

Translational pharmacology of dopamine receptor agonists and antagonists

Prolactin and oxytocin as biomarkers



Translational pharmacology of dopamine receptor agonists and antagonists

Prolactin and oxytocin as biomarkers

PROEFSCHRIFT

ter verkrijging van de graad van Doctor aan de Universiteit van Leiden,
op gezag van Rector Magnificus prof. mr. P. F. van der Heijden,
volgens besluit van het College voor Promoties,
te verdedigen op donderdag 22 september 2011, klokke 11.15 uur
door Jasper Stevens, geboren te Geldrop in 1979.

PROMOTIECOMMISSIE

Promotor

Prof. dr. M. Danhof

Co-promotoren

Dr. E. C. M. de Lange

Dr. P. H. van der Graaf

Overige leden

Dr. J. H. Proost, Rijksuniversiteit Groningen

Dr. A. Vermeulen, Johnson & Johnson

Prof. Dr. A. P. IJzerman

Prof. Dr. J. Bouwstra

Prof. Dr. M. Oitzl.

***THE RESEARCH DESCRIBED IN THIS THESIS WAS FINANCIALLY SUPPORTED BY PFIZER
AND CONDUCTED AT THE LEIDEN/AMSTERDAM CENTER FOR DRUG RESEARCH,
LEIDEN UNIVERSITY, THE NETHERLANDS.***



Translational pharmacology of dopamine receptor agonists and antagonists

Prolactin and oxytocin as biomarkers

For Nienke and my parents.



Contents

- 1 Background, objectives and outline 9
- 2 Translational pharmacology of intranasal administration of dopamine receptor agonists and antagonists 13
- 3 A new minimal-stress freely-moving rat model for preclinical studies on intranasal administration of CNS drugs 43
- 4 Online solid phase extraction with liquid chromatography-tandem mass spectrometry to analyze remoxipride in small plasma-, brain homogenate-, and brain microdialysate samples 59
- 5 Systemic- and direct nose-to-brain transport in the rat; a pharmacokinetic model for remoxipride after intravenous and intranasal administration 77
- 6 Mechanism-based PK-PD model for the prolactin biological system response following a dopamine inhibition challenge - quantitative extrapolation to humans 97
- 7 Conclusions and general discussion 123

Appendices

- Nederlandse samenvatting 135
- Nawoord 143
- List of Publications 145
- Abbreviations 147

Background, objectives and outline

The dopaminergic system organizes many behavioral mechanisms in the brain. Dysfunctions of the dopaminergic system can result in disease states like e.g. schizophrenia, Parkinson's disease and sexual disorders (Marsden, 2006). Dopamine receptor antagonists have been developed to block hallucinations and delusions that occur in schizophrenic patients, whereas dopamine receptor agonists are effective in alleviating the hypokinesia of Parkinson's disease. However, blockade of dopamine receptors can induce extrapyramidal effects similar to those resulting from dopamine depletion in Parkinson's disease, and high doses of dopamine agonists can cause psychoses. Also, the occurrence of sexual dysfunctions is high in Parkinson's disease patients, but dopamine replacement therapy can cause hyper sexuality and aberrant sexual behavior (Meco, et al., 2008). The therapies of disorders resulting from dopamine imbalances are thus associated with severe side effects.

To develop treatments with improved safety and efficacy, one of the scientific challenges is to understand the biological mechanisms underlying the pharmacokinetic- and pharmacodynamic (PK-PD) relationships of (partial) dopamine agonists and antagonists. PK-PD modeling is the gold standard to investigate such complex mechanisms. Often, these models include plasma drug concentration-effect relationships. However, for dopaminergic compounds, the target site is the brain extracellular fluid (ECF) that surrounds the dopamine receptors. Consequently, a more mechanistic approach should be aimed at understanding the drug concentrations at the target site (De Lange, et al., 2005; Danhof, et al., 2007; Ploeger, et al., 2009).

Also, to achieve a more rapid onset of action and an increased therapeutic window for compounds that have high clearance and/or low oral bioavailability characteristics, alternative routes of administration are developed. Intranasal administration of dopaminergic compounds avoids gastrointestinal- and hepatic first-pass elimination and is hypothesized to circumvent the blood-brain barrier by direct nose-to-brain transport (Dhuria, et al., 2009). This administration route is therefore anticipated to improve the time to onset- and/or the selectivity of action, specifically for drugs acting on the central nervous system.

This thesis addresses different aspects of the PK-PD correlations of dopaminergic drugs following intravenous and intranasal administration.

Chapter 2 reviews how detailed preclinical investigations in combination with mechanistic PK–PD modeling may provide a scientific basis for the translational pharmacology of dopaminergic drugs to man, following systemic and intranasal administration.

Chapter 3 of this thesis reports on the development and validation of a new ‘minimum-stress’ animal model that allows intranasal- and, for comparative purposes, intravenous drug administration. In this preclinical model, PK–PD parameters can be obtained over time in blood- and brain ECF samples in freely moving animals. A staining study was performed to confirm the selectivity of intranasal administration and corticosterone concentrations were determined over time to exclude stress-related experimental influences. Subsequently, acetaminophen was administered intravenously and intranasal as a model compound to test the animal model.

To investigate dopaminergic PK–PD relationships, the weak but selective dopamine D₂-receptor antagonist remoxipride was chosen as a paradigm compound. To detect low remoxipride concentrations in small plasma-, brain ECF- and brain homogenate samples, novel analytical methods were required. *Chapter 4* reports on the development, optimization and validation of these methods, for which online solid phase extraction and liquid chromatography-tandem mass spectrometry techniques were used.

Following intranasal administration, compounds can enter the brain by direct nose-to-brain transport or via systemic absorption followed by blood-brain barrier transport. Comparison to intravenous administration provides insight on intranasal bioavailability. Using the newly developed animal model and analytical methods, we can obtain serial datapoints in plasma and close to, if not at, the target site following intravenous and intranasal administration of remoxipride. In *chapter 5*, nonlinear mixed effect modeling (Beal and Sheiner, 1992) was applied to quantitate the PK of remoxipride in plasma and brain ECF following intranasal and intravenous administration. This approach provides, for the first time, quantitation of direct nose-to-brain transport of remoxipride.

The next step was to develop a mechanism-based PK–PD model on data obtained in rats, which could be used to predict the PK–PD relationship in different situations and systems, including the biological system response in humans. To that end, the effects of brain ECF remoxipride concentrations on prolactin concentrations, as translational biomarker for dopaminergic system activity, were assessed following intravenous administration of remoxipride.

We report in *chapter 6* on the development and validation of a novel mechanism-based PK–PD model containing:

- a PK model for remoxipride concentrations in plasma and brain ECF after intravenous remoxipride administration
- a pool model incorporating the rate of synthesis of prolactin in lactotrophs, and the rate constants for prolactin release into- and elimination from plasma
- a biological system response model for homeostatic feedback
- a drug concentration–effect model for prolactin release in response to brain ECF remoxipride concentrations.

The dataset obtained following intranasal administration of remoxipride was used to challenge the predictive value of the model for alternative routes of administration. Finally, a first step towards translation from rat to humans was performed and compared to clinical data, to investigate if the structural model can be applied for both species.

In *chapter 7* the conclusions and general discussion of this scientific basis for the translational pharmacology of dopaminergic drugs following systemic and intranasal administration are discussed.

REFERENCES

- Beal SL and Sheiner BL (1992) NONMEM user's guide, Part 1, in *NONMEM user's guide, Part 1* University of California at San Francisco.
- Danhof M, de Jongh J, De Lange EC, Della PO, Ploeger BA and Voskuyl RA (2007) Mechanism-based pharmacokinetic-pharmacodynamic modeling: biophase distribution, receptor theory, and dynamical systems analysis. *Annu Rev Pharmacol Toxicol* **47**:357-400.
- De Lange EC, Ravenstijn PG, Groenendaal D and Van Steeg TJ (2005) Toward the prediction of CNS drug-effect profiles in physiological and pathological conditions using microdialysis and mechanism-based pharmacokinetic-pharmacodynamic modeling. *AAPS J* **7**:E532-E543.
- Dhuria SV, Hanson LR and Frey WH (2009) Intranasal delivery to the central nervous system: Mechanisms and experimental considerations. *Journal of Pharmaceutical Sciences* **99**:1654-1673.
- Marsden CA (2006) Dopamine: the rewarding years. *Br J Pharmacol* **147**:S136-S144.
- Meco G, Rubino A, Caravona N and Valente M (2008) Sexual dysfunction in Parkinson's disease. *Parkinsonism & Related Disorders* **14**:451-456.
- Ploeger BA, Van der Graaf PH and Danhof M (2009) Incorporating receptor theory in mechanism-based pharmacokinetic-pharmacodynamic (PK-PD) modeling. *Drug Metab Pharmacokinet* **24**:3-15.

Translational pharmacology of intranasal administration of dopamine receptor agonists and antagonists

J. Stevens, M. Danhof, E. C. M. de Lange.

*Division of Pharmacology, LACDR, Leiden University, Leiden,
The Netherlands.*

ABSTRACT

Many central nervous system (CNS) diseases related to dysfunction of the dopaminergic system are treated with dopaminergic drugs, but with varying degrees of success. Dopaminergic drugs often suffer from extensive and/or variable gastrointestinal- and hepatic first-pass elimination, as well as limited brain distribution. Therefore, the intranasal administration route is of interest as it may enhance brain target site distribution of these drugs, and may reduce side-effects, therewith improving the therapeutic possibilities of dopaminergic drugs.

The data obtained in investigations on intranasal administration to date, have not provided insight on the rate of brain distribution nor on the route; via the systemic circulation and/or direct from nose to brain. Most importantly, such data lacked information on brain target site pharmacokinetics (PK) that drives the pharmacodynamics (PD). Therefore these data are not suited to aid in quantitative prediction of PK–PD relationships in human.

It is anticipated that quantitative prediction of the time course of CNS drug effects of dopaminergic drugs in human is possible, using detailed PK and PD data following intranasal- as well as systemic administration and advanced mechanistic PK–PD modeling. To that end there is a need for refined animal models and biomarkers to provide insight into brain target site PK in relation to dopaminergic brain activity, to be extrapolated to the human situation using translational pharmacology approaches.

INTRODUCTION

The dopaminergic system is involved in many CNS functions, including behavior and cognition, voluntary movement, motivation and reward, inhibition of prolactin production, sleep, mood, attention, and learning. Many CNS diseases are related to dysfunction of this important system, such as Parkinson's disease, schizophrenia and sexual disorders (Marsden, 2006), and are symptomatically treated with dopaminergic drugs, with varying degrees of success (Kvernmo, et al., 2008). Unfortunately, many dopaminergic drugs often suffer from extensive and/or variable gastrointestinal- and hepatic first-pass elimination (Deleu, et al., 2002), while the blood-brain barrier (BBB) may also limit their brain distribution (El Ela, et al., 2004). This commenced, amongst others initiatives, the search for alternative routes of administration (Mahmood, et al., 1997; Degim, et al., 2003).

The intranasal administration route is of interest as it may increase brain target site pharmacokinetics (PK) of these drugs, and therewith may improve the effects (PD) of the dopaminergic drugs (Illum, 2004; Costantino, et al., 2007; Dhuria, et al., 2009). Intranasal administration is anticipated to rapidly target compounds into; 1) the systemic circulation by the respiratory epithelial pathway, and 2) into the CNS via olfactory epithelial- and olfactory nerve pathways. In a limited number of human studies, the merit of intranasal administration has been based on improvement of drug effects (Kapoor, et al., 1990).

Preclinical investigations to date have studied the potential added value of intranasal administration on the basis of descriptive analysis of concentrations (at best area under the curve (AUC) in brain or cerebrospinal fluid (CSF) compared to plasma (Dhuria, et al., 2009; Vyas, et al., 2005; Van den Berg, et al., 2005)). CSF, however, does not necessarily provide direct information on the target site concentration of dopaminergic drugs (De Lange and Danhof, 2002). The brain extracellular fluid (ECF) PK, is a much better sampling site as it represents most closely the site of action for most dopamine targets such as receptors, reuptake transporters and metabolizing enzymes (De Lange, et al., 2005; Jeffrey and Summerfield, 2010).

To quantitatively predict the time course of CNS drug concentrations and effects in human, insight on the rate of brain distribution and on the route of brain distribution either via the systemic circulation or direct from nose-to-brain is needed, as well as on the brain target site PK (De Lange, et al., 2005; Danhof, et al., 2007; Ploeger, et al., 2009), together with other bio-

markers on the causal chain between dose and effect. Having such information, translational PK–PD modeling approaches can be used for extrapolation of *in vivo* preclinical data to the human situation.

To that end, mechanism-based PK–PD modeling concepts are useful, as this allows explicit distinction between drug-specific- and biological-system (animal, human) specific parameters (Danhof, et al., 2008). Consequently, following intranasal administration studies, mechanism-based PK–PD modeling has the potential to provide quantitative information on the absorption pathways, target site distribution and effect.

This review provides a short overview on the pharmacology of the dopaminergic system and its associated diseases, with subsequent description of the various anatomical and biological aspects of intranasal administration and currently used experimental approaches to investigate this route of administration. This is followed by a disquisition on the prospect of quantitative prediction of the time course of human dopaminergic CNS drug effects using detailed PK and PD data on intranasal as well as systemic administration, combined with advanced mechanistic PK–PD modeling.

Finally, as obtainment of such human data is highly restricted and extremely expensive, it is stated that important information should be derived from *in vivo* animal studies and translational pharmacology approaches. This indicates the need for refined animal models and biomarkers to gain insight into brain target site PK in relation to dopaminergic brain activity. It is concluded that preclinical mechanistic PK–PD models can provide the scientific basis for the translational pharmacology of dopaminergic drugs after intravenous and intranasal administration.

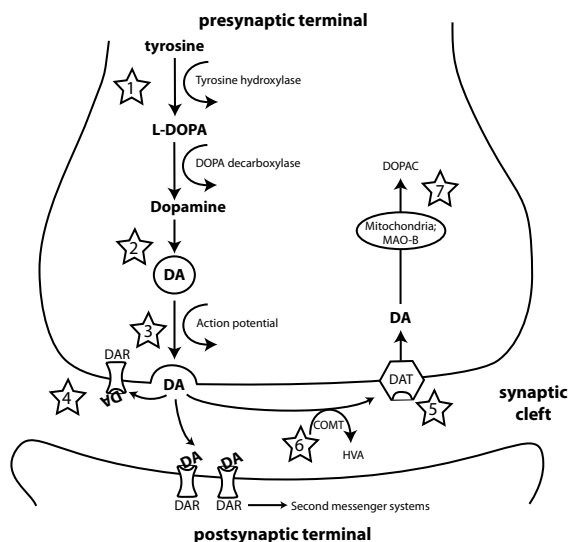
THE DOPAMINERGIC SYSTEM

Dopamine is the predominant catecholamine neurotransmitter in the mammalian brain, where it controls a variety of CNS functions including locomotor activity, cognition, emotion, positive reinforcement, food intake, and endocrine regulation. It also plays multiple roles in the periphery as a modulator of cardiovascular function, catecholamine release, hormone secretion, vascular tone, renal function, and gastrointestinal motility (Kandel, et al., 2000). The dopaminergic brain systems have been the focus of much research over the past 30 years, mainly because important pathological conditions have been linked to a dysregulation of dopaminergic transmission, such as Parkinson's disease, schizophrenia, sexual disorders, Tourette's syndrome, and hyperprolactinemia (Marsden, 2006).

■ Dopamine synthesis, release and metabolism

Dopamine is biosynthesized in the cell bodies of dopaminergic neurons in the brain. It is stored in neuronal vesicles and released into the synaptic cleft in response to presynaptic action potentials. In this extracellular space, dopamine may bind and activate dopamine receptors, which can be present at post- and presynaptic membranes (Carlson, 2001). The effect of dopamine is ended upon reuptake by reuptake-transporters (Chen and Reith, 2000), extracellular metabolism by catechol-O-methyl transferase (Bilder, et al., 2004) and/or outer mitochondrial membrane associated monoamine oxidase B (Ben Jonathan and Hnasko, 2001) (Figure 1).

Figure 1 Synthesis and metabolism of dopamine (DA) and site of action of drugs that affect dopamine transmission (numbered stars). Drugs can affect the synthesis (1), storage (2) and release (3) of DA. Many drugs act on the DA receptors (DAR) in the synaptic cleft (4), while some interfere with DA reuptake (5) by DA transporter proteins (DAT) or on the metabolic pathways of catechol-O-methyl transferase (COMT, 6) or mitochondrial monoamine oxidase B (MAO-B, 7). 3M =, 3-methoxytyramine; HVA =, homovanillic acid; DOPAC = 3,4-dihydroxy-phenylacetic acid.



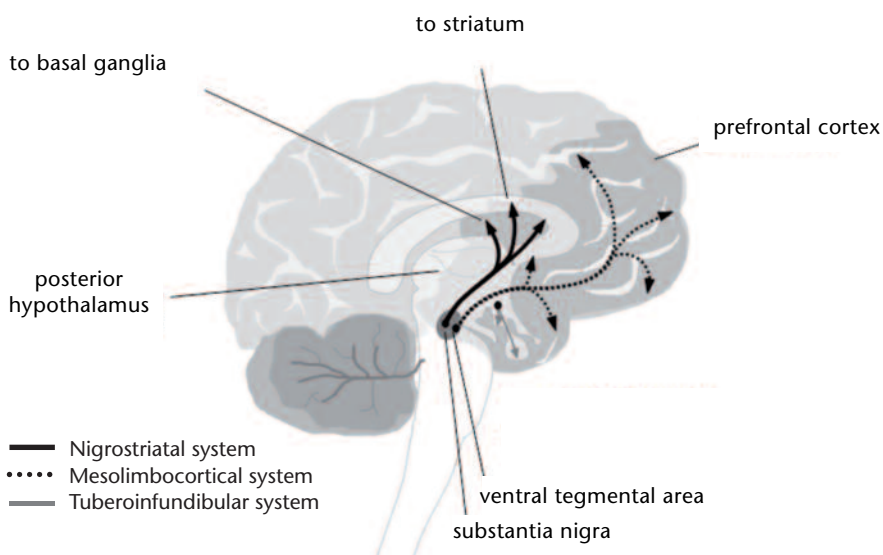
■ Dopaminergic pathways

Dopamine containing neurons are mainly located in the substantia nigra pars compacta, the ventral tegmental area and the hypothalamus, and pro-

ject their axons to large areas in the brain (Kandel, et al., 2000; Freeman, et al., 2000; Ben Jonathan and Hnasko, 2001; Ben Jonathan, et al., 2008). Dopamine is transmitted via three major pathways (Figure 2):

- the first, the nigrostriatal system, extends from the substantia nigra to the caudate nucleus-putamen (neostriatum) and is concerned with sensory stimuli and movement
- the second, the mesolimbocortical system, projects from the ventral tegmentum to the mesolimbic forebrain and is thought to be associated with cognitive, reward and emotional behavior
- and the third, the tuberoinfundibular system, is concerned with neuronal control of the hypothalamic-pituitary endocrine system.

Figure 2 Major dopaminergic pathways in the brain (redrawn from CNS-Forum educational resources <http://www.cnsforum.com/educationalresources/imagebank/>).



■ Dopaminergic drugs

Dopaminergic activity in the brain can be modulated by drugs via different targets (Figure 1).

• Dopamine synthesis

Several drugs of clinical importance act indirectly on the synthesis of dopamine e.g. L-DOPA, which is converted into dopamine (Deleu, et al., 2002). Compounds like for example alpha-methyl-para-tyrosine can act directly on

dopamine synthesis by inhibiting the hydroxylation of tyrosine to dopamine (Ankenman and Salvatore, 2007).

- **Dopamine vesicles**

Monoamine oxidase inhibitors like e.g. selegiline (Caslake, et al., 2009) may decrease intracellular metabolism and potentially increase vesicular dopamine.

- **Dopamine release**

Other compounds influence the amount of dopamine reaching the synaptic cleft. For example reserpine, which depletes dopamine vesicles (Peter, et al., 1995), or amphetamine, which releases dopamine from terminal stores (Goodwin, et al., 2009).

- **Dopamine transmission**

Many drugs affect dopamine transmission directly by either blocking or stimulating dopamine receptors in the synaptic cleft. Dopamine antagonists include antipsychotic drugs, whereas e.g. bromocriptine is a dopamine agonist, used to treat hyperprolactinemia and Parkinson's disease (Kvernmo, et al., 2006).

- **Dopamine elimination from synaptic cleft**

Several drugs increase the synaptic concentration of dopamine by blocking the re-uptake or metabolism of dopamine. As an example, cocaine is a potent inhibitor of the dopamine re-uptake transporter (Schmitt and Reith, 2010), and OR-611 is a catechol-O-methyl transferase inhibitor (Kaakkola and Wurtman, 1992).

■ Pharmacology of the dopamine receptors

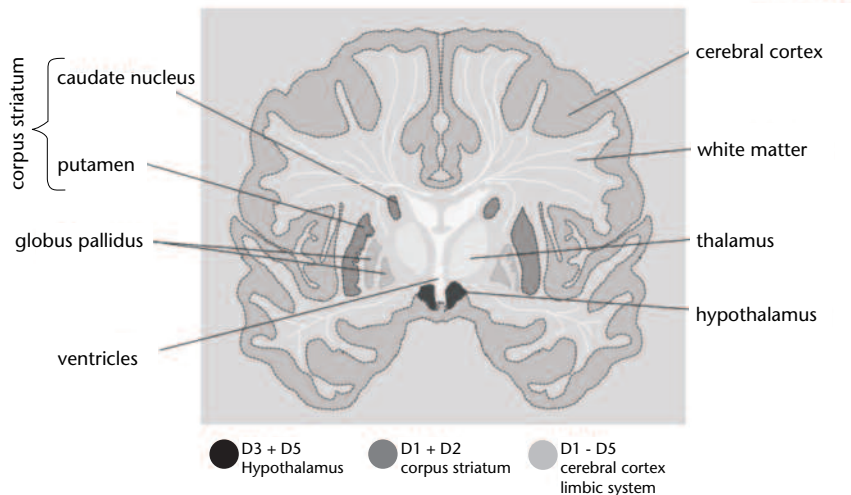
All dopamine receptor subtypes are expressed in the brain in distinct but overlapping areas (Defagot, et al., 1997; Missale, et al., 1998; Khan, et al., 2000; Marsden, 2006).

□ Receptor types and brain distributions

There are five subtypes of dopamine receptors and these D1–D5 subtypes are widely distributed throughout both the cerebral cortex and the limbic system of the brain. Certain sub-types are also found in other specific areas of the brain, for example the D1- and D2-receptors are expressed in the striatum (Figure 3).

□ Receptor subfamilies

The dopamine receptor subtypes can be divided into two families, the D1-like and D2-like receptors. The D1-like receptors comprise D1- and D5-receptor subtypes that are associated with *stimulation* of adenylate cyclase. The D2-like receptors comprise D2-, D3- and D4-receptor subtypes and these are associated with *inhibition* of adenylate cyclase.

Figure 3 Brain distribution of dopamine receptor subtypes.

■ Dopaminergic dysfunctions and associated therapies

Dysfunctions of the dopaminergic system can result in disease states like e.g. Parkinson's disease, schizophrenia and sexual disorders. Other neurotransmitter systems may be involved as well, but are not further discussed here.

• Parkinson's Disease

Very low levels of dopamine in the motor areas of the brain that result from neural cell death in the substantia nigra pars compacta, and often also the formation of Lewy Bodies are known to produce Parkinson's Disease (Dauer and Przedborski, 2003). Symptoms include muscle rigidity and stiffness, stooped/unstable posture, loss of balance and coordination, gait (walking pattern) disturbance, slow movements and difficulty with voluntary movements, tremors and shaking, mask-like facial expression, and impairment in cognitive/intellectual ability.

Although research is directed toward prevention of dopamine neuron degeneration, all current therapies focus on (symptomatic) replacement of dopamine treatment with its precursor L-DOPA. This is combined with a peripheral decarboxylase inhibitor (like benserazide or carbidopa) as to prevent dopamine formation in the periphery, and a COMT inhibitor (like tolcapone or entacapone) to prolong the effect of L-DOPA.

In addition, elimination of dopamine is slowed down by MAO-B inhibitors (like rasagiline and selegiline).

However, unwanted effects of chronic L-DOPA administration are associated with end-of-dose deterioration of function, on/off oscillations, freezing during movement, and dyscoordination of movement (dyskinesias) at peak dose, accompanied by depression anxiety, pain, panic, and delusions.

Although L-DOPA is still accepted as “gold standard” in Parkinson’s Disease treatment, D1- and D2-receptor stimulation by dopamine-agonists may improve therapeutic response (Deleu, et al., 2002; Kvernmo, et al, 2008).

Dopamine agonists include ropinirole, cabergoline, bromocriptine, pergolide, pramipexole, rotigotine, and apomorphine.

In general, sole dopamine agonists treatment is less effective than L-DOPA treatment. However, dopamine agonists do not depend on neuronal uptake and release and have in general a longer duration of action. This reduces the risk of the development of dyskinesias (Savitt, et al., 2006). It has been suggested that several ergot derived dopamine agonists (pramipexole, ropinirole) reduce neuronal cell death, thereby slowing down disease progression relative to L-DOPA (Yamamoto and Schapira, 2008; Kvernmo, et al., 2008). It is however a major challenge to demonstrate a disease modifying effect in clinical trials (Ploeger and Holford, 2009).

- **Schizophrenia**

Although direct evidence is lacking, it seems that when dopamine levels increase in the thinking areas of the brain (forebrain, hindbrain and limbic system), hallucinations start to occur in hearing, sensing, tasting and smell. At the more extreme, this results in schizophrenia, characterized by the loss of contact with reality by hallucinations, delusions, disordered thinking, unusual speech or behavior, and social dysfunction. The symptoms of schizophrenia are classified in categories as positive (delusions, hallucinations, thought disorder), negative (flat affect, poverty of thought, amotivation, social withdrawal), cognitive (distractibility, impaired working memory, impaired executive function), and mood (mania, depression) (Eon and Durnham, 2009).

Pharmacological studies indicate that the potency of antipsychotic drugs are strongly correlated to the ability to block D2-receptors (Kapur, et al., 2000; Seeman, 2010). Antagonizing D1-like receptors do not lead to antipsychotic activity, but rather to aggravation of symptoms. In contrast, evidence is accumulating that administration of low doses of D1-receptor agonists can alleviate symptoms. The role of antagonizing or partially agonizing D3-receptors remains unclear (Miyamoto, et al., 2005).

In the treatment of schizophrenia, antipsychotic drugs are often very effective in treating certain symptoms of schizophrenia, particularly hallucina-

tions and delusions. Unfortunately, the drugs may not be as helpful with other symptoms, such as reduced motivation and emotional expressiveness. Especially, the older antipsychotics (“neuroleptics”), like haloperidol and chlorpromazine, may produce short-term side effects including drowsiness, restlessness, muscle spasms, dry mouth, tremor, or blurred vision, while one important long-term side effect is tardive dyskinesia. In such cases, a lower dose may help, or the use of newer antipsychotic drugs like olanzapine, quetiapine, and risperidone, which appear less likely to have this problem. Some-times when schizophrenic patients become depressed, other symptoms can appear to worsen. The severity of the symptoms may be reduced by the addition of an antidepressant drug.

- **Sexual dysfunction**

Sexual dysfunction is often referred to as either disturbances in sexual desire or functioning. In the brain, sexual function is under control of inhibitory and stimulatory processes. For the treatment of erectile dysfunction, the use of the D1/D2-dopamine receptor agonist apomorphine provides a strong support in favor of a participation of the dopaminergic system in the control of sexual function. However, the exact involvement of dopamine in sexual motivation and in the control of genital arousal in humans is unknown (Giuliano and Allard, 2001; Kruger, et al., 2005). Pfaus (2009) reported on studies implicating D1-receptors being involved, while Baskerville and Douglas (2008) reported that merely D2-receptors mediate sexual behavior. This leaves the need for more investigations on specific dopamine receptor interactions in hypothalamic brain areas implicated in sexual behavior, being the medial preoptic area and periventricular nucleus.

■ Problems and future perspectives in dopaminergic therapies

Treatment of disorders associated with dopamine imbalance involves drug treatment in order to increase or decrease dopamine levels in the brain. Dopamine receptor antagonists have been developed for too high dopamine concentrations, to block hallucinations and delusions that occur in schizophrenic patients, whereas dopamine receptor agonists are effective in alleviating the hypokinesia of Parkinson's disease in which dopamine action is too low. However, blockade of dopamine receptors can induce effects similar to those resulting from dopamine depletion in Parkinson's disease, and high doses of dopamine agonists can cause psychoses. Also, the occurrence of sexual dysfunctions is high in Parkinson's disease patients, but dopamine replacement therapy can cause hyper sexuality and aberrant sexual behavior (Meco, et al., 2008). The therapies of disorders resulting from dopamine

imbalances are thus associated with severe side effects. Newer therapies are more specifically targeted to one of the dopamine receptor types, or focus on partial agonist in which in the absence of a full agonist the partial agonists will help to increase the response, while in the presence of a full agonist the partial agonist will reduce the response (Lieberman, 2004; Ohlsen and Pilowsky, 2005).

Another issue is the problem associated with target site distribution of the dopaminergic drugs, that drive their effects. Between dosing and target site distribution, a lot of factors are involved that may contribute significantly to intra-individual variability and therefore inadequate/unpredictable outcome. Thus, many dopaminergic drugs often suffer from extensive and/or variable gastrointestinal- and hepatic first-pass elimination (e.g. apomorphine, chlorpromazine, bromocryptine, pergolide, lisuride, and risperidone) (Contin, et al., 2000; Deleu, et al., 2002; Blin, et al., 2003; Del Dotto and Bonuccelli 2003; Nyholm, et al., 2006; Menon and Stacy, 2007), while for a number of dopaminergic drugs (e.g. pramipexole, amisulpiride, fluphenazine, olanzapine, and risperidone) active transport mechanisms are involved in BBB transport (El Ela et al., 2004; Wang, et al., 2004a, Wang, et al., 2004b; Zhu, et al., 2006; Okura, et al., 2007). This initiated, amongst others, the search for alternative routes of administration (Mahmood, et al., 1997; Contin, et al., 2000; Degim, et al., 2003). One of the options is intranasal administration.

INTRANASAL ADMINISTRATION

Intranasal administration has gained special interest as a strategy to circumvent unfavorable absorption and/or extensive first-pass metabolism characteristics of orally administered compounds, as well as a potential means to circumvent the blood-brain barrier (BBB) when this barrier restricts brain distribution of a compound (Dhuria, et al., 2009). As the nasal cavity is covered by a thin mucosa and a well vascularised epithelium, a drug molecule can quickly be transferred across the single epithelial cell layer directly into the systemic blood circulation. On the other hand, direct nose-to-brain transport may result in brain distribution enhancement (Illum, 2004; Costantino, et al., 2007; Dhuria, et al., 2009; Pires, et al., 2009).

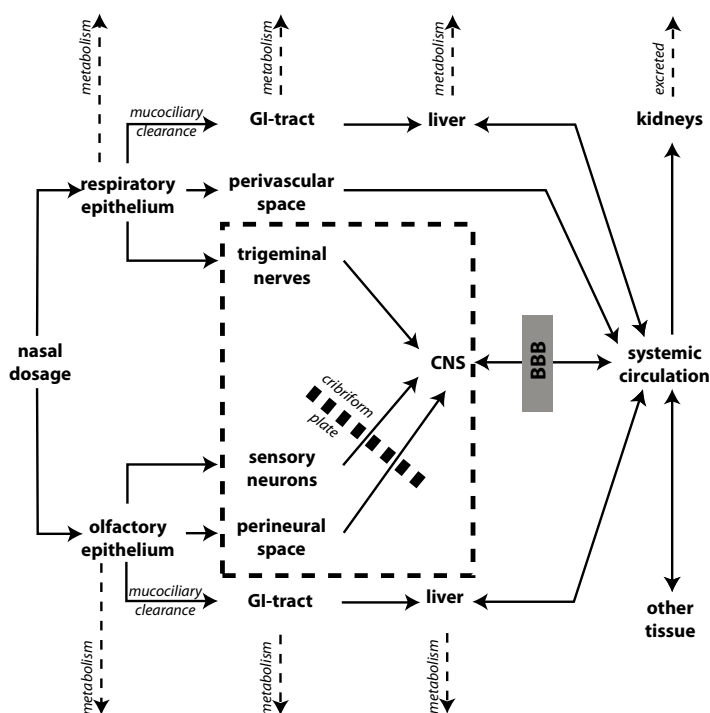
Thus, intranasal administration may offer a more rapid onset of action and an increased therapeutic window due to targeted drug delivery for compounds having a high clearance, low oral bioavailability and/or low BBB transport characteristics. Intranasal administration can therefore be used as an alternative to oral administration if a fast effect is desired or if the drug

is extensively degraded in the gut or liver. To identify its potential to circumvent the BBB, the different nasal transportation routes need to be considered.

■ Nasal transport

Part of the nasal cavity is covered by respiratory epithelium, across which systemic drug absorption can be achieved. The olfactory epithelium is located in the upper posterior part of the nasal cavity (Gross, et al., 1982). The nerve cells of the olfactory epithelium project into the olfactory bulb of the brain, which provides a direct connection between the brain and the external environment. Two major routes of transport can be distinguished in direct nose-to-brain transport (Figure 4). The respiratory and the olfactory epithelial pathway (Illum, 2000; Dhuria, et al., 2009).

Figure 4 Schematic presentation of direct nose-to-brain (dotted square) and systemic absorption and elimination routes following intranasal administration. CNS, central nervous system; BBB, blood brain barrier; GI-tract, gastrointestinal tract. Adjusted from Illum 2000.



- **Respiratory epithelial pathway**

Following absorption over the respiratory epithelium, compounds diffuse into trigeminal nerves which may allow compounds to further enter the brain.

- **Olfactory epithelial pathway**

Compounds that enter the brain by the olfactory epithelial pathway may diffuse into the perineural spaces that cross the cribriform plate, ending up in the cerebrospinal fluid of the subarachnoid space, and may further diffuse throughout the brain. The olfactory epithelial pathway also allows intracellular transport through the sensory neurons, into the olfactory bulb. On the cell surface of sensory neurons, transporter proteins (glycoproteins) are present allowing compounds to bind and to be absorbed via endocytosis. After intracellular transport, the compound is exocytosed in the olfactory bulb.

■ **Intranasal administration of dopaminergic compounds**

For quite a number of dopaminergic drugs the intranasal route has been investigated. A few examples are shortly described below.

- **Dopamine**

Following intranasal administration of dopamine, higher plasma bioavailability was found compared to dermal, buccal, or rectal administration in beagle dogs (Ikeda, et al., 1992). For radiolabeled dopamine, direct transport of radioactivity from nose into brain was indicated in the olfactory tract and -bulb, while also radioactivity was found to be increased in the striatum, indicating distribution into deeper brain areas (Dahlin, et al., 2000). Interestingly, dopamine uptake transporters have been identified in rat- and bovine respiratory- and olfactory epithelia, indicating potential active uptake of dopamine (Chemuturi, et al., 2006).

- **L-DOPA**

Being the precursor for dopamine, intranasal administration of L-DOPA might directly increase dopamine levels in the brain following intrabrain decarboxylation. De Souza Silva and colleagues found an increase in the extracellular dopamine concentrations in the neostriatum of the brain upon intranasal L-DOPA administration to anaesthetized rats, as determined by microdialysis (Souza Silva, et al., 1997). Recently, Kim and colleagues (Kim, et al., 2009) investigated intranasal dosing of L-DOPA together with carbidopa, compared to oral administration of these drugs. Plasma and brain data, analyzed by compartmental modeling, indicated that L-DOPA was rapidly transported into the brain, and nasal administration of the drugs resul-

ted in ~3-fold higher bioavailability than oral administration. Intranasal administration of L-DOPA and carbidopa was suggested as a good rescue therapy for Parkinson's disease patients who experience symptom fluctuation with oral L-DOPA administration.

- **Apomorphine**

Several clinical results have been published on apomorphine following intranasal administration. Improved pharmacodynamics were found compared to subcutaneous administration in Parkinson patients (Kapoor, et al., 1990). In more longitudinal studies, however, nasal blockage, burning sensation and nasal vestibulitis were indicated (Kleedorfer, et al., 1991; Van Laar, et al., 1992). Several preclinical formulations have been tested to overcome these issues, and bioavailability could be increased up to ~70% (Ugwoke, et al., 1999). For the treatment of sexual dysfunctions, several clinical intranasal apomorphine formulations were found to result in a rapid time to maximal plasma concentration while CSF-plasma ratios increased significantly (from 5% to approximately 35%), compared to subcutaneous administration (Kendirci and Hellstrom, 2004). This was accompanied by an improvement of the effect (sexual activity) in the majority of the cases (Kendirci and Hellstrom, 2004).

These studies indicate that intranasal administration may indeed be a useful route of administration, although also limitations should be considered.

- Nasal administration is primarily suitable for potent drugs since only a limited volume can be administered into the nasal cavity (Dhuria, et al., 2009; Stevens, et al. 2009).
- For continuous and frequent administration of drugs and vehicles, the risk of harmful long term effects on the nasal epithelium exists (like for apomorphine, as described previously).
- For nasal administration, a high variability in the amount of drug absorbed may be encountered. Variability may result from variation of the method of nasal administration, e.g. position of the tip upon spraying, therefore exposing nasal tissues differentially, as well as by upper airway infections, irritation of the nasal mucosa, and by partial swallowing of the sprayed drug solution. As a note, such variability should always be put into perspective, and compared to that following oral (or other routes of) administration (Coda, et al., 2003; Studd et al., 1999; Kublik, et al., 1998).
- Furthermore, following intranasal administration, compounds can be subjected to extensive metabolism in the nasal mucosa and tissue by several enzymes (e.g. cytochrome P450 isoenzymes, amino peptidases and carboxyl esterases (Minn, et al., 2005; Zhang et al., 2009; Benedetti, et al., 2009).

- Finally, also several transporter proteins have been identified, which are responsible for active efflux of compounds, for example P-glycoprotein, and organic anion/multidrug resistance associated proteins (Jones, 2001; Graff and Pollack, 2003).

■ Considerations in preclinical studies on intranasal administration

There are several issues that need to be considered in obtaining preclinical data following intranasal administration studies.

• Impact of anesthesia and/or restrain stress

Many preclinical PK–PD studies on intranasal administration so far have been performed on anaesthetized animals, whether or not in combination with complete isolation of the nasal cavity and cannulated trachea to aid breathing. Alternatively, restrained animals are used. Such experimental conditions have major influence on physiological parameters, like blood flow, mucocilliary clearance, nasal cycle, and airflow dynamics (Van den Berg, et al., 2002; Ross, et al., 2004; Thorne, et al., 2008). These are all factors that may influence the rate and/or extent of absorption and widens the gap between animal and human conditions. Altogether, this indicates the need for more refined, minimum-stress animal models for intranasal administration (Dhuria, et al., 2009; Stevens, et al., 2009).

• Sampling techniques

To have information on brain distribution of nasally administered drugs, the use of brain tissue allows only one time-point per animal, and thus large numbers of animals are required. Puncturing the cisterna magna induces a high risk of blood contamination, while also puts a limit to the number of samples that can be obtained (Van den Berg, et al., 2002). The use of a CSF cannula has provided a major improvement as it allows serial CSF-sampling and decreases the risk of blood contaminations (Van Bree, et al., 1989). However, still, by serial CSF sampling, the potential effects of CSF-removal on brain fluid pressure and brain physiology remain.

• Parameters used for comparison of data on brain distribution

For quantification of brain distribution following intranasal versus other routes of administration, often the ratio of AUC in CSF over AUC in plasma is used and compared to the ratio following other routes of administration (Van den Berg, et al., 2005). Such AUC ratios identify differences in total brain exposure (extent) after intranasal administration, rather than provide the quantitative distinction between brain distribution via the systemic circulation and direct nose-to-brain transport, in terms of absorption rate

and bioavailability. For that reason, such descriptive pharmacokinetic models are of limited value for translational purposes, especially for animal to human extrapolation.

TRANSLATIONAL MECHANISM-BASED PK–PD MODELING

Mechanism-based PK–PD models are based on principles from systems pharmacology and contain specific expressions to characterize processes on the causal path between drug exposure and drug response. An important feature of mechanism-based PK–PD models is the strict distinction between drug-specific and biological system-specific parameters to describe *in vivo* drug effects. In this regard PK–PD modeling has developed from an empirical and descriptive approach into a mechanistic science recognizing the (patho)-physiological mechanisms which are underlying PK–PD relationships.

With time, it has become clear that mechanism-based PK–PD models have indeed much improved properties for extrapolation and prediction (Danhof, et al., 2008). To that end, a mechanism-based approach should include specific expressions to describe target site distribution, target binding and activation, and the transduction, including the homeostatic control mechanisms (Danhof, et al., 2007; Ploeger, et al., 2009; Gabrielsson and Green, 2009). The use of more detailed biological system information will improve the accuracy in PK–PD relationships in humans (Danhof, et al., 2008). As in most cases direct measurement of the anticipated effect is difficult or impossible, the use of biomarkers of the effects may provide quantitative information on the causal path between drug PK and effect.

■ Biomarker classification and application

Biomarkers can be classified according to the biomarker classification scheme (Danhof, et al., 2005). In short:

- **Type 0 biomarkers** refer to the genotype- or phenotype as determinant of the drug response, that influences target site exposure or response due to variation in the expression of e.g. enzymes or receptors. They are commonly used as covariates in PK–PD models.
- **Type 1 biomarkers** refer to drug concentrations in general and at the target site in particular. As previously pointed out, quantitative biomarkers that represent the target site distribution of drugs and metabolites for compounds that act in the CNS are difficult to obtain in man, but readily available *in vivo* in animal (De Lange, et al., 2005).

- **Type 2 biomarkers** refer to the degree of target occupancy. In theory, effects may occur at different degrees of target occupancy and may be species dependent. The relationship between target occupancy and effect is therefore important for the understanding of inter- and intra-individual variability. Information on target occupancy is available by bioassays *in vitro* and can also be non-invasively measured in humans by positron emission tomography (Kapur, et al., 2000).
- **Type 3 biomarkers** refer to quantification of the target site activation. By means of *in vitro* bioassays information can be obtained on receptor activation in animal and man. Techniques like electroencephalograms (Kropf and Kuschinsky, 1993; Vorobyov, et al., 2003) and functional-magnetic resonance imaging can obtain specific receptor activation in a clinical *in vivo* setting.
- **Type 4 biomarkers** refer to physiological measures in the integral biological system, which are often controlled by homeostatic feedback mechanisms. Since dopamine is an important neurotransmitter in hypothalamic control, pituitary hormones have high potential as (translational) type 4 biomarkers for dopaminergic activity in the brain (Freeman et al., 2000).
- **Type 5 biomarkers** characterize disease processes and are particularly useful in clinical settings. An important question is whether type 5 biomarkers can be identified in animal models of disease.
- **Type 6 biomarkers** refer to clinical endpoints and lie outside the scope of this review.

Obtaining information concerning multiple types of biomarkers allows better quantification of the causal chain of events, and increases the accuracy of the model. It is however, not always necessary to obtain information on each step/type of biomarker, as the parsimony of the biological system can be applied in mechanism-based PK–PD modeling. Still, to obtain enough information from the clinical setting is extremely costly, and for clear reasons limited. This makes that we have to make use of *in vivo* animal studies and apply translational pharmacology approaches. To that end, quantitative pre-clinical PK data should be obtained in refined animal models and, for biomarkers of the effect, emphasis should be on the ones that can be measured in both animal and human.

■ Drug concentrations at the target site

As the aim is for the drug to reach its target site to be able to interact with its target, it is important to have information on target site concentrations. CSF concentrations do not provide direct information on the target site concentration of dopaminergic drugs, as dopamine receptors are facing the ECF of the brain parenchyma. Indeed many factors contribute to the distribution between CSF and the target site concentrations, indicating that CSF concentrations do not necessarily reflect brain target site concentrations (De Lange and Danhof, 2002). In many cases, brain targets are membrane receptors facing the brain ECF, or enzymes within the brain ECF. This makes information on brain ECF concentrations highly valuable (De Lange and Danhof, 2002; Watson, et al., 2009). For intracellular targets, things get more complicated. There are no means to directly obtain brain intracellular concentration-time profiles. Moreover, the intracellular space is highly heterogeneous. Total brain concentrations may provide some information, but without temporal resolution. Information on brain cell exposure by brain ECF might still be of value.

Altogether, measurement of brain ECF pharmacokinetics is anticipated to provide a better basis to describe PK–PD relations (Jeffrey and Summerfield, 2010). To this end, the intracerebral microdialysis technique is of special interest, as it offers the advantage of multiple samples collected over time from the brain ECF, without removal of fluid, therefore maintaining normal fluid pressure and physiological conditions (De Lange, et al., 1994; De Lange, et al., 1999; Chaurasia, et al., 2007). It should however be mentioned that proper quantification of microdialysate concentrations relative to brain ECF concentrations is important. The microdialysis technique has been applied to date in a few studies following intranasal administration (Souza Silva, et al., 1997; Bagger and Bechgaard, 2004; Shi, et al., 2005; Yang, et al., 2005; Souza Silva, et al., 2008).

■ Translational biomarkers on the activity of the dopaminergic system

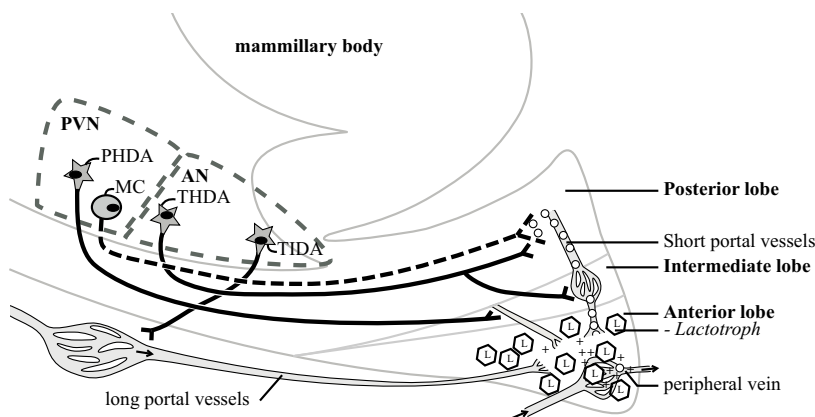
Dopamine is an important neurotransmitter in hypothalamic control of the pituitary. Therefore, pituitary hormones have a high potential as biomarker for dopaminergic activity in the brain. Of special interest are prolactin and oxytocin. These hormones are released in plasma, and blood sampling may provide information on the functioning of the dopaminergic system. As blood sampling can be performed in man and in animals, prolactin and oxytocin are of interest as translational biomarkers in investigations on (intranasal) administration of dopaminergic compounds.

- **Prolactin**

Prolactin is mainly associated with reproductive and metabolic functions. It is synthesized and stored in lactotrophs located in the anterior lobe of the pituitary. The release of prolactin is predominantly under hypothalamic inhibitory control by dopaminergic neurons.

Dopaminergic neurons project dopamine into the anterior lobe of the pituitary via several pathways (Figure 5). Activation of dopamine D2-receptors on the cell surface of lactotrophs inhibits the release of prolactin into plasma. Likewise, blockade of D2-receptors leads to release of prolactin. Besides the dopaminergic control on prolactin release, prolactin concentrations in plasma are also influenced by changes in synthesis rate, lactotroph storage capacity, homeostatic feedback mechanisms and rate of plasma elimination (Freeman, et al., 2000; Ben Jonathan and Hnasko, 2001; Fitzgerald and Dinan, 2008).

Figure 5 Neurons in the periventricular nucleus (PVN) and arcuate nucleus (AN) of the hypothalamus influence the release of prolactin (+) and oxytocin (o) by the pituitary. Prolactin release into peripheral veins by lactotrophs (L) is under inhibitory control of tuberoinfundibular (TIDA), periventricular hypothalamic (PHDA) and tuberohypothalamic (THDA) dopamine pathways. Oxytocin is released by terminals of magnocellular neurons (MC) into short portal vessels that transport oxytocin to the peripheral vein (adapted from Freeman, et al., 2000).



Interestingly, for prolactin, the synthesis, pathways of release and homeostatic feedback, and elimination half-life are similar in rats when compared to man. This makes prolactin concentrations in plasma an interesting candidate for evaluation as a translational biomarker for D2-receptor activity (Ben Jonathan, et al., 2008), in particular for dopamine receptor antagonists and possibly also partial agonists.

- **Oxytocin**

The synthesis and release of oxytocin into plasma is mainly associated with birth, lactation, parenting, sexual behavior and stress management. Oxytocin is synthesized and stored in magnocellular neurons located in the periventricular- and supraoptic nucleus of the hypothalamus. Activation of dopamine D1- but primarily dopamine D2-receptors present on the cell surface of these neurons, induces oxytocin release from the terminals located in the pituitary. Also, dopamine release from the tuberohypothalamic axons in the posterior lobe of the pituitary activate dopamine receptors on the magnocellular neurons, leading to the release of oxytocin in plasma. This makes also oxytocin an attractive biomarker for dopamine D1/D2-receptor activation. A limitation however is that the physiology of oxytocin release is much less understood than that of prolactin. Although baseline oxytocin concentrations appear to be similar in rat and man (Uckert, et al., 2003; Kramer, et al., 2004), comparative information on oxytocin synthesis, pathways of release, and feedback mechanisms in animal and man is currently lacking.

- **Clinical PK–PD models for dopaminergic action and prolactin response**

In general, the physiology of prolactin release and the discrepancies in the biological systems between animal and man (Ben Jonathan, et al., 2008) are better described for prolactin compared to oxytocin.

Several clinical PK–PD models have been published on the relationships between dopaminergic drug concentrations in plasma and prolactin concentrations in plasma, as a biomarker for dopaminergic activity, following intravenous administration. The corresponding feature of these models is a precursor pool model describing prolactin synthesis, storage in lactotrophs, release into- and elimination from plasma (Movin-Osswald and Hammarlund-Udenaes, 1995). In this first publication, a clinical PK–PD model described the drug effects of two consecutive intravenous doses of the dopamine D2/D3-antagonist remoxipride on the prolactin release (Movin-Osswald and Hammarlund-Udenaes, 1995). Since this model was less able to describe the data of subsequent clinical studies, another PK–PD model (Bagli, et al., 1999) integrated a physiological indirect-response PD/tolerance model, including putative concentrations of the agonist dopamine, following administration of the D1/D2/D3-dopamine receptor antagonist chlorprothixene. However, actual dopamine concentrations could not be obtained, hence limiting quantitation of biological system-specific parameters. More recently, circadian rhythmicity in prolactin release has also been included in the model (Friberg, et al., 2008; Ma, et al., 2010). From these studies it is clear that pro-

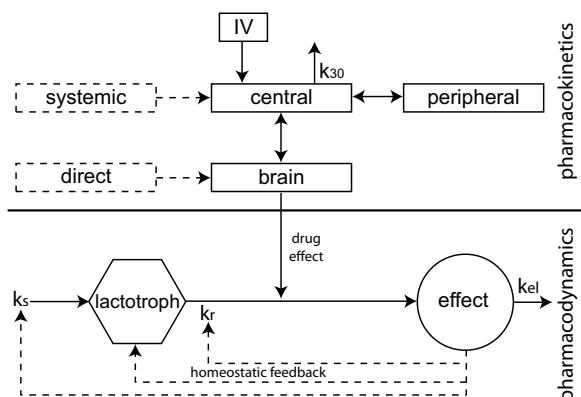
lactin release is highly regulated in the brain, and that some feedback model is required to accurately describe prolactin concentrations in plasma. However, such a feedback model remains to be optimized in a quantitative, mechanistic manner. Also, these models interconnect plasma drug concentrations to prolactinergic effects. As previously mentioned, a more mechanistic approach should be aimed at understanding the drug concentrations at the target site (brain ECF).

In animals, obtaining *in vivo* information on (part of) the seven biomarker types over time is more straightforward than in humans. Animal studies also provide the opportunity to investigate broader dosing regimens and different administration routes. Consequently, preclinical mechanism-based PK–PD models have high accuracy in quantitatively describing the drug specific- and the biological system specific characteristics that lie at the basis of drug–effect relationships and biological system responses. Challenging the model with other dopaminergic compounds provides an even stronger basis for the estimation of the biological system parameters, and should be pursued in order to validate the biological system in a proposed model structure. Figure 6 provides an example of such a mechanism-based PK–PD approach for intravenous and intranasal administration of dopamine receptor antagonists. The pharmacokinetics of the compound are described by a three compartmental approach; i) a central (plasma) compartment that describes the plasma drug concentrations over time, ii) a brain compartment, that represents the brain ECF concentrations over time, and iii) a peripheral compartment, describing the concentration-time profiles of compound in peripheral tissues. Modeling of obtained plasma- and brain ECF compound concentrations following intravenous administration provides an accurate description of the PK at the target site. When comparing intravenous and intranasal administration, pharmacokinetic modeling of brain ECF concentrations provides another unique feature. The predictive properties of mechanism-based PK–PD models that either include or exclude direct nose-to-brain transport can be compared. This would provide, for the first time, quantitative information on different intranasal absorption routes.

As the target site (brain ECF) PK is accurately described, this will also positively affect the accuracy of pharmacodynamic parameter estimates. In figure 6, the biological system of prolactin secretion is depicted as a two compartmental pool model (Movin-Osswald and Hammarlund-Udenaes, 1995). Modeling of target site PK of the compound (type 1 biomarker) and plasma concentrations of prolactin (type 4 biomarker) provides quantitative information on drug–effect relations, in which information on type 2 and 3 biomarkers can be included. Also, based on empirical approaches, direct

homeostatic feedback mechanisms that act on the prolactin secretion, can be separately and quantitatively investigated. The drug-specific- and system-specific parameters thus acquired can be used in a translational approach to predict the effect in humans.

Figure 6 An example of a structural PK-PD model (solid lines) and hypotheses that can be tested (dotted lines) in a mechanism-based PK-PD approach. Information on dose and route of absorption is provided following intravenous-(IV) or intranasal (by systemic- or direct nose-to-brain transport) administration of compound. Three compartments describe the pharmacokinetics, and the pharmacodynamics are described by synthesis (k_s), storage (lactotroph) and secretion (k_r) of prolactin into plasma (effect), and plasma elimination (k_{el}). Brain ECF concentrations (brain) induce a drug-effect via the k_r . Homeostatic biological systems effects can be investigated by feedback of prolactin plasma concentrations on k_s , storage, or k_r . k_{30} represents the elimination rate constant.



■ Link between animal and human

Quantification of drug specific- and biological system specific parameters in mechanism-based PK-PD models provides the opportunity to scale the animal PK-PD model to man. Allometric scaling of drug PK and biological system specific parameters has been used in translational investigations, with reasonable degree of success, to predict drug effects in humans (Yassen, et al., 2007; Zuideveld, et al., 2007).

Pharmacodynamic properties are more difficult to scale compared to PK properties, since parameters that establish an effect are often not related to bodyweight (e.g. receptor occupancy, transduction, maximal effect, etc.).

However, this information can be obtained by *in vitro* bioassays, and, for many drugs and endogenous compounds, clinical information is readily available in literature (e.g. target binding characteristics of dopaminergic compounds (Kvernmo, et al., 2006)). This provides the opportunity to replace the drug- and biological system parameters estimated in rat by the human values, and thus provide an extrapolation step in man. Subsequent simulation studies can provide early insight on the clinical applicability of a drug, at an early stage in drug development. Also, as the preclinical derived translational mechanism-based PK–PD model describes the drug–effect relationship and the biological system, clinical studies suffice with fewer individuals and less samples per individual, for proof of concept in man. Ultimately, simultaneous modeling of relatively large animal- and small clinical datasets, allows further investigations on critical factors of animal-to-human extrapolation in a strict quantitative manner.

CONCLUSIONS

To develop treatments with improved safety and efficacy, one of the scientific challenges is to understand the biological mechanisms underlying the PK–PD relationships of (partial-) dopamine agonists and antagonists. PK–PD modeling is the golden standard to investigate such complex mechanisms. Often, these models include plasma drug concentration–effect relationships. However, for dopaminergic compounds, the target site is the brain ECF that surrounds the dopamine receptors. Consequently, a more mechanistic approach should be aimed at understanding the drug concentrations at the target site.

A second challenge is to achieve a more rapid onset of action and/or increased therapeutic window for dopaminergic compounds that have high clearance and/or low oral bioavailability characteristics. Intranasal administration of dopaminergic compounds avoids gastrointestinal- and hepatic first-pass elimination and is hypothesized to circumvent the BBB by direct nose–to–brain transport. This administration route is therefore anticipated to improve the time to onset- and/or the selectivity of action, specifically for drugs acting on the CNS.

To study (intranasal) administration of dopaminergic compounds, more advanced animal models are required that preferably; i) make use of freely moving animals under minimum stress conditions, ii) allow measurement of PK and PD parameters in serially obtained plasma- and brain ECF samples, and iii) allow intranasal and, for comparison, intravenous administration within the same individual. PK modeling of thus acquired rich datasets would allow

quantification of PK parameters in plasma and brain ECF following intranasal and intravenous administration. Such an approach has high potential to identify direct nose-to-brain transport in a quantitative manner.

Several clinical PK–PD models have been published on the relationships between dopaminergic drug- and prolactin concentrations, as a biomarker for dopaminergic activity, following intravenous administration. From these studies it is clear that prolactin release is highly regulated in the brain, and that some homeostatic feedback model is required to accurately describe prolactin concentrations in plasma. As measurement at the target site is easier in animal studies, preclinical models allow for more mechanistic PK–PD approaches and can hence contribute to more accurate identification of drug-specific and biological system-specific parameters (including homeostatic feedback). This approach would allow for confirmation of potential improved onset- and/or selectivity of action following intranasal administration of dopaminergic drugs.

An important feature of mechanism-based PK–PD models is the strict distinction between drug-specific and biological system-specific parameters to describe *in vivo* drug responses. This is important since pertinent information on differences in biological system parameters enables the prediction of drug effects in biological systems other than the system in which the model has been developed. Consequently, translational modeling and simulation can be applied to quantitatively predict the time course of effect in man. Ultimately, preclinical derived mechanistic PK–PD models can provide the scientific basis for the translational pharmacology of dopaminergic drugs after intravenous and intranasal administration in humans.

REFERENCES

- Ankenman R and Salvatore MF (2007) Low Dose Alpha-Methyl-Para-Tyrosine (AMPT) in the Treatment of Dystonia and Dyskinesia. *J Neuropsychiatry Clin Neurosci* **19**:65-69.
- Bagger M and Bechgaard E (2004) A microdialysis model to examine nasal drug delivery and olfactory absorption in rats using lidocaine hydrochloride as a model drug. *Int J Pharm* **269**:311-322.
- Bagli M, Suverkrup R, Quadflieg R, Hoflich G, Kasper S, Moller HJ, Langer M, Barlage U and Rao ML (1999) Pharmacokinetic-pharmacodynamic modeling of tolerance to the prolactin-secreting effect of chlorprothixene after different modes of drug administration. *J Pharmacol Exp Ther* **291**:547-554.
- Baskerville TA and Douglas AJ (2008) Interactions between dopamine and oxytocin in the control of sexual behavior. *Progress in Brain Research* **170**: 277-290.
- Ben Jonathan N and Hnasko R (2001) Dopamine as a Prolactin (PRL) Inhibitor. *Endocrin Rev* **22**:724-763.
- Ben Jonathan N, LaPensee CR and LaPensee EW (2008) What Can We Learn from Rodents about Prolactin in Humans? *Endocrin Rev* **29**:1-41.
- Benedetti MS, Whomsley R, Poggesi I, Cawello W, Mathy FX, Delporte ML, Papeleu P, Wa-telet JB (2009) Drug metabolism and pharmacokinetics. *Drug Metab Rev.* **41**(3):344-90.
- Bilder RM, Volavka J, Lachman HM and Grace AA (2004) The catechol-O-methyltransferase polymorphism: relations to the tonic-phasic dopamine hypothesis and neuropsychiatric phenotypes. *Neuropsychopharmacol* **29**:1943-1961.
- Blin O. (2003) The pharmacokinetics of pergolide in Parkinson's disease. *Curr Opin Neurol.* **16** Suppl 1:S9-12.
- Carlson NR (2001) Physiology of behaviour. Allyn and Bacon, Needham Heights.
- Caslake R, Macleod A, Ives N, Stowe R and Counsell C (2009) Monoamine oxidase B inhibitors versus other dopaminergic agents in early Parkinson's disease. *Cochrane Database of Systematic Reviews* **4** Art No. CD006661.
- Chaurasia CS, Muller M, Bashaw ED, Benfeldt E, Bolinder J, Bullock R, Bungay PM, De Lange ECM, Derendorf H, Elmquist WF, Hammarlund-Udenaes M, Joukhadar C, Kellogg DL, Jr., Lunte CE, Nordstrom CH, Rollema H, Sawchuk RJ, Cheung BWY, Shah VP, Stahle L, Ungerstedt U, Welty DF and Yeo H (2007) AAPS-FDA Workshop White Paper: Microdialysis Principles, Application, and Regulatory Perspectives. *J Clin Pharmacol* **47**:589-603.
- Chemuturi NV, Haraldsson JE, Prisinzano T and Donovan M (2006) Role of dopamine transporter (DAT) in dopamine transport across the nasal mucosa. *Life Sci* **79**:1391-1398.
- Chen N and Reith ME (2000) Structure and function of the dopamine transporter. *Eur J Pharmacol* **405**:329-339.
- Coda BA, Rudy AC, Archer SM, and Wermeling DP. (2003) Pharmacokinetics and bioavailability of single-dose intranasal hydromorphone hydrochloride in healthy volunteers. *Anesth Analg.* **97**:117-123.
- Contin M, Riva R, Albani F, Baruzzi A. (2000) Pharmacokinetic optimisation of dopamine receptor agonist therapy for Parkinson's disease. *CNS Drugs* **14**:439-455
- Costantino HR, Illum L, Brandt G, Johnson PH and Quay SC (2007) Intranasal delivery: physicochemical and therapeutic aspects. *Int J Pharm* **337**:1-24.
- Dahlin M, Bergman U, Jansson B, Bjork E and Brittebo E (2000) Transfer of dopamine in the olfactory pathway following nasal administration in mice. *Pharm Res* **17**:737-742.
- Danhof M, Alvan G, Dahl SG, Kuhlmann J and Paintaud G (2005) Mechanism-based pharmacokinetic-pharmacodynamic modeling-a new classification of biomarkers. *Pharm Res* **22**:1432-1437.
- Danhof M, De Jongh J, De Lange EC, Della Pasqua OE, Ploeger BA and Voskuyl RA (2007) Mechanism-based pharmacokinetic-pharmacodynamic modeling: biophase distribution, receptor theory, and dynamical systems analysis. *Annu Rev Pharmacol Toxicol* **47**:357-400.
- Danhof M, De Lange EC, Della Pasqua OE, Ploeger BA and Voskuyl RA (2008) Mechanism-based pharmacokinetic-pharmacodynamic (PK-PD) modeling in translational drug research. *Trends Pharmacol Sci* **29**:186-191.

- Dauer W and Przedborski S (2003) Parkinson's Disease: Mechanisms and Models. *Neuron* **39**:889-909.
- De Lange EC and Danhof M (2002) Considerations in the use of cerebrospinal fluid pharmacokinetics to predict brain target concentrations in the clinical setting: implications of the barriers between blood and brain. *Clin Pharmacokinet* **41**:691-703.211-227.
- De Lange EC, Danhof M, De Boer AG and Breimer DD (1994) Critical factors of intracerebral microdialysis as a technique to determine the pharmacokinetics of drugs in rat brain. *Brain Res* **666**:1-8.
- De Lange EC, De Boer BA and Breimer DD (1999) Microdialysis for pharmacokinetic analysis of drug transport to the brain. *Adv Drug Deliv Rev* **36**:211-227.
- De Lange EC, Ravenstijn PGM, Groenendaal D, and Van Steeg TS (2005) Toward the Prediction of CNS Drug Effect Profiles in Physiological and Pathological Conditions Using Microdialysis and Mechanism-Based Pharmacokinetic-Pharmacodynamic Modeling. *AAPS Journal* **7**(3) article 54.
- De Souza Silva MA, Mattern C, Häcker R, Nogueira PJ, Huston JP, Schwarting RK (1997) Intranasal administration of the dopaminergic agonists L-DOPA, amphetamine, and cocaine increases dopamine activity in the neostriatum: a microdialysis study in the rat. *J Neurochem*. **68**:233-9.
- Defagot MC, Malchiodi EL, Villar MJ and Antonelli MC (1997) Distribution of D4 dopamine receptor in rat brain with sequence-specific antibodies. *Brain Res Mol Brain Res* **45**:1-12.
- Degim IT, Acartürk F, Erdogan D, Demirez Lortlar N (2003) Transdermal administration of bromocriptine. *Biol Pharm Bull*. **26**:501-5.
- Del Dotto P, Bonuccelli U (2003) Clinical pharmacokinetics of cabergoline. *Clin Pharmacokinet*. **42**:633-45.
- Deleu D, Northway MG and Hanssens Y (2002) Clinical pharmacokinetic and pharmacodynamic properties of drugs used in the treatment of Parkinson's disease. *Clin Pharmacokinet* **41**:261-309.
- Deleu D, Northway MG, Hanssens Y (2002) Clinical pharmacokinetic and pharmacodynamic properties of drugs used in the treatment of Parkinson's disease. *Clin Pharmacokinet*. **41**:261-309.
- Dhuria SV, Hanson LR and Frey WH (2009) Intranasal delivery to the central nervous system: Mechanisms and experimental considerations. *J Pharm Sci* **99**:1654-1673.
- El Ela AA, Härtter S, Schmitt U, Hiemke C, Spahn-Langguth H, Langguth P (2004) Identification of P-glycoprotein substrates and inhibitors among psychoactive compounds—implications for pharmacokinetics of selected substrates. *J Pharm Pharmacol*. **56**:967-75.
- Eon S, Durham J (2009) Schizophrenia: A Review of Pharmacologic and Nonpharmacologic Treatments. *US Pharm*. **34**:HS-2-HS-9.
- Fisher A.N., Brown K., Davis S.S., Parr G., Smith D. (1987) The effect of molecular size on the nasal absorption of water-soluble compounds in the albino rat. *J Pharmacy and Pharmacol* **39**:357-362.
- Fitzgerald P and Dinan TG (2008) Prolactin and dopamine: What is the connection? A Review Article. *J Psychopharmacol*, **22**(Suppl):12-9.
- Freeman ME, Kanyicska B, Lerant A and Nagy G (2000) Prolactin: structure, function, and regulation of secretion. *Physiol Rev* **80**:1523-1631.
- Friberg LE, Vermeulen AM, Petersson KJF and Karlsson MO (2008) An Agonist-Antagonist Interaction Model for Prolactin Release Following Risperidone and Paliperidone Treatment. *Clin Pharmacol Ther* **85**:409-417.
- Gabrielsson J and Green AR (2009) Quantitative Pharmacology or Pharmacokinetic Pharmacodynamic Integration Should Be a Vital Component in Integrative Pharmacology. *J Pharmacol Exp Ther* **331**:767-774.
- Giuliano F and Allard J (2001) Dopamine and sexual function. *Int J Impot Res* **13 Suppl 3**:S18-S28.
- Goodwin JS, Larson GA, Swant J, Sen N, Javitch JA, Zahniser NR, De Felice LJ and Khoshbouei H (2009) Amphetamine and Methamphetamine Differentially Affect Dopamine Transporters in Vitro and in Vivo. *J Biol Chem* **284**:2978-2989.

- Graff CL, Pollack GM (2003) P-Glycoprotein attenuates brain uptake of substrates after nasal instillation. *Pharm Res* **20**:1225-30.
- Gross EA, Swenberg JA, Fields S and Popp JA (1982) Comparative morphometry of the nasal cavity in rats and mice. *J Anat* **135**:83-88.
- Ikeda K, Murata K, Kobayashi M and Noda K (1992) Enhancement of bioavailability of dopamine via nasal route in beagle dogs. *Chem Pharm Bull (Tokyo)* **40**:2155-2158.
- Illum L (2000) Transport of drugs from the nasal cavity to the central nervous system. *Eur J Pharm Sci* **11**:1-18.
- Illum L (2004) Is nose-to-brain transport of drugs in man a reality? *J Pharm Pharmacol* **56**:3-17.
- Jeffrey P and Summerfield S (2010) Assessment of the blood-brain barrier in CNS drug discovery. *Neurobiol Dis* **37**:33-37.
- Jones N (2001) The nose and paranasal sinuses physiology and anatomy. *Adv Drug Deliv Rev* **51**:5-19.
- Kaakkola S and Wurtman RJ (1992) Effects of COMT inhibitors on striatal dopamine metabolism: a microdialysis study. *Brain Res* **587**:241-249.
- Kandel ER, Schwartz JH and Jessell TM (2000) Principles of neural science. McGraw-Hill Companies.
- Kapoor R, Turjanski N, Frankel J, Kleedorfer B, Lees A, Stern G, Bovington M and Webster R (1990) Intranasal apomorphine: a new treatment in Parkinson's disease. *J Neurol Neurosurg Psychiatry* **53**:1015.
- Kapur S, Zipursky R, Jones C, Remington G and Houle S (2000) Relationship Between Dopamine D2 Occupancy, Clinical Response, and Side Effects: A Double-Blind PET Study of First-Episode Schizophrenia. *Am J Psychiatry* **157**:514-520.
- Kendirci M and Hellstrom WJ (2004) Intranasal apomorphine. Nastech Pharmaceutical. *IDrugs* **7**:483-488.
- Khan ZU, Gutierrez A, Martin R, Penafiel A, Rivera A and de la CA (2000) Dopamine D5 receptors of rat and human brain. *Neurosci* **100**:689-699.
- Kim TK, Kang W, Chun IK, Oh SY, Lee YH, Gwak HS (2009) Pharmacokinetic evaluation and modeling of formulated levodopa intranasal delivery systems. *Eur J Pharm Sci* **38**:525-32.
- Kleedorfer B, Turjanski N, Ryan R, Lees AJ, Milroy C and Stern GM (1991) Intranasal apomorphine in Parkinson's disease. *Neurol* **41**:761-762.
- Kramer KM, Cushing BS, Carter CS, Wu J and Ottinger M (2004) Sex and species differences in plasma oxytocin using an enzyme immunoassay. *Can J Zool* **82**:1194-1200.
- Kropf W and Kuschinsky K (1993) Effects of stimulation of dopamine D1 receptors on the cortical EEG in rats: different influences by a blockade of D2 receptors and by an activation of putative dopamine autoreceptors. *Neuropharmacol* **32**:493-500.
- Kruger TH, Hartmann U and Schedlowski M (2005) Prolactinergic and dopaminergic mechanisms underlying sexual arousal and orgasm in humans. *World J Urol* **23**:130-138.
- Kublik H and Vidgren MT (1998) Nasal delivery systems and their effect on deposition and absorption. *Adv Drug Deliv Rev* **29**:157-177.
- Kvernmo T, Hartter S and Burger E (2006) A review of the receptor-binding and pharmacokinetic properties of dopamine agonists. *Clin Therapeutics* **28**:1065-1078.
- Kvernmo T, Houben J, Sylte I (2008) Receptor-binding and pharmacokinetic properties of dopaminergic agonists. *Curr Top Med Chem* **8**:1049-67.
- Lieberman JA (2004) Dopamine Partial Agonists: A New Class of Antipsychotic. *CNS Drugs* **18**:251-267.
- Ma G, Friberg LE, Movin-Osswald G, and Karlsson M (2010) Comparison of the agonist-antagonist interaction model and the pool model for the effect of remoxipride on prolactin. *Br J Clin Pharmacol* **70**:815-824.
- Mahmood I (1997) Clinical pharmacokinetics and pharmacodynamics of selegiline. An update. *Clin Pharmacokinet* **33**:91-102.
- Marsden CA (2006) Dopamine: the rewarding years. *Br J Pharmacol* **147**:S136-S144.

- Mathison S., Nagilla R., Kompella U.B. (1998) Nasal route for direct delivery of solutes to the central nervous system: fact or fiction? *J Drug Target* **5**: 415-441.
- McMartin C., Hurchinson L.E.F., Hyde R., Peters G.E. (1987) Analysis of structure requirements for the absorption of drugs and macromolecules from the nasal cavity. *J Pharm Sci* **76**:535-540.
- Meco G, Rubino A, Caravona N and Valente M (2008) Sexual dysfunction in Parkinson's disease. *Parkinsonism Relat Disord* **14**:451-456.
- Menon R, Stacy M (2007) Apomorphine in the treatment of Parkinson's disease. *Expert Opin Pharmacother*. **8**:1941-50.
- Minn A, Leclerc S, Heydel JM, Minn AL, Denizcot C, Cattarelli M, Netter P and Gradinaru D (2002) Drug transport into the mammalian brain: the nasal pathway and its specific metabolic barrier. *J Drug Target* **10**:285-296.
- Minn AL, Pelczar H, Denizot C, Martinet M, Heydel JM, Walther B, Minn A, Goudonnet H, Artur Y (2005) Characterization of microsomal cytochrome P450-dependent monooxygenases in the rat olfactory mucosa. *Drug Metab Dispos*. **33**:1229-37.
- Missale C, Nash SR, Robinson SW, Jaber M and Caron MG (1998) Dopamine receptors: from structure to function. *Physiol Rev* **78**:189-225.
- Miyamoto S, Duncan GE, Marx CE and Lieberman JA (2005) Treatments for schizophrenia: a critical review of pharmacology and mechanisms of action of antipsychotic drugs. *Mol Psychiatry* **10**:79-104.
- Montastruc JL, Rascol O, Senard JM, Houin G, Rascol A (1995) Sublingual apomorphine: a new pharmacological approach in Parkinson's disease? *J Neural Transm Suppl*. **45**:157-61.
- Morrison E.E., Costanzo R.M. (1992) Morphology of the human olfactory epithelium. *J Comp Neurol* **297**: 1-13.
- Movin-Osswald G and Hammarlund-Udenaes M (1995) Prolactin release after remoxipride by an integrated pharmacokinetic-pharmacodynamic model with intra- and interindividual aspects. *J Pharmacol Exp Ther* **274**:921-927.
- Neef C and van Laar T (1999) Pharmacokinetic-pharmacodynamic relationships of apomorphine in patients with Parkinson's disease. *Clin Pharmacokinet* **37**:257-271.
- Nyholm D (2006) Pharmacokinetic optimisation in the treatment of Parkinson's disease: an update. *Clin Pharmacokinet* **45**:109-36.
- Ohlsen RI and Pilowsky LS (2005) The place of partial agonism in psychiatry: recent developments. *J Psychopharmacol* **19**:408-413.
- Okura T, Ito R, Ishiguro N, Tamai I, and Deguchi Y (2007) Blood-brain barrier transport of pramipexole, a dopamine D2 agonist. *Life Sci* **80**:1564-71.
- Peter D, Liu Y, Sternini C, de Giorgio R, Brecha N and Edwards RH (1995) Differential expression of two vesicular monoamine transporters. *J Neurosci* **15**:6179-6188.
- Pfaus JG (2009) Pathways of sexual desire. *J Sex Med* **6**:1506-1533.
- Pires A, Fortuna A, Alves G and Falcao A (2009) Intranasal drug delivery: how, why and what for? *J Pharm Pharm Sci* **12**:288-311.
- Ploeger BA and Holford NHG (2009) Washout and delayed start designs for identifying disease modifying effects in slowly progressive diseases using disease progression analysis. *Pharmaceut Statist* **8**:225-238.
- Ploeger BA, van der Graaf PH and Danhof M (2009) Incorporating receptor theory in mechanism-based pharmacokinetic-pharmacodynamic (PK-PD) modeling. *Drug Metab Pharmacokinet* **24**:3-15.
- Ross TM, Martinez PM, Renner JC, Thorne RG, Hanson LR and Frey WH (2004) Intranasal administration of interferon beta bypasses the blood-brain barrier to target the central nervous system and cervical lymph nodes: a non-invasive treatment strategy for multiple sclerosis. *J Neuroimmunol* **151**:66-77.
- Sakane T, Akizuki M, Yamashita S, Nadai T, Hashida M, Sekazi H (1991) The transport of a drug to the cerebrospinal fluid directly from the nasal cavity: The relation to the lipophilicity of the drug. *Chem Pharm Bull Tokyo* **39**:2456-2458.

- Sakane T., Akizuki M., Yamashita S., Sekazi H., Nadai T. (1994) Direct transport from the rat nasal cavity to the cerebrospinal fluid: The relation to the dissociation of the drug. *J Pharm and Pharmacol* **46**:378-379.
- Savitt JM, Dawson VL and Dawson TM (2006) Diagnosis and treatment of Parkinson disease: molecules to medicine. *J Clin Invest* **116**:1744-1754.
- Schmitt KC and Reith MEA (2010) Regulation of the dopamine transporter. *Ann NY Acad Sci* **1187**:316-340.
- Seeman P (2010) Dopamine D2 receptors as treatment targets in schizophrenia. *Clin Schizophr Relat Psychoses* **4**:56-73.
- Shi Z, Zhang Q and Jiang X (2005) Pharmacokinetic behavior in plasma, cerebrospinal fluid and cerebral cortex after intranasal administration of hydrochloride meptazinol. *Life Sci* **77**:2574-2583.
- Souza Silva MA, Mattern C, Hacker R, Nogueira PJ, Huston JP and Schwarting RK (1997) Intranasal administration of the dopaminergic agonists L-DOPA, amphetamine, and cocaine increases dopamine activity in the neostriatum: a microdialysis study in the rat. *J Neurochem* **68**:233-239.
- Souza Silva MA, Topic B, Huston JP and Mattern C (2008) Intranasal dopamine application increases dopaminergic activity in the neostriatum and nucleus accumbens and enhances motor activity in the open field. *Synapse* **62**:176-184.
- Stevens J, Suidgeest E, van der Graaf PH, Danhof M and de Lange EC (2009) A new minimal-stress freely-moving rat model for preclinical studies on intranasal administration of CNS drugs. *Pharm Res* **26**:1911-1917.
- Studd J, Pornel B, Marton I, Bringer J, Varin C, Tsouderos Y, and Christiansen C (1999) Efficacy and acceptability of intranasal 17 beta-oestradiol for menopausal symptoms: randomised dose-response study. Aerodiol Study Group. *Lancet* **353**:1574-1578.
- Thorne RG, Hanson LR, Ross TM, Tung D and Frey WH (2008) Delivery of interferon-beta to the monkey nervous system following intranasal administration. *Neurosci* **152**:785-797.
- Uckert S, Becker A, Ness B, Stief C, Scheller F, Knapp W and Jonas U (2003) Oxytocin plasma levels in the systemic and cavernous blood of healthy males during different penile conditions. *World J Urol* **20**:323-326.
- Ugwoke MI, Exaud S, Van Den MG, Verbeke N and Kinget R (1999) Bioavailability of apomorphine following intranasal administration of mucoadhesive drug delivery systems in rabbits. *Eur J Pharm Sci* **9**:213-219.
- Van Bree JB, Baljet AV, van Geyt A, de Boer AG, Danhof M and Breimer DD (1989) The unit impulse response procedure for the pharmacokinetic evaluation of drug entry into the central nervous system. *J Pharmacokinet Biopharm* **17**:441-462.
- Van den Berg MP, Romeijn SG, Verhoef JC and Merkus FW (2002) Serial cerebrospinal fluid sampling in a rat model to study drug uptake from the nasal cavity. *J Neurosci Methods* **116**:99-107.
- Van den Berg MP. Uptake of fluorescein isothiocyanate-labelled dextran into the CSF after nasal and intravenous administration to rats. 2005. PHD-thesis.
- Van Laar T, Jansen EN, Essink AW and Neef C (1992) Intranasal apomorphine in parkinsonian on-off fluctuations. *Arch Neurol* **49**:482-484.
- Vorobyov VV, Schibaev NV, Morelli M and Carta AR (2003) EEG modifications in the cortex and striatum after dopaminergic priming in the 6-hydroxydopamine rat model of Parkinson's disease. *Brain Res* **972**:177-185.
- Vyas T.K., Salphati I., Benet L.Z. (2005) Intranasal drug delivery for brain targeting. *Current Drug Delivery* **2**: 165-175.
- Wang JS, Ruan Y, Taylor RM, Donovan JL, Markowitz JS, DeVane CL (2004b) The brain entry of risperidone and 9-hydroxyrisperidone is greatly limited by P-glycoprotein. *Int J Neuropsychopharmacol.* **7**:415-9.
- Wang JS, Taylor R, Ruan Y, Donovan JL, Markowitz JS, Lindsay De Vane C (2004a) Olanzapine penetration into brain is greater in transgenic Abcb1a P-glycoprotein-deficient mice than FVB1 (wild-type) animals. *Neuropsychopharmacol.* **29**:551-7.

- Watson J, Wright S, Lucas A, Clarke KL, Viggers J, Cheetham S, Jeffrey P, Porter R and Read KD (2009) Receptor occupancy and brain free fraction. *Drug Metab Dispos* **37**:753-760.
- Wei G, Wang D, Lu H, Parmentier S, Wang Q, Scott S, Panter SS, Frey WH, Ying W. (2007) Intranasal administration of a PARG inhibitor profoundly decreases ischemic brain injury. *Front Biosci* **12**: 4986-4996.
- Yamamoto M and Schapira AH (2008) Dopamine agonists in Parkinson's disease. *Expert Rev Neurother* **8**:671-677.
- Yang Z, Huang Y, Gan G and Sawchuk RJ (2005) Microdialysis evaluation of the brain distribution of stavudine following intranasal and intravenous administration to rats. *J Pharm Sci* **94**:1577-1588.
- Yassen A, Olofsen E, Kan J, Dahan A and Danhof M (2007) Animal-to-human extrapolation of the pharmacokinetic and pharmacodynamic properties of buprenorphine. *Clin Pharmacokinet* **46**:433-447.
- Ying W., et al. (2007) Intranasal administration with NAD⁺ profoundly decreases brain injury in a rat model of transient focal ischemia. *Front Biosci* **12**: 2728-2734.
- Zhang X, Zhang QY, Liu D, Su T, Weng Y, Ling G, Chen Y, Gu J, Schilling B, Ding X (2005) Expression of cytochrome p450 and other biotransformation genes in fetal and adult human nasal mucosa. *Drug Metab Dispos.* **33**:1423-1428.
- Zhu HJ, Wang JS, DeVane CL, Williard RL, Donovan JL, Middaugh LD, Gibson BB, Patrick KS, Markowitz JS (2006) The role of the polymorphic efflux transporter P-glycoprotein on the brain accumulation of d-methylphenidate and d-amphetamine. *Drug Metab Dispos.* **34**:1116-1121.
- Zuideveld KP, van der Graaf PH, Peletier LA and Danhof M (2007) Allometric scaling of pharmacodynamic responses: application to 5-Ht_{1A} receptor mediated responses from rat to man. *Pharm Res* **24**:2031-2039.

A new minimal-stress freely-moving rat model for preclinical studies on intranasal administration of CNS drugs *Pharm Res* (2009) 26:1911-1917

J. Stevens¹, E. Suidgeest¹, P. H. van der Graaf², M. Danhof¹,
E. C. M. de Lange¹.

¹ Division of Pharmacology, LACDR, Leiden University, Leiden,
The Netherlands.

² Pfizer, Pharmacometrics/Global Clinical Pharmacology, Sandwich, Kent,
England.

ABSTRACT

Purpose. To develop a new minimal-stress model for intranasal administration in freely moving rats and to evaluate in this model the brain distribution of acetaminophen following intranasal versus intravenous administration.

Methods. Male Wistar rats received one intranasal cannula, an intracerebral microdialysis probe, and two blood cannulas for drug administration and serial blood sampling respectively. To evaluate this novel model, the following experiments were conducted; 1) Evans Blue was administered to verify the selectivity of intranasal exposure. 2) During a 1 minute infusion 10, 20, or 40 µl saline was administered intranasally or 250 µl intravenously. Corticosterone plasma concentrations over time were compared as biomarkers for stress. 3) 200 µg of the model drug acetaminophen was given in identical setup and plasma, and brain pharmacokinetics were determined.

Results. In 96% of the rats, only the targeted nasal cavity was deeply colored. Corticosterone plasma concentrations were not influenced, neither by route nor volume of administration. Pharmacokinetics of acetaminophen were identical after intravenous and intranasal administration, although the C_{max} in microdialysates was reached a little earlier following intravenous administration.

Conclusion. A new minimal-stress model for intranasal administration in freely moving rats has been successfully developed and allows direct comparison with intravenous administration.

INTRODUCTION

Targeting the central nervous system (CNS) by intranasal delivery is a promising alternative for oral or parenteral administration, and is investigated to directly target the brain, thereby increasing CNS target site bioavailability and the efficacy of CNS drugs (American Academy of Pediatrics: Committee on Drugs, 1997; Graff and Pollack, 2005a; Jansson and Bjork, 2002). Little is known however on the distribution of CNS drugs into the target site, i.e. the extracellular fluid (ECF) surrounding the pharmacologic receptors in brain tissue, following intranasal administration.

Current pharmacokinetic-pharmacodynamic (PK–PD) studies after intranasal administration in small laboratory animals are performed with anesthetized animals, whether or not in combination with complete isolation of the nasal cavity and a cannulated trachea to aid breathing (Veronesi, et al., 2007; Dahlin, et al., 2001; Dufes, et al., 2003; Van den Berg, et al., 2004). Other research is based upon restrained animals (Shi, et al., 2005). All methods currently used have major influence on physiology (i.e. blood flow, nasal immunology, mucociliary clearance, nasal cycle, airflow dynamics, and stress), which all play important roles in the PK and/or PD of compounds (Raphael, et al., 1996b; Schipper, et al., 1991; Selwyn, et al., 1996; Raphael, et al., 1996a; Raphael and Butt, 1997; Schindler, et al., 1996; Lennox, et al., 1996; Sapolsky, et al., 2000; Ugwoke, et al., 2001). Therefore, this methodology complicates quantification of PK–PD endpoints and consequently the extrapolation to the *in vivo* human situation.

To meet the demands for animal PK/biomarker models and nasal administration techniques, which allow better interpretation and translation of PK–PD parameters from animal to man, a new animal model is needed that allows drug administration under minimal stress conditions in freely moving animals.

The objective of this study was to develop and validate a new preclinical, refined minimal stress animal model, in which we can administer compounds intranasally and intravenously, while blood- and brain ECF samples can be taken over time, to obtain PK–PD parameters in plasma and brain of freely moving animals. After comparing the size of nasal cavities, the highly vascular olfactory epithelium ratios, and cost-considerations of eight different species, as described by Ugwoke *et al.*, (Ugwoke, et al., 2001), we focused on the rat as animal of choice. An intranasal cannula was manufactured and implanted together with an intracerebral microdialysis probe. Also, the animals received two blood cannulas for drug administration and serial blood

sampling respectively. The intranasal site of administration needed to be substantiated by a staining study. Through corticosterone measurements and comparison with literature, any stress effects during our experimental- and administration techniques had to be excluded (Cano, et al., 2008). Then, our model had to be validated, which was done by the administration of a model compound and comparing the pharmacokinetics between the groups. Acetaminophen was used for its linear plasma and blood-brain barrier (BBB) transport kinetics (De Lange, et al., 1994; Schaiquevich, et al., 2004; Kandimalla and Donovan, 2005; Graff and Pollack, 2005b; Van Bree, et al., 1989). P-glycoprotein (P-gp) efflux did not have to be considered since acetaminophen is no P-gp substrate (Schaiquevich, et al., 2004; Kandimalla and Donovan, 2005; Graff and Pollack, 2005b). To explain concentration-time profiles and include both intraindividual and interindividual variability, pharmacokinetic modeling was used to calculate population parameter estimates of blood- and brain PK.

MATERIALS AND METHODS

■ Surgery and Methods

All animal procedures were performed in accordance with Dutch laws on animal experimentation. The study protocol was approved by the Animal Ethics Committee of Leiden University (UDEC nr. 6023 and 6132). Male Wistar WU rats (245 ± 18 g, Charles River, The Netherlands), $n = 89$, were housed in groups for 7–13 days (Animal Facilities, Gorlaeus Laboratoria, Leiden, The Netherlands), under standard environmental conditions (ambient temperature 21°C; humidity 60%; 12/12 h light, background noise, daily handled), with *ad libitum* access to food (Laboratory chow, Hope Farms, Woerden, The Netherlands) and acidified water. Between surgery and experiments, the animals were kept individually in Makrolon type three cages for 7 days to recover from the surgical procedures.

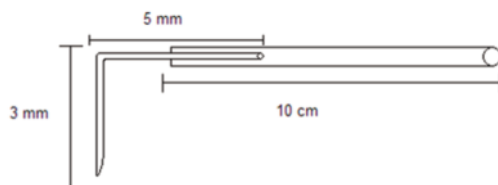
All surgical procedures were performed under complete anesthesia with subcutaneous administration of 0.1 ml/100 g Ketanest (ketamine base 25 mg/ml, Pfizer B.V., Capelle a/d IJssel, The Netherlands), and 0.01–0.017 ml/100 g Domitor (medetomidine hydrochloride 1 mg/ml, Pfizer Animal Health B.V. Capelle a/d IJssel, The Netherlands). Body temperature was maintained at 37°C by an electric heating pad. All cannulas were disinfected with 0.1% benzalkoniumchloride.

The animals were chronically instrumented with a CMA/ 12 microdialysis guide (Aurora Borealis Control, Schoonebeek, The Netherlands) in the olfactory bulb. The guide was inserted at 53° from the dorsoventral axis (towards posterior) parallel to the sagittal plane, at the coordinates AP –2.5 mm,

L -0.9 mm, V -6.4 mm from bregma. The intranasal probe was manufactured (Figure 1) by bending the sawn off tip of a 27 gauge needle (90°) and glueing the blunt end to 10 cm tubing (Portex Fine Bore polythene tubing, Smiths Industries, Kent, England). With a 1.0 mm drill, a hole was drilled through the nasal bone (AP 12 mm and L -0.5 mm), the metal tip was pressed into the hole and attached with histo-acryl (B. Braun Medical B.V., Oss, The Netherlands). The nasal cannula was tunneled subcutaneously to the back of the head. The end was melted shut to prevent infection. Consequently, the animals received two cannulas. To obtain blood samples, 3 cm of ID 0.28 mm cannula (SIMS Portex LTD, England) was inserted in the femoral artery, connected to 16 cm x 0.58 mm internal diameter (ID) cannula (Portex Fine Bore polythene tubing Smiths Industries, Kent, England). For drug administration, 4 cm of ID 0.58 mm cannula was inserted in the femoral vein, and 16 cm of ID 0.58 mm cannula was, similar to the sampling cannula, led subcutaneously to the back of the head where it was fixated with a rubber ring. After the surgery the animals received 0.03 ml Temgesic® intramuscular (Schering-Plough, The Netherlands) and 0.3 ml Ampicillin® (Alfasan B.V. Woerden) subcutaneously. After 6 days the guide was replaced by the microdialysis probe (CMA/12, 4 mm Polycarbonate membrane, cut-off 20 kD) at a pre-experiment interval of 24 ± 1 h.

Figure 1 Schematic representation of the intranasal cannula.

The 0.28 mm internal diameter, and 0.61 mm outer diameter tubing is glued to the bended (90°), sawn off tip of a 27 gauge needle.



In the corticosterone study, a control group of seven rats received 500 μ l intravenously administered saline (B. Braun Melsungen AG, Melsungen, Germany) during a 1 minute infusion with an automated pump (Harvard apparatus 22, model 55-2222, Holliston, MA, USA). The experimental groups received 10, 20, or 40 μ l of saline intranasally ($n = 8, 10$, and 9 respectively). Blood samples of 200 μ l were taken from the arterial cannula at $t = 0$ (blank), 5, 10, 20, 35, 60, 90, 120, 150, and 180 min, shaken in heparin (10 IE) coated eppendorf cups (Sarstedt, Nümbrecht, Germany), and tempo-

rarily stored on ice. After the experiment the samples were centrifuged for 15 minutes at 5000 rpm and stored at -20°C .

Using the aforementioned automated pump, in the acetaminophen study the control group received a dose of 200 μg acetaminophen (Leiden University Medical Center Pharmacy, Leiden, The Netherlands) in 250 μl saline intravenously in 30 seconds. In the experimental groups, 200 μg acetaminophen in 20, 30, or 40 μl saline was administered intranasally during a 1 minute infusion. Start and duration of infusion was corrected for internal volume of the tubing so that infusion started at $t = 0$ min. Blood samples of 200 μl were taken from the arterial cannula at $t = 0$ (blank), 5, 10, 20, 35, 60, 90, 120, 150, and 180 minutes, and temporarily stored in heparin (10 IE) coated eppendorf cups on ice.

After the experiment the samples were centrifuged for 15 minutes at 5000 rpm and stored at -20°C .

Microdialysis perfusion fluid (PF) was prepared (Moghaddam and Bunney, 1989), consisting of phosphate buffer (2 mM, pH 7.4), containing 145 mM sodium, 2.7 mM potassium, 1.2 mM calcium, 1.0 mM magnesium, 150 mM chloride, and 0.2 mM ascorbate, which was filtered, stored in glass vials (-20°C), and sonified before use. Tubing (1.2 $\mu\text{l}/100$ mm FEP-tubing CMA/Microdialysis AB, Stockholm, Sweden) was connected with tubing adapters (CMA/Microdialysis, Stockholm, Sweden) to the microdialysis probe's inlet and outlet. Microdialysis vials were preweighed and placed in a cooled fraction collector (Univentor 820 Microsampler, Antec, Netherlands) to collect the microdialysate samples. Microdialysis probes were continuously flushed with PF (2 $\mu\text{l}/\text{min}$, Bee-Hive, Bioanalytical Systems Inc. W-Lafayette, USA), and 10 minute interval samples were collected between $t = -1$ h to $t = 1$ h, followed by 20 minute interval samples until $t = 3$ h.

After sample collection, vials were weighed to determine true probe perfusion rate (a maximal deviation of 5% was allowed for the sample to be included in the data), and stored at -80°C .

In 27 rats of the intranasal groups, 30 μl 0.5% Evans blue was administered in 30 seconds at the end of the experiments. 10 to 15 minutes later, the animals were sacrificed with an overdose of Nembutal (Ceva Sante Animale, Naaldwijk, The Netherlands). The nose tip, nasal cavities, brain, mouth, lungs, and intestines were visually examined for blue coloration and scored on a scale; 3, 2, 1, and 0, representing full, medium, light, and no coloration respectively.

■ Analysis

For the plasma corticosterone (CORT) concentrations, a commercially available 125I-corticosterone Radio Immunoassay (RIA) was used (Immun Chem™ Double Antibody Corticosterone 125I RIA kit, MP Biomedicals, Orangeburg, NY, USA), according to the instructions of the manufacturer. Data acquisition was performed on a Gamma Scintillation Counter (Minaxi 5000 series, Packard). Concentrations were calculated using R 2.5.0 (The R Foundation for Statistical Computing, Vienna, Austria). Data exceeding 1.5 times the interquartile range was excluded from the dataset. Geometric means of the CORT concentrations for the control group and all the animals at $t = 0$ min were calculated, and compared with literature to determine the amount of stress induced by our operational and handling techniques. Heteroscedasticity was eliminated by calculating logarithmic conversion of the data (Lew, 2007; Flynn, et al., 1974), and data were normalized to their own baseline to minimize interindividual variability. Thereafter, the groups were tested at every time point by a single factor ANOVA to determine the amount of stress induced by our experimental techniques.

Acetaminophen concentrations in plasma and microdialysate were determined using High Pressure Liquid Chromatography with Electro-Chemical Detection (HPLC-ECD). For all procedures Purified Millipore water (MQ, resistivity 18.2 MΩ.cm) from a Milli-Q® PF Plus system was used (Millipore B.V., Amsterdam, The Netherlands). Sigma, Zwijndrecht, The Netherlands delivered 3,4-dihydroxybenzylamine hydrobromide (DHBA), L-cysteine, and 1-octane-sulfonic acid (OSA). Ethylenediaminetetraacetic acid (EDTA), perchloric acid, sodiumacetate, and L-(+)-ascorbic acid were obtained from Baker, Deventer, The Netherlands. Ortho-phosphoric acid, di-sodium hydrogen phosphate dihydrate, and sodium dihydrogen phosphate monohydrate were obtained from Merck, Amsterdam, The Netherlands. Methanol and acetic acid from Biosolve B.V., Valkenswaard, The Netherlands. Calibration solutions were prepared by adding 50 µl blank plasma to 50 µl calibration standard; 10, 25, 50, 100, 200, 300, 400, 500, and 1,000 ng/ml acetaminophen in antioxidant (0.1 M acetic acid, 3.3 mM L-cysteine, 0.27 M EDTA, 0.0125 mM L-(+)-ascorbic acid, S. Sarre, personal communications).

To 50 µl of the plasma samples 50 µl MQ was added. To these samples 25 µl internal standard (IS), containing 150 ng/ml DHBA, was added and proteins were precipitated by adding 100 µl 6% perchloric acid. After vortexing and centrifugation (10 minutes at 4000 rpm), the supernatant was transferred into a clean glass tube; 150 µl 1 M sodiumacetate was added, and after vortexing, injected into the HPLC-ECD. 20 µl of the microdialysate samples was

vortexed with 20 μ l IS and directly injected into the HPLC-ECD system. The analytical equipment consisted of a LC-10 AD pump (Shimadzu, 's Hertogenbosch, The Netherlands), a Waters 717plus Autosampler (Waters, Etten-Leur, The Netherlands), a pulse damper (Antec Leyden, Zoeterwoude, The Netherlands), a C18 ODS Ultrasphere 5 μ m column (4.6 mm x 15 cm) with C18 refill guard column (Alltech Netherlands B.V., Ridderkerk, The Netherlands), an electrochemical amperometric detector (DECADE, software version 3.02, Antec Leyden B.V., Zoeterwoude, The Netherlands), a VT-03 electrochemical flow cell, 25 μ m spacer, and in situ AG/AgCl (ISAAC) reference electrode (filled with a saturated potassiumchloride solution) operating in DC mode. The mobile phase (MP) consisted of a 85% phosphate buffer (96,4% 1.0 M NaH_2PO_4 , 3,6% 1.0 M Na_2HPO_4 , diluted with MQ to 50 mM phosphate buffer, and OSA was added to obtain 2 mM OSA), 15% MeOH and 100 mg/l EDTA. MP was filtered through a 0.2 μ m nylon filter membrane (Alltech Netherlands B.V., Ridderkerk, The Netherlands).

Data acquisition and processing was performed using Empower® data acquisition software (Waters, Etten-Leur, The Netherlands). For constructing the calibration curve, linear regression analysis was applied using weight factor $1/Y^2$. Data exceeding 1.5 times the interquartile range were excluded from the dataset before plotting geometric mean concentrations over time. Data analysis, statistical analysis, and plotting was performed using Microsoft® Office Excel 2003 (Microsoft Corporation, USA) and OriginPro® 7.5 (Origin-Lab Corporation, Northampton, MA, USA).

Heteroscedasticity was eliminated before executing a single factor ANOVA on every time point (Flynn, et al., 1974; Lew, 2007). When $p < 0.05$, a Student T-test (one-tailed homoscedastic) was performed between the individual groups per time point. Areas Under the Curve (AUC) were calculated by the trapezoidal rule and microdialysis AUC's were corrected for *in vitro* recovery. AUC's were plotted, and tested for differences between groups by single factor ANOVA. The absolute recovery was calculated by dividing the plasma AUC after IN administration by the plasma AUC after IV administration.

Nonlinear mixed effect modeling (NONMEM 6.2, run in the PSN module (Lars et al., 2004) under Windows XP Professional 2002 (service pack3) on an Intel Pentium D CPU3.2 GHz processor) was used to model the pharmacokinetic parameters clearance and volume of distribution. 1-, 2- and 3-compartment models were entered in various subroutines in NONMEM for the experiments with acetaminophen, and identified by likelihood ratio test ($p < 0.05$; decrease in objective function value of 3.84 points), pharmacokinetic parameter estimate endpoint, and goodness-of-fit plots. The inter-

individual variability of the blood PK model was assumed log-linear and optimized by taking possible correlation between parameters into account, and by testing the intraindividual variability through an additive error model versus a constant coefficient of variation model. The individual parameter estimates of the blood PK model allowed estimation of intercompartmental clearance and volume of distribution in the brain compartment. Population parameter estimates were assumed to be normally distributed, and considered equal when the 95% confidence intervals of the parameter estimates overlap (1.96 times the standard error).

RESULTS

■ Evans Blue

Of the 27 rats that had received Evans Blue through the intranasal probe in the right nasal cavity, one had a broken septum and was excluded in the determination of the nasal coloration. One animal experienced blocking of the intranasal probe, thereby decreasing the amount of Evans Blue reaching the right nasal cavity. Full coloration of the right nasal cavity was observed in 96% of the animals. The nose tip, tongue, palate and intestine were light colored in 81%, 89%, 93%, and 79% of the animals respectively. In the left nasal cavity 67% was not colored. In 96% of the animals the lungs as well as the olfactory bulb were not colored. Table 1, shows all the acquired data.

Table 1 Colouration of several tissues after intranasal administration of 30 µl 0.5% Evans blue in 30 seconds.

Score	Nose tip	Lungs	Olfactory Bulb	Right cribrif. plate	Left cribrif. plate	Right nasal cavity	Left nasal cavity	Esophagus	Bowels	Stomach	Tongue	Palate
0	5	26	26	1	2	0	18	6	7	3	3	2
1	22	1	1	26	25	0	4	21	20	23	24	25
2	0	0	0	0	0	1	3	0	0	1	0	0
3	0	0	0	0	0	25	1	0	0	0	0	0

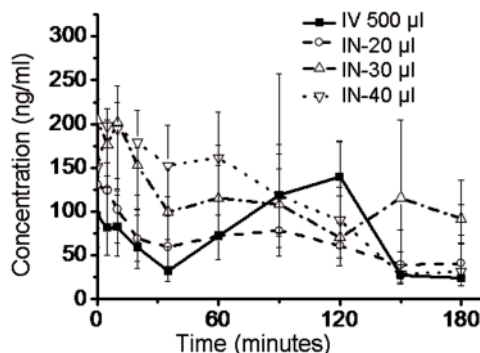
Tissue of 27 rats has been observed for full, medium, light, or no colouration scored by 3, 2, 1, and 0 respectively. The table shows the number of rats with accompanying scores.

■ Corticosterone as Biomarker for Stress

Geometric mean (\pm S.E.M.) of CORT concentrations in plasma at $t = 0$ were 166 ± 14 ng/ml ($n = 33$). The groups did not show significant differences (p -values > 0.23) over the time period of 180 minutes (Figure 2).

Figure 2 Concentration-time profiles of corticosterone (geometric mean \pm S.E.M.) in plasma after intranasal administration of different volumes of saline (IN-20, -30, and -40 μ l), compared to intravenous (IV-500 μ l) administration.

Single factor ANOVA proves no differences between the groups ($p > 0.23$). $n = 9, 9, 8$, and 6 for the IV, IN-20 μ l, IN-30 μ l, and IN-40 μ l groups respectively.



■ Acetaminophen as Model Compound

The log-normal geometric mean-time profiles of the concentrations in plasma after administration of acetaminophen (Figure 3) showed the same profiles for all groups. At $t = 10$ min there were differences between the groups when tested IV vs. 30 μ l, 20 μ l vs. 30 μ l, and 20 μ l vs. 40 μ l (p -values are 0.04, 0.00, and 0.02 respectively). At $t = 180$ differences were found between IV and 20 μ l, 20 μ l vs. 30 μ l, and 20 μ l vs. 40 μ l (p -values were 0.00, 0.04, and 0.02 respectively). Areas under the curve (AUC) in plasma with their standard error of the means were calculated (Figure 4); 10.5 ± 0.7 , 11.6 ± 0.6 , 8.8 ± 0.9 , and 9.6 ± 0.8 (μ g*min)/ml for IV, 20, 30, and 40 μ l IN administration respectively. No statistically significant differences between the groups were found ($p = 0.07$).

After measuring and plotting the geometric mean (\pm S.E.M., Figure 3) of acetaminophen brain microdialysate concentrations over time, single factor ANOVA revealed a difference in profiles at $t = 5, 35$ and 90 min (p -values

were 0.00, 0.04 and 0.03 respectively). The maximal brain microdialysate acetaminophen concentration was reached earlier after intravenous administration.

Figure 3 Concentration-time profiles (geometric means \pm S.E.M.) of acetaminophen in plasma and brain microdialysate after intranasal (IN) administration of 200 μ g acetaminophen in different volumes, compared to intravenous (IV) administration. At $t = 10$ min concentrations in plasma (solid line) differed when tested IV vs. IN-30 μ l, IN-20 μ l vs. IN-30 μ l, and IN-20 μ l vs. IN-40 μ l ($p = 0.04$, 0.00, and 0.02 respectively). At $t = 180$ differences were found between IV and 20 μ l, 20 μ l vs. 30 μ l, and 20 μ l vs. 40 μ l ($p = 0.00$, 0.04 and 0.02 respectively). In the brain microdialysates (dotted line) differences were found at $t = 5$, 35, and 90 min ($p = 0.00$, 0.04, and 0.03 respectively).

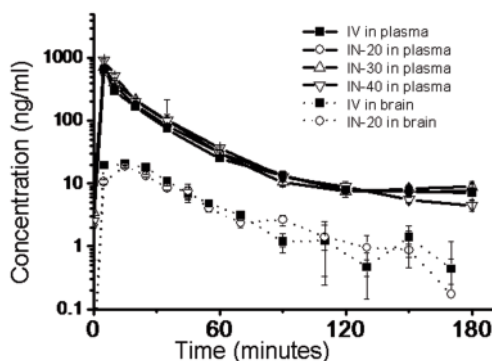
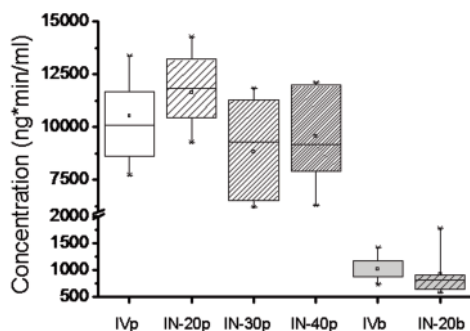


Figure 4 Box plots of the Area's Under the Curve (AUC) of acetaminophen concentration-time profiles in plasma (p) and brain microdialysate (b), following intranasal (IN) administration of 200 μ g acetaminophen in different volumes (-20, -30, and -40 μ l), compared to intravenous (IV) administration. No differences between plasma AUC's were found ($p > 0.07$). The AUC's of the brain microdialysates also show no difference ($p = 0.98$).



Microdialysis *in vitro* recovery was 40%. The mean AUCs \pm S.E.M. of the brain concentrations were 2.54 ± 0.31 ($\mu\text{g} \cdot \text{min}$)/ml and 2.55 ± 0.44 ($\mu\text{g} \cdot \text{min}$)/ml for the control group and experimental group receiving 20 μl solution respectively and did not differ (Figure 4, $p = 0.98$). The absolute recovery of acetaminophen was 95%.

After comparing several models, a 2-compartment model with the brain compartment as an effect compartment, constant coefficient of variation for intraindividual variability and correlation between the clearance and volume of distribution of compartment 1 and 3 proved to fit the data best for both the experimental and the control study. Estimating interindividual variability on clearance and volume of distribution in effect compartment 2 did only improve the model (decrease in objective function value > 3.84) of intranasal administration. Parameter estimates with their 95% confidence interval acquired from NONMEM are listed in table 2.

Table 2 Population model parameter values.

Blood and peripheral pharmacokinetic model							Brain pharmacokinetic model	
		CL1 (L/h)	V1 (L)	CL2 (L/h)	V2 (L)	KA (mg/h)	Q3 (L/h)	V3 (ml)
θ	IV	0.86 ± 0.12	0.19 ± 0.05	0.27 ± 0.21	$0.07 \pm 0.02^*$		8.32 ± 5.3	1050 ± 300
	IN	0.89 ± 0.11	0.17 ± 0.04	0.40 ± 0.06	0.13 ± 0.03	86.3 ± 19.4	2.63 ± 1.96	886 ± 286
η^2	IV	0.03 ± 0.03	0.07 ± 0.06	-	-	-	0.62 ± 0.53	0.16 ± 0.12
	IN	0.09 ± 0.07	0.31 ± 0.21	-	0.16 ± 0.15	-	0.88 ± 1.20	0.19 ± 0.22
σ^2	IV			0.01 ± 0.005			0.05 ± 0.02	
	IN			0.02 ± 0.01			0.06 ± 0.04	

Data represented are population parameter estimates (θ) with their interindividual variability (η^2) and the population intraindividual variability (σ^2) with their 95% confidence interval after intravenous (IV) or intranasal (IN) administration of 200 mg acetaminophen.

Parameters of the first central compartment are clearance (CL1) and volume of distribution (V1). For the second peripheral compartment clearance (CL2) and volume of distribution (V2) were determined, as well as the absorption rate constant (KA) after IN administration. In the brain the intercompartmental clearance(Q) and volume of distribution (V3) were estimated. Parameter estimates that differ between the studies are denoted with *.

DISCUSSION

The aim of this study was to develop and validate a new preclinical, refined minimal stress animal model, in which we can administer compounds intranasally and intravenously, with blood- and brain ECF samples to be taken over time. Our results indicate that IN administration in freely moving rats does not induce stress, while for the model compound acetaminophen it was observed that the pharmacokinetics following IN and IV administration were similar.

■ Evans Blue

Evans Blue is a dye with a high affinity for albumin which is present in nasal mucosa. Besides the expected full coloration of the targeted nasal cavity, 93% of the animals showed light coloration of the palate caused by leakage through the nasopalatine duct that connects the nose and mouth. This might be an indication for buccal absorption in rats, which should be considered in the PK and extrapolation of data to clinical situations, since in humans the nasopalatine duct does not extend to the mouth. However, due to its role, in cooperation with the vomeronasal organ, in food recognition, sex recognition, and courtship we found it not advisable to close the nasopalatine duct (Jacob, et al., 2000). Also, after the 10 minutes following Evans Blue administration a small part was swallowed, which could indicate the possibility of partial oral uptake after intranasal administration. This can be caused by passive leakage to the oesophagus and/or active sweeping by the cilia in the nose. Since rats are obligate nose breathers (Krinke, 2000) this obviously cannot be prevented in freely moving animals. The concentration-time curves of acetaminophen however, excluded substantial uptake of compound through oral absorption. Use of other (more viscous) formulations could possibly eliminate this problem in future research.

■ Corticosterone

In our study, the CORT data show no influence of administration techniques, nor of volume of administration. Cano *et al.* (Cano, et al., 2008) performed a circadian rhythm study concerning the CORT concentrations in Wistar rats during high-fat induced stress and compared it to a normally fed control group. In that study, plasma concentrations of CORT were found to be 283 ± 35 ng/ml (mean \pm S.E.M.) in the control group, with an amplitude of 97 ± 11 ng/ml, *versus* 456 ± 42 ng/ml in the experimental group, showing a significant difference compared to the control group ($p < 0.01$). Also, in that study, CORT concentrations were roughly 200 ng/ml straight after onset

of the light phase, indicating higher basal concentrations when compared with our experiments 166 ± 14 ng/ml (basal average \pm S.E.M.). Additionally, Perello *et al.* (Perello, et al., 2006) discovered in individually housed Wistar rats, after decapitation under conditions of minimal stress after the onset of the light phase, basal concentrations of 363 ± 35 ng/ml (mean \pm S.E.M.) in animals. This was significantly higher when compared to their group-housed animals (206 ± 32) and to our individually housed freely moving animals. Perello *et al.* (Perello, et al., 2006) stated their CORT concentrations to be low when compared to restraining studies and bacterial lipopolysaccharide injection. In our freely moving animals, we find no evidence that stress levels are increased due to our handling techniques or experiments, moreover, when compared to aforementioned studies, we have less CORT release indicating less stress.

■ Acetaminophen

In principle, differences in the concentration time profiles in both plasma and brain data can be explained by the absorption phase over the nasal epithelium *versus* IV administration, as well as by the difference in infusion time. Equal plasma AUCs indicate that the same amount of drug as IV is absorbed after IN administration. Although differences are found when testing data per time point, the comparison of the concentration-time profiles with NONMEM show no differences in parameter estimates, except for V2. Adding interindividual variability for V2 in the IV model did not increase the predictability and was therefore left out of the model, but this can cause the difference in the population estimates for V2 since adding interindividual variability did improve the IN model. The individual- and population estimates described the data well. We can consider the free drug concentrations in the ECF in terms of intercompartmental clearance (Q3) and V3, which gives us information on the blood-brain-barrier transport and whether direct transport from the nasal epithelium into the brain could be an issue. Since the plasma pharmacokinetics after IV and IN administration are similar, increased CNS target site bioavailability after IN administration should result in increased brain concentrations after IN administration compared to IV administration, which is not the case. Acetaminophen is subject to metabolism by P450, that is highly present in the nasal epithelium (Sarkar, 1992), but this did not influence the PK of acetaminophen following intranasal administration relative to that following intravenous dosing. Furthermore, we found no evidence of substantial buccal or oral absorption in the concentration-time profiles of acetaminophen. The population estimates of the brain showed no differences in intercompartmental clearance, volume of distribution, interindividual- or intraindividual variability.

CONCLUSIONS

The animals showed clear coloration in the right nasal cavity, so after intranasal administration, the major part of the administered 30 μ l Evans Blue remained in the nasal cavity and the cannula can be used to administer compounds in the right nasal cavity in freely moving animals, with little or no drainage to other absorption sites.

When compared to other studies reported in literature, our experimental and handling techniques resulted in lower CORT concentrations, which indicates less stress during the experiments in freely moving animals.

The intranasal administration did not increase CORT concentrations, and there were no differences in CORT concentrations when volumes up to 40 μ l are administered, compared to IV administration.

With respect to the plasma and brain pharmacokinetics of acetaminophen we conclude that following IN administration no evidence was found for selective distribution enhancement to the brain. The administration of acetaminophen is site specific, as also concluded from the Evans Blue study. We do emphasize however that the administration of acetaminophen by the intranasal route shows a very rapid absorption indicated by identical PK when compared to IV administration.

In summary, the new intranasal administration method in freely moving animals allows the local, stress free administration of acetaminophen, while blood and brain pharmacokinetics can be observed over time.

REFERENCES

- American Academy of Pediatrics: Committee on Drugs (1997) Alternative Routes of Drug Administration---Advantages and Disadvantages (Subject Review). *Pediatrics* **100**:143-152.
- Cano P, Jimenez-Ortega V, Larrad A, Reyes Toso CF, Cardinali DP and Esquifino AI (2008) Effect of a high-fat diet on 24-h pattern of circulating levels of prolactin, luteinizing hormone, testosterone, corticosterone, thyroid-stimulating hormone and glucose, and pineal melatonin content, in rats. *Endocrine* **33**:118-125.
- Dahlin M, Jansson B and Bjork E (2001) Levels of dopamine in blood and brain following nasal administration to rats. *Eur J Pharm Sci* **14**:75-80.
- De Lange EC, Danhof M, De Boer AG and Breimer DD (1994) Critical factors of intracerebral microdialysis as a technique to determine the pharmacokinetics of drugs in rat brain. *Brain Res* **666**:1-8.
- Dufes C, Olivier JC, Gaillard F, Gaillard A, Couet W and Muller JM (2003) Brain delivery of vasoactive intestinal peptide (VIP) following nasal administration to rats. *Int J Pharm* **255**:87-97.
- Flynn FV, Piper KA, Garcia-Webb P, McPherson K and Healy MJ (1974) The frequency distributions of commonly determined blood constituents in healthy blood donors. *Clin Chim Acta* **52**:163-171.
- Graff CL and Pollack GM (2005a) Nasal drug administration: potential for targeted central nervous system delivery. *J Pharm Sci* **94**:1187-1195.
- Graff CL and Pollack GM (2005b) Functional Evidence for P-glycoprotein at the Nose-Brain Barrier. *Pharmaceutical Research* **22**:86-93.
- Jacob S, Zelano B, Gungor A, Abbott D, Naclerio R and McClintock MK (2000) Location and Gross Morphology of the Nasopalatine Duct in Human Adults. *Arch Otolaryngol Head Neck Surg* **126**:741-748.
- Jansson B and Bjork E (2002) Visualization of in vivo olfactory uptake and transfer using fluorescein dextran. *J Drug Target* **10**:379-386.
- Kandimalla KK and Donovan MD (2005) Localization and Differential Activity of P-glycoprotein in the Bovine Olfactory and Nasal Respiratory Mucosae. *Pharmaceutical Research* **22**:1121-1128.
- Krinke GJ (2000) *The laboratory rat*. Academic Press.
- Lars L, Jakob R and Niclas J (2004) Perl-speaks-NONMEM (PsN)-a Perl module for NONMEM related programming. *Comput Methods Programs Biomed* **75**:85-94.
- Lennox P, Hern J, Birchall M and Lund V (1996) Local anaesthesia in flexible nasendoscopy. A comparison between cocaine and co-phenylcaine. *J Laryngol Otol* **110**:540-542.
- Lew M (2007) Good statistical practice in pharmacology Problem 1. *Br J Pharmacol* **152**:295-298.
- Moghaddam B and Bunney BS (1989) Ionic composition of microdialysis perfusing solution alters the pharmacological responsiveness and basal outflow of striatal dopamine. *J Neurochem* **53**:652-654.
- Perello M, Chacon F, Cardinali DP, Esquifino AI and Spinedi E (2006) Effect of social isolation on 24-h pattern of stress hormones and leptin in rats. *Life Sciences* **78**:1857-1862.
- Raphael JH and Butt MW (1997) Comparison of isoflurane with propofol on respiratory cilia. *Br J Anaesth* **79**:473-475.
- Raphael JH, Selwyn DA, Mottram SD, Langton JA and O'Callaghan C (1996a) Effects of 3 MAC of halothane, enflurane and isoflurane on cilia beat frequency of human nasal epithelium in vitro. *Br J Anaesth* **76**:116-121.
- Raphael JH, Strupish J, Selwyn DA, Hann HCL and Langton JA (1996b) Recovery of respiratory ciliary function after depression by inhalation anaesthetic agents: an in vitro study using nasal turbinate explants. *Br J Anaesth* **76**:854-859.
- Sapolsky RM, Romero LM and Munck AU (2000) How Do Glucocorticoids Influence Stress Responses? Integrating Permissive, Suppressive, Stimulatory, and Preparative Actions. *Endocr Rev* **21**:55-89.

- Sarkar MA (1992) Drug Metabolism in the Nasal Mucosa. *Pharmaceutical Research* **9**:1-9.
- Schaiquevich P, Niselman V, Tumilasci O and Modesto R (2004) Evaluation of acetaminophen P-glycoprotein-mediated salivary secretion by rat submandibular glands. *Archives of Oral Biology* **49**:895-901.
- Schindler E, Müller M, Zickmann B, Kraus H, Reuner KH and Hempelmann G (1996) Blood supply to the liver in the human after 1 MAC desflurane in comparison with isoflurane and halothane. *Anesthesiol Intensivmed Notfallmed Schmerzther* **31**:344-348.
- Schipper NGM, Verhoef JC and Merkus FWHM (1991) The Nasal Mucociliary Clearance: Relevance to Nasal Drug Delivery. *Pharmaceutical Research* **8**:807-814.
- Selwyn DA, Raphael JH, Lambert DG and Langton JA (1996) Effects of morphine on human nasal cilia beat frequency in vitro. *Br J Anaesth* **76**:274-277.
- Shi Z, Zhang Q and Jiang X (2005) Pharmacokinetic behavior in plasma, cerebrospinal fluid and cerebral cortex after intranasal administration of hydrochloride meptazinol. *Life Sci* **77**:2574-2583.
- Ugwoke MI, Verbeke N and Kinget R (2001) The biopharmaceutical aspects of nasal mucosal adhesive drug delivery. *J Pharm Pharmacol* **53**:3-21.
- Van Bree JB, Baljet AV, Van Geyt A, De Boer AG, Danhof M and Breimer DD (1989) The unit impulse response procedure for the pharmacokinetic evaluation of drug entry into the central nervous system. *J Pharmacokinet Biopharm* **17**:441-462.
- Van den Berg M, Merkus P, Romeijn S, Verhoef JC and Merkus F (2004) Uptake of Melatonin into the Cerebrospinal Fluid After Nasal and Intravenous Delivery: Studies in Rats and Comparison with a Human Study. *Pharmaceutical Research* **21**:799-802.
- Veronesi MC, Kubek DJ and Kubek MJ (2007) Intranasal delivery of a thyrotropin-releasing hormone analog attenuates seizures in the amygdala-kindled rat. *Epilepsia* **48**:2280-2286.

Online solid phase extraction with liquid chromatography-tandem mass spectrometry to analyse remoxipride in small plasma-, brain homogenate-, and brain microdialysate samples

Journal of Chromatography B (2010) **878**:969-975

J. Stevens¹, D. J. van den Berg¹, S. de Ridder¹, H. A. G. Niederländer¹,
P. H. van der Graaf², M. Danhof¹, E. C. M. de Lange¹.

¹ *Division of Pharmacology, LACDR, Leiden University, Leiden, The Netherlands.*

² *Pfizer, Pharmacometrics/Global Clinical Pharmacology, Sandwich, Kent, England.*

ABSTRACT

Remoxipride is a selective dopamine D2-receptor antagonist, and useful as a model compound in mechanism-based pharmacological investigations. To that end, studies in small animals with serial sampling over time are needed. For these small volume samples currently no suitable analytical methods are available. We propose analytical methods for the detection of low concentrations remoxipride in small sample volumes of plasma, brain homogenate, and brain microdialysate, using online solid phase extraction with liquid chromatography-tandem mass spectrometry.

Method development, optimization and validation are described in terms of calibration curves, extraction yield, lower limit of quantification (LLOQ), precision, accuracy, inter-day- and intra-day variability. The 20 μ l plasma samples showed an extraction yield of 76%, with a LLOQ of 0.5 ng/ml.

For 0.6 ml brain homogenate samples the extraction yield was 45%, with a LLOQ of 1.8 ng/ml. The 20 μ l brain microdialysate samples, without pre-treatment, had a LLOQ of 0.25 ng/ml. The precision and accuracy were well within the acceptable 15% range.

Considering the small sample volumes, the high sensitivity and good reproducibility, the analytical methods are suitable for analyzing small sample volumes with low remoxipride concentrations.

INTRODUCTION

Mechanism-based pharmacokinetic–pharmacodynamic (PK–PD) modeling of dopaminergic agents following different routes of administration of in preclinical studies *in vivo* is anticipated to provide key knowledge to predict efficacious doses and the time-course of dopaminergic drug effects in man. Remoxipride is a substituted benzamide and is a weak, but very selective, dopamine D2-receptor antagonist. It was originally intended to be used as an atypical antipsychotic (Roxiam®) but taken from the market in 1993. Remoxipride is, however, very useful as a model compound in mechanism-based PK–PD studies on the dopaminergic system in small animals. With our ultimate aim being to build a mechanism-based PK–PD model of remoxipride, we first need to characterize the pharmacokinetic part of the model, i.e. determining the transport of remoxipride across the blood–brain barrier (Hammarlund-Udenaes, et al., 1997) and consecutive distribution between extracellular and intracellular space. Especially the free drug concentrations in the brain extracellular fluid surrounding the membrane receptors, as can be measured with intracerebral microdialysis, are of interest as membrane receptors are important targets for many drugs including remoxipride (Nadal, 2001). Plasma pharmacokinetics can be derived from serial plasma samples, brain extracellular fluid pharmacokinetics can be determined from collecting brain microdialysates, and total brain concentrations can be obtained from the brain, obtained from each animal at the end of the experiment.

As summarized in table 1, in 1987, De Ruiter *et al.* (de Ruiter, et al., 1987) described an analytical method for remoxipride in plasma using reversed-phase (RP) liquid chromatography (LC) with direct injection of 1ml untreated plasma diluted with 10mM phosphate buffer (1:1, v/v) into a disposable precolumn (C-18) treated with hexadecyltrimethylammonium bromide. A post-column ionpair extraction with 9,10-demethoxy-anthracene-2-sulphonate allowed detection with a fluorescence detector. In 1990 Nilsson (Nilsson, 1990) described a more simple and robust analytical method using a two-step liquid–liquid extraction, with higher sensitivity. This was followed by the method of Chiou and Lo (Chiou and Lo, 1992) who, in 1992, described a faster way of measuring remoxipride concentrations, using an easier extraction step, RP high-pressure liquid chromatography (HPLC) with ultraviolet detection (UV). In 1997, DePuy *et al.* (DePuy, et al., 1997) described an analysis using a chiral OD-R column, HPLC, and UV detection, allowing the separate measurement of the remoxipride enantiomers. In the research, evidence was provided that *in vivo* conversion of the R- to S-

enantiomer does not occur, and confirmed stability in repetitive freeze–thaw cycles. Pharmacological investigations comprise full understanding of the distribution of drug throughout the body, including the determination of free drug concentrations in brain. Therefore, Main *et al.* (Main, et al., 1996) measured remoxipride in cerebrospinal fluid using the method described by Nilsson (Nilsson, 1990).

The earlier published analytical methods presented above (Chiou and Lo, 1992; Main, et al., 1996; de Ruiter, et al., 1987; DePuy, et al., 1997; Widman, et al., 1993; Nilsson, 1990) require rather large plasma or cerebrospinal fluid samples ranging from 0.5 to 2 ml, which can be obtained from humans in clinical studies (Table 1). In preclinical PK–PD studies, however, small laboratory animals are mostly used, thereby limiting the sample size. Based on Dutch legislation, quality of research, and animal ethics, the maximal obtainable blood volume in rats is 8 ml/kg/day (Van Zutphen, et al., 2001).

Table 1 Overview of analytical methods to determine remoxipride concentrations in plasma.

	De Ruiter, et al., 1987	Nilsson, 1992	Chiou and Lo, 1992	DePuy, et al., 1997
sample volume plasma (ml)	>0.5	1	2 (*)	0.5
sample preparation	PCE	LLE	LLE	LLE+P
internal standard	-	3B	-	3B
injection volume (ml)	1	0.2	0.05	0.1
flow rate (ml/min)	1	1.3	1.3	0.58-0.70
chromatography	RP LC	RP LC	RF HPLC	HP LC
detection	FL	FL	UV	UV
run time (min)	8	-	6	>40.6
retention time (min)	-	-	2.8	22.6
Extraction yield (%)	88 +/- 4	85 (*)	75	88.1 +/- 10.2 (**)
LLOD (ng/ml)	1	-	-	0.01
LLOQ (ng/ml)	-	0.742	12.5	20
intraday (%)	3.5	5.2	0.6-9.7	7
interday (%)	3.5	2.3	1.1-4.4	4.5

RP, reverse phase; LC, liquid chromatography; HP, high pressure; LLOD, lower limit of detection (3* noise ratio); LLOQ, lower limit of quantification; PCE, post column extraction; LLE, liquid-liquid extraction; p, prefilter; 3B, 3-bromo-N-[(1-propyl-2-pyrrolidiny)methyl]-2,6-dimethoxybenzamide; -, unknown; (*), for low concentration range only; (**), extraction recovery only.

Together with the strong need for sampling over time in pharmacokinetic studies, 9–10 blood samples of 200 μl can be taken per day, resulting in approximately 100 μl plasma samples, to analyze often both PK and PD parameters.

In rats, total brains of ± 1.8 g are obtained and homogenized. Only one sample can be taken, therefore the sample size is large. There is currently no analysis available for the measurement of remoxipride in brain homogenate. Brain microdialysis studies are bound to low perfusion speed resulting in typical microdialysate sample volumes of 10–60 μl (Chaurasia, et al., 2007; De Lange and Danhof, 2002; Nadal, 2001).

Analytical procedures for measuring both plasma and brain homogenate samples are complicated by the presence of interfering compounds. For plasma samples, dilution and/or protein precipitation are standard methods to clean up the samples before analysis. To analyze brain homogenate samples liquid–liquid extraction is often used as a pre-treatment. The microdialysis samples are far less polluted with interfering compounds, therefore, it remains to be seen whether sample pre-treatment is a necessity.

For experiments in rats, we here propose analytical methods for the detection of low concentrations remoxipride in small sample volumes of plasma, brain homogenate, and microdialysate, using online solid phase extraction (SPE) coupled to liquid chromatography (LC) with tandem mass spectrometry (MS–MS). The analytical method should cover the PK concentration range in all tissue types in our future experiments. For the plasma analysis a simple precipitation step was needed, and for the brain homogenates a liquid–liquid extraction step was implemented. The measurement of remoxipride in microdialysate could be performed without pre-treatment of the samples.

MATERIALS AND METHODS

To validate our method and increase the sensitivity and throughput, we tested plasma dilution and protein precipitation by acetonitrile or perchloric acid for positive contribution to the remoxipride analysis. Several SPE cartridges were tested; hysphere silica based cyanopropyl phase (CN), resin general phase (GP), and resin strong hydrophobic phase (SH) (Spark, Emmen, The Netherlands), mixed mode cationic exchange (MCX), and weak cationic exchange (WCX) cartridges (Waters, Etten-Leur, The Netherlands). The performance of these cartridges was tested alone as well as in combination with micro-column LC. Remoxipride was injected at the SPE column under acidic- and alkaline conditions. The effect of the addition of trifluoroacetic acid was investigated as well as different mobile phase ratios, to

increase peak performance. The final method is presented hereunder, together with an illustrative application of these analyses after remoxipride administration in individual rats. Because of its structural resemblance and previous use as internal standard in remoxipride measurements in plasma (Ogren, et al., 1993), we used raclopride as internal standard.

■ Chemical and reagents

For all procedures Purified Millipore water (MQ, 18.2 MΩ cm) from a Milli-Q® PF Plus system was used (Millipore B.V., Amsterdam, The Netherlands). Remoxipride ((S)-3-bromo- N-[1-ethyl-2-pyrrolidinyl)methyl]-2,6-dimethoxybenzamide, 371.27 g/mol, pKa 8.9 (Budavari, et al., 1996), was obtained from TOCRIS, Bristol, United Kingdom. The internal standard raclopride (IS, 3,5-dichloro-N-[(2S)-1-ethyl-2-pyrrolidinyl)methyl]-2-hydroxy-6-methoxybenzamide, 347.24 g/mol, pKa,basic 9.5, pKa,acidic 6.11 (Bouchard, et al., 2002)), and L-cysteine were obtained from Sigma, Zwijndrecht, The Netherlands. Acetonitrile, acetic acid (both ULC/MS grade), trifluoro acetic acid (TFA, ULC/MS grade), ammonium acetate and t-butyl-methyl-ether (HPLC grade) were obtained from Biosolve B.V., Valkenswaard, The Netherlands. Ammonium hydroxide (25%), ammonium acetate (99.1%), sodium carbonate (99.9%), potassium iodide (99.9%), ethylenediaminetetraacetic acid (EDTA), perchloric acid, and L-(+)-ascorbic acid were obtained from Baker, Deventer, The Netherlands. All pH measurements were performed using a Schott CG 820 pH meter (Schott-Geräte, Germany). 10 mM Sodium phosphate homogenization buffer (pH 7.4) was prepared using di-sodium hydrogen phosphate di-hydrate (99.5%, E. Merck Nederland B.V., Amsterdam, The Netherlands) and sodium di-hydrogen phosphate monohydrate (99%, Sigma-Aldrich, Zwijndrecht, The Netherlands). Anti-oxidant (0.1M acetic acid, 3.3mM l-cysteine, 0.27M EDTA, 0.0125 mM L-(+)-ascorbic acid; S. Sarre, personal communications) and microdialysis perfusion fluid (PF (Moghaddam and Bunney, 1989)) was prepared, filtered, stored in glass vials (−20 °C), and sonified before use.

■ Samples

Blank plasma-, whole brain-, and brain microdialysis samples were obtained from Male Wistar WU rats (245 ± 18 g, Charles River, The Netherlands). All animal procedures were performed in accordance with Dutch laws on animal experimentation. The study protocol was approved by the Animal Ethics Committee of Leiden University (UDEC nr. 05156). A microdialysis guide was implanted in the striatum, and 6 days later replaced by a microdialysis probe (CMA/12, 4 mm polycarbonate membrane, cut-off 20 kD,

Aurora Borealis Control, Schoonebeek, The Netherlands). The next day the probe was perfused with 2 $\mu\text{l}/\text{min}$ perfusion fluid, and blank microdialysate samples were collected in a cooled fraction collector (Univentor 820 Micro-sampler, Antec, Netherlands) for 5 hours. After administration of an over-dose of Nembutal, blank blood was obtained by open heart puncture. The whole brains were harvested after transcardial transfusion with 50 mM phosphate buffer (pH 7.4), and the blank brains were stored at -80°C .

■ Pharmacokinetic study in rats

The described analytical methods have been applied to the pharmacokinetic study of remoxipride in rats. Intranasal delivery of remoxipride was investigated to directly target the brain. Intranasal delivery is a promising alternative for oral or parenteral administration, since it avoids the high first-pass clearance of remoxipride (American Academy of Pediatrics: Committee on Drugs, 1997; Widman, et al., 1993; Graff and Pollack, 2005; Jansson and Bjork, 2002). All animal procedures were performed in accordance with Dutch laws on animal experimentation. The study protocol was approved by the Animal Ethics Committee of Leiden University (UDEEC 6132). Rat experiments were performed as described by Stevens *et al.* (Stevens, et al., 2009) in seven male Wistar WU rats. In short, during anaesthetized surgery, two blood cannulas were implanted in the femoral artery and -vein for blood sampling and drug administration, respectively. Next to that, a microdialysis guide was implanted in the striatum, and 6 days later replaced by a microdialysis probe (CMA/12, 4 mm polycarbonate membrane, cut-off 20 kD). The next day the probe was perfused with 2 $\mu\text{l}/\text{min}$ perfusion fluid, and microdialysate samples were collected in the mentioned cooled fraction collector. After a 30 min blank perfusion period, remoxipride in saline (B. Braun Melsungen AG, Melsungen, Germany) was administered (16 mg/kg, $t = 0$) during a 30 min intravenous infusion, using an automated pump (Harvard apparatus 22, model 55-2222, Holliston, MA, USA). A total number of 10 blood samples per animal, of 200 μl each, were collected from the arterial cannula in EDTA-coated vials at 10 time points during the experiment ($t = 0, 5, 10, 20, 35, 60, 90, 120, 150$, and 180 min). Blood was centrifuged for 15 min at 5000 rpm and the plasma was stored at -20°C . Microdialysate samples were collected every 20 min for the first 2 h, and every 30 thereafter, until the end of the experiments. The microdialysate samples were stored at -80°C . At $t = 240$ min, transcardial perfusion was performed with 50 mM phosphate buffer (pH 7.4), and the whole brain was removed and stored at -80°C . The concentrations of remoxipride in the samples were measured using the described methods. Plasma- and microdialysate geometric means (\pm standard deviation (S.D.)) were plotted over time. The geometric mean of

the brain homogenates were used to calculate the ratio of the concentration remoxipride in the brain versus the microdialysate concentrations.

■ Sample preparation, calibration curves and quality controls

For the plasma analysis a calibration curve of 0, 5, 10, 20, 50, 100, 200, 500, 1000, and 2000 ng/ml remoxipride in MQ was prepared from a stock solution (100 µg remoxipride per ml MQ). For the quality controls (QCs), standard solutions containing remoxipride were added to 1.9 ml blank plasma (0.05:0.95, v/v), resulting in concentrations of 5, 50, 200, and 2000 ng/ml remoxipride. To 20 µl experimental plasma samples and QCs, IS (100 ng/ml) and MQ (1:1:1, v/v/v) was added and vortexed. Standard calibration solutions were mixed with IS (100 ng/ml) and blank plasma (1:1:1, v/v/v). 6% perchloric acid (HClO₄) was added to these mixtures (2:3, v/v) to precipitate the proteins. After brief vortexing (Vortex-Genie CM-9, Wilton en Co B.V., Etten-Leur, The Netherlands), the samples were centrifuged in eppendorf vials at 8000 rpm during 10 min (Labofuge GL centrifuge, Micro CL 21R, Thermo Fisher Scientific, Breda, The Netherlands) and 60 µl supernatant was added to 45 µl 0.5 M Na₂CO₃ and vortexed. 10 µl of sample was injected onto the online SPE.

Brains were defrosted and homogenized with a Potter S apparatus (B. Braun, Melsungen) in phosphate buffer in a 1:5 ratio (m/v) and kept on ice.

To 0.6 ml blank brain homogenate (100 mg brain) samples 100 µl of calibration standard was added resulting in concentrations of 0, 5, 10, 20, 50, 100, 200, 400, and 500 ng remoxipride/gram brain. The quality controls (QCs) contained 5, 20, 100, and 400 ng/gram brain. To the spiked homogenates (calibration curve), QCs and samples, 20 µl of IS (1000 ng/ml) and/or MQ was added (60:2:10, v/v/v). After vortexing, potassium iodide and 1 M Na₂CO₃ were added (72:10:10, v/v/v) and subsequently vortexed. t-Butyl-methyl-ether was added (0.92:5, v/v), and thorough vortexing supplied transfer of remoxipride and IS from aqueous to organic phase. After centrifugation at 4000 rpm during 10 min, organic phase was transferred to clean glass tubes and evaporated in a vacuum vortex at 40 °C (Labconco vortex evaporator, Beun de Ronde, Breda, The Netherlands). 100 µl SPE solvent (Section Online SPE-LC-MS-MS system) was added, mixed and sonified for 20 s. After spinning down the liquid, sample was transferred to eppendorf vials and centrifuged at 15000 rpm. 10 µl of supernatant was injected onto the online SPE.

For the microdialysate analysis, calibration standards were prepared in PF, resulting in concentrations of 0, 0.5, 1.0, 2.0, 5.0, 10, and 20 ng/ml remoxipride, all containing 10 ng/ml IS. The QCs were prepared containing 0.5, 5 and 20 ng/ml remoxipride. To 20 µl calibration standards, QCs, or micro-

dialysate samples, 5 μl anti-oxidant was added and vortexed prior to injection of 10 μl into the LC system. Anti-oxidant was used in microdialysate to prevent oxidation of molecules, other than remoxipride, that we might like to measure in the future.

■ Online SPE-LC–MS–MS system

After each injection (8 °C, Surveyor auto sampler, Thermo Fischer Scientific, Breda, The Netherlands), the injection needle was washed with 100 μl acetonitrile in MQ (1:9, v/v) and acetonitrile in MQ with acetic acid (1:3, v/v) to reduce carry-over. A Gynkotek P580 Solvent Delivery pump (Dionex Benelux B.V., Amsterdam, The Netherlands) flushed sample onto the SPE column (Hysphere Resin GP SPE in SPE cartridge holder, Spark, Emmen, The Netherlands: ambient temperature). SPE solvent A (SPE-A) consisted of acetonitrile in 10mM ammonium acetate/ammonium hydroxide (pH 8.3, 1:4, v/v). SPE solvent B (SPE-B) consisted of 50mM ammonium acetate/ammonium hydroxide (pH 8.3), and SPE solvent C (SPE-C) consisted of acetonitrile mixed with 16 mM acetic acid (7:3, v/v, 0.1% TFA, pH 2). The flow rate was 1 ml/min. At basic conditions, including $t = 0$ min, the SPE was flushed with SPE-A solvent. After 1 min of washing, a six-port switching valve diverted the SPE to the LC system. At 5 min the SPE was switched back to the SPE pump, and flushed with SPE-C solvent C, SPE-A, and SPE-B for 3, 3, and 2 minutes, respectively, to precondition the column for a next injection. The SPE was used only during one LC-sequence with a maximum of about 90 injections, finalizing with QCs to verify quality. After switching to the LC system in back flush mode, the MS pump (Surveyor MS pump, Thermo Fischer Scientific, 100 $\mu\text{l}/\text{min}$) was used to separate the analytes on an Alltima HP C18 HPLC column (ambient temperature, 150 mm \times 1.0 mm, 5 μm , Alltech Applied Science, Breda, The Netherlands). The mobile phases (MP) consisted of acetonitrile, 10 mM acetic acid/ammonium acetate at pH 3.7, and 0.05 % TFA. The latter was added to enhance peak shape and resolution. For the plasma- and brain analysis the ratio for MP-1 was 1:3 (v/v) and for MP-2 the ratio was 2:3 (v/v). A linear gradient (0–6 min, MP-1–MP-2) was applied to elute remoxipride and IS. At 10 min the LC system was reset to MP-1. The microdialysate samples were directly injected into the LC system using a mixture of MP-A and MP-B (6:4, v/v). Since no SPE was used, the flow was diverted to waste at the onset of the elution, and after 2 minutes the switching valve directed the flow to the MS–MS.

The Finnigan TSQ Quantum Ultra Mass Spectrometer System (Thermo Fischer Scientific) was tuned by infusing standard solutions of remoxipride or IS with the aid of a T-piece in the LC-eluent. Since remoxipride and the

IS are charged, electro spray-ionization was preferred above atmospheric pressure chemical ionization, and nitrogen was used as the desolvation gas. After collision-induced dissociation by argon gas (0.8 psi), the total ion current (TIC) was measured using the fragmented ions of remoxipride ($MH^+ = 371$) and raclopride ($MH^+ = 347$). Data acquisition was performed using the software package LC-Quan provided by Thermo Scientific. For all three analysis a separate tuning of the mass spectrometer was performed.

After analysis, linear regression was used to determine the slope, intercept and correlation coefficient (R^2) of the relation between the peak-area ratio and the drug concentration in the calibration standards data, and accepted when $R^2 > 0.98$. For the calibration curves weighting factors of 1, $1/Y$ and $1/Y^2$ were compared.

■ Extraction yield, LLOD, LLOQ, accuracy, precision, inter- and intra-day variability

Peak-area ratios of remoxipride over IS were calculated, and remoxipride concentrations were corrected for the dilution with IS and anti-oxidant. The extraction yield was calculated by dividing the peak area's of remoxipride either before and after LLE or LC with and without SPE. The lower limit of detection (LLOD) was defined as the lowest concentration measurable by a signal–noise ratio (S/N) of 3, lower limit of quantification (LLOQ) as the lowest concentration measurable by a S/N of 10. Intra-day, inter-day variability, and accuracy for the analysis were determined by measuring replicates of the QCs. Precision was calculated as the relative standard deviation (RSD) for both intra-day and inter-day variability, and accuracy as the degree off closeness of the determined value to the true value. Acceptable precision was defined by a RSD $<15\%$ for the standards, and $<20\%$ at LLOQ. Accuracy was allowed to deviate $<15\%$ for the standards, and $<20\%$ at LLOQ compared to the nominal values. Extraction yield, LLOD, LLOQ, accuracy, precision, inter- and intra-day variability methods and acceptance ranges are based on guidelines distilled from the Third Bioanalytical Workshop of the American Association of Pharmaceutical Scientists and Food and Drug Administration in 2006 (Viswanathan, et al., 2007).

RESULTS AND DISCUSSION

■ Method development and optimization SPE-LC–MS–MS

Online SPE was used for rat plasma and brain homogenate samples in order to provide an adequate sample clean up. As cleaning and preconditioning

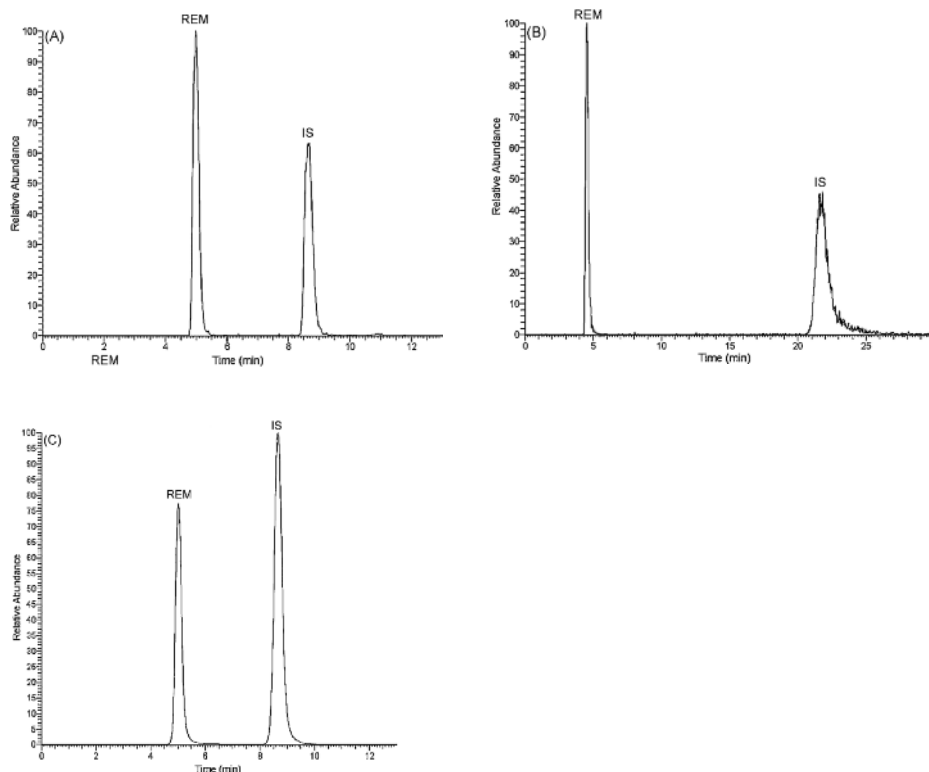
the SPE could be performed during elution of remoxipride and IS at the LC column, time loss due to the cleansing step was reduced. Several SPE cartridges were tested for the optimal adsorption and elution properties. Hysphere CN was suitable for remoxipride adsorption and elution, but the internal standard raclopride already eluted during the washing phase. On the WCX phase, remoxipride behaved as a neutral and already eluted at 100% methanol, so no proper washing could take place. The Waters MCX showed bad resolution for remoxipride, so this method was abandoned. When using the Hysphere Resin SH material, the IS behaved differently from remoxipride and showed a poor peak shape. The Hysphere Resin GP SPE gave adequate separation, retention and peak shape for both remoxipride and IS. As we wanted to use material with another separation mechanism for the SPE as for the LC, this phase was chosen. Stability of this type of material over a wide range of pH (0–14) was favorable for our application. Both remoxipride and IS are trapped on the SPE at pH 8.3 and released when the SPE is switched to the LC system that is flushing MP at pH 3.7. To optimize the peak shape, several mobile phases (MPs) were tested by varying acetonitrile content, buffer composition and pH. This resulted in the MPs as described in the section Online SPE-LC-MS-MS system. In the plasma- and brain analysis the addition of TFA (0.05%) enhanced the peak shape of both remoxipride and IS. After tuning, using a syringe at 5 $\mu\text{l}/\text{min}$ and LC flow of 100 $\mu\text{l}/\text{min}$, the main fragments of remoxipride and IS were identified (Table 2). For the plasma analysis the retention times of remoxipride and IS were 5.0 and 8.7 min, respectively, for the brain analysis 5.1 and 8.7 min, respectively, and for the microdialysate analysis the retention times were 4.8 and 20.7 min, respectively (Figure 1).

Table 2 Tandem mass spectrometer settings.

	20 μl plasma or 0.6 ml brainhomogenate		20 μl microdialysate	
	REM	IS	REM	IS
measure window (min)	0-7	7-13	0-12	12-25
desolvation gas (psi)	27	27	25	10
ionization voltage (kV)	3.5	3.5	3	3.5
fragments (m/z)	112	112	112	112
	228	129	228	129
	242	219	242	204

REM, remoxipride; IS, internal standard.

Figure 1 Relative abundances of remoxipride (REM) and raclopride (IS) in different matrices. A; Chromatogram of plasma spiked with 20 ng/ml remoxipride. B; 2 ng/ml remoxipride in microdialysate. C; 20 ng/ml remoxipride in brain homogenate.



■ Method validation

Table 2 provides an overview of the MS settings regarding measure window, desolvation gas pressure, ionization voltage, and measured fragment sizes derived from the total ion currents, for the plasma, brain microdialysate, and brain homogenate analysis. Specific information for the different types of samples is described below. For the plasma analysis in which 20 μ l plasma sample was used, the online SPE allowed us to only use a simple precipitation step, in contrast with the liquid–liquid extraction or post-column extraction described in literature (DePuy, et al., 1997; de Ruiter, et al., 1987; Nilsson, 1990; Chiou and Lo, 1992). Evaluation of the pretreatment methods showed that using acetonitrile or precipitation with perchloric acid gave similar results. The results were better when compared to diluting

plasma, which caused clogging of the system. Because of the extra evaporation step needed in the acetonitrile method, we proceeded with the more simple perchloric acid precipitation method. Rigid flushing of the SPE after injection, prevented non-volatile ions from entering the LC-MS-MS system. The thus developed sample preparation method caused an extraction yield of remoxipride of 76% (Table 3).

This extraction yield was the product of the recovery of the pre-treatment, the SPE and the matrix effect. Three measurements of the SPE recovery revealed a mean recovery \pm S.D. of $92 \pm 2.6\%$. The combined mean recovery of the pre-treatment and matrix effect was $80 \pm 4.6\%$ ($n = 17$). LLOD and LLOQ were 0.15 and 0.5 ng/ml, respectively. This indicates that while using a smaller sample volume a similar LLOD and LLOQ were obtained when compared to literature (Table 1). Using a weighting factor of $1/Y^2$, calibration was performed within two calibration ranges. Both calibration ranges were measured during the same run. The high standards caused a considerable memory effect. R^2 for the concentration range 100 – 2000 ng/ml was acceptable: 0.990 ± 0.017 (\pm S.D.). The lower concentration range gave an average R^2 of 0.966 ± 0.017 , which was most likely caused by the memory effect that increased the error on the lowest concentrations of the calibration curve. The memory effect could later on be circumvented by injection of blanks after samples in the high range of the calibration curve. The memory effect also influenced the intra-day RSD for QCs in the low (5 ng/ml) concentration samples. The inter-day RSD for the other QCs ranged from 4.9 to 14.7%, with an average of 9.0%. The intraday variability is thereby higher than described with other methods (Table 1), which should decrease by reducing the memory effect. For the intra-day RSD this range was 1.8–3.6%, with an average of 2.6 ng/ml which is low compared to literature, and the average accuracy \pm S.D. was $103.7 \pm 5.3\%$. Despite the memory effect, the precision, as indicated by the RSDs and accuracy, are within ranges (Table 3) which were suitable for the samples derived from our *in vivo* remoxipride experiments in rats.

For the analysis of the brain homogenate we needed a liquid–liquid extraction step (LLE) for the clean up of our samples. Adding potassium iodide resulted in a low, but reproducible extraction yield of $45 \pm 2.3\%$ (mean \pm S.D.). The extraction yield consisted of the recovery of remoxipride during the LLE, the SPE and the matrix effect of brain homogenate extracts. The mean recovery \pm S.D. of the SPE was $96 \pm 5.2\%$ ($n = 12$), and of the matrix effect $68 \pm 11\%$ ($n = 8$). The recovery of the LLE could therefore be calculated to be approximately 69%. LLOD and LLOQ were 0.53 and 1.8 ng/ml, respectively. The calibration curves ($1/Y$) showed an average $R^2 \pm$ S.D. of 0.998 ± 0.001 . The inter-day RSD ranged from 5.6 to 11.3%, with an average of 8.7%.

For the intra-day RSD this range was 2.2 – 4.0%, with an average of 2.7% and average accuracy \pm S.D. of $94.8 \pm 4.7\%$. The RSD and accuracy were within the acceptable ranges. Of the 100 μ l supernatant we needed 10 μ l for injection, so scaling down the amount of brain tissue needed for sample preparation would be feasible. Although from analytical perspective the extraction yield could be improved, for our experiments it is sufficient to draw conclusions about the amount of remoxipride in the intracellular brain fluid (Section pharmacokinetic study in rats).

Table 3 Validation results of remoxipride analysis.

Plasma (n = 5 over 5 consecutive days)				
LLOD (ng/ml)			0.15	
LLOQ (ng/ml)			0.5	
REM Extraction yield (%)			76	
added (ng/ml)	mean (ng/ml)	RSD (%)		Accuracy (%)
		interday	intraday	
5	5.1	18.1	11.8	100.6
50	48.3	4.9	3.6	108.6
200	192.5	14.7	2.1	109.8
200	195.9	11.4	1.8	97.2
2000	2091.0	5.0	2.9	102.1
Brain homogenate (n = 5 over 7 consecutive days)				
LLOD (ng/ml)			0.53	
LLOQ (ng/ml)			1.8	
REM Extraction yield (% \pm SD)			45 \pm 2.3	
added (ng/ml)	mean (ng/ml)	RSD (%)		Accuracy (%)
		interday	intraday	
5	5.0	11.0	4.0	100.3
20	18.7	6.8	2.3	93.3
100	96.4	11.3	2.2	96.4
400	357.3	5.6	2.4	89.3
Microdialysate (n = 6 over 4 consecutive days)				
LLOD (ng/ml)			0.08	
LLOQ (ng/ml)			0.25	
added (ng/ml)	mean (ng/ml)	RSD (%)		Accuracy (%)
		interday	intraday	
0.5	0.6	9.2	4.1	117.8
5	4.7	10.1	7.5	93.5
20	20.7	11.3	7.0	103.7

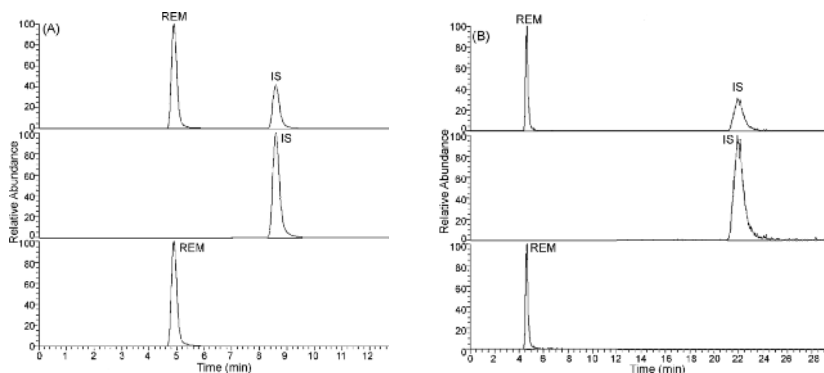
LLOD, lower limit of detection; LLOQ, lower limit of quantification;
REM, remoxipride;
S.D., standard deviation; RSD, relative standard deviation.

For the microdialysate analysis no extraction step was needed, allowing direct injection of the 20 μ l brain microdialysate samples in the LC system, although this caused the LLOD to be slightly higher than in the plasma analysis. Diverting the first 2 min to waste reduced the noise, thereby reducing the LLOD and LLOQ to 0.08 and 0.25 ng/ml, respectively. The calibration curves ($1/Y^2$) showed an R^2 of 0.986 ± 0.015 . The average intra-day and inter-day RSD were 6.2 and 10.2%, respectively. The average accuracy \pm S.D. was $105 \pm 12.2\%$. The RSD and accuracy were within the acceptable ranges. When previous reported analysis in cerebrospinal fluid (Main, et al., 1996) would be used, sample sizes ranging from 500 to 1500 μ l would be necessary. Our method allows 20 μ l sampling over time in an individual animal using microdialysis techniques.

■ Pharmacokinetic study in rats

The concentration of remoxipride was successfully measured in plasma-, brain homogenate-, and brain microdialysate samples after intravenous administration of 16 mg/kg remoxipride. Figure 2 depicts examples of real sample chromatograms in all three matrices. Figure 3 shows the concentration-time profiles in plasma and brain microdialysate.

Figure 2 Relative abundances of remoxipride (REM) and raclopride (IS) in different matrices in an individual rat after administration of 16 mg/kg remoxipride at $t = 0$. The upper panel shows the chromatogram of the sample. The lower panels show the peaks of the IS (middle panel) and remoxipride (lower panel) within that sample. (A) Chromatograms of plasma sample at $t = 40$ min, (B) chromatograms of microdialysate sample at $t = 140$ -160 min and (C) chromatograms of a brain homogenate sample at $t = 240$ min.



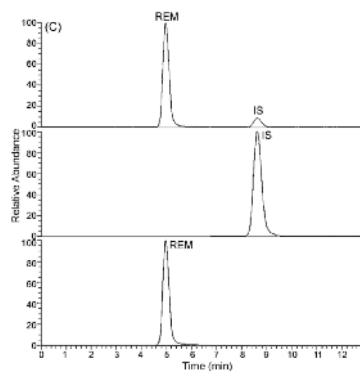
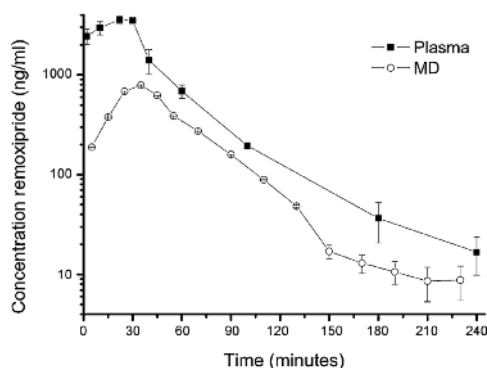


Figure 3 Remoxipride concentrations (geometric mean \pm standard deviation) in plasma (closed symbols) and brain microdialysate (MD, open symbols) after a 30 min intravenous infusion of 16 mg/kg remoxipride at $t = 0$ in 7 Wistar rats.



The lowest measured concentrations are above the LLOQ. As expected, the maximum concentration (C_{max}) in plasma is reached at the end of the infusion; 30 min. The C_{max} of the microdialysate concentrations lies between 30 and 40 min. The delay in the microdialysate time to C_{max} implies activity at the site of the blood-brain barrier (BBB). Remoxipride acts on dopaminergic neurons that are located on the cell membranes of dopaminergic neurons. When investigating the PD in terms of efficacy and safety of compounds, understanding of the time to onset of action is vital. Interaction with the BBB has, in the case of remoxipride, evidently an effect on the time to onset of action. Although from a preclinical perspective, these results endorse the assumption that full understanding of the distribution of compound to the site of action is essential for dose-finding studies.

Moreover, the geometric mean (\pm S.D.) of the concentration in brain homogenate at $t = 240$ min was found to be 1096 ± 153.3 ng/ml, with corresponding microdialysate concentration of 8.77 ± 1.46 ng/ml in the microdialysate. The ratio that is present in the brain normalized by the microdialysate concentrations is therefore 125. Since this is larger than one, it is proven that a significant portion of bound remoxipride is still present in the brain, thereby increasing the complexity of the PK of remoxipride in a rat.

A single dose study does not provide sufficient information on the distribution over the BBB. To fully understand the mechanistic interpretation of the brain distribution, these studies must first be expanded with several other dosages. Secondly, after expansion, population approach non-linear mixed effect modeling should be performed to fully comprehend the PK of remoxipride in a mechanistic way. Full understanding of the PK then allows building of a mechanism-based PK–PD model of remoxipride in rat. The small sample volumes used in the analytical methods described in this article allow, for the first time, in-depth analysis of the PK of remoxipride over time in small laboratory animals.

CONCLUSIONS

We have successfully developed online SPE–LC–MS–MS methods for the rapid analysis of remoxipride in plasma, brain microdialysates and brain homogenate.

A simple protein precipitation proved to be sufficient as plasma sample (20 μ l) clean up, before online SPE. One SPE cartridge could be used for about ninety injections, with a high extraction yield. For the measurement of remoxipride in rat brain homogenate (0.6 ml), an additional LLE was performed before online SPE. This is the first report for analyzing remoxipride in whole brain samples and although the extraction yield is relatively low, it is feasible for our *in vivo* experiments. For brain microdialysate samples (20 μ l), no pre-treatment was needed and the samples were directly injected in the LC system.

For all three sample types a good precision and accuracy of the remoxipride analysis was obtained. The LLODs are appropriate for the use in preclinical experiments. When compared to previous reports, we accomplished the analysis of remoxipride in small sample volumes, to allow collection of concentration data suitable for mechanistic pharmacological studies on remoxipride in small laboratory animals.

REFERENCES

- American Academy of Pediatrics: Committee on Drugs (1997) Alternative Routes of Drug Administration---Advantages and Disadvantages (Subject Review). *Pediatrics* **100**:143-152.
- Bouchard G, Pagliara A, Carrupt PA, Testa B, Gobry V and Girault HH (2002) Theoretical and experimental exploration of the lipophilicity of zwitterionic drugs in the 1,2-dichloroethane/water system. *Pharm Res* **19**:1150-1159.
- Budavari S, O'Neil MJ, Smith A, Heckelman PA and Kinneary JF (1996) *The Merck Index, an encyclopedia of chemicals, drugs, and biologicals*. Merck & Co., Inc., Whitehouse Station, N.J., U.S.A.
- Chaurasia CS, Muller M, Bashaw ED, Benfeldt E, Bolinder J, Bullock R, Bungay PM, De Lange ECM, Derendorf H, Elmquist WF, Hammarlund-Udenaes M, Joukhadar C, Kellogg DL, Jr., Lunte CE, Nordstrom CH, Rollema H, Sawchuk RJ, Cheung BWY, Shah VP, Stahle L, Ungerstedt U, Welty DF and Yeo H (2007) AAPS-FDA Workshop White Paper: Microdialysis Principles, Application, and Regulatory Perspectives. *J Clin Pharmacol* **47**:589-603.
- Chiou RH and Lo MW (1992) Determination of remoxipride in human plasma and urine by reversed-phase ion-pair high-performance liquid chromatography. *J Chromatogr* **581**:300-305.
- De Lange EC and Danhof M (2002) Considerations in the use of cerebrospinal fluid pharmacokinetics to predict brain target concentrations in the clinical setting: implications of the barriers between blood and brain. *Clin Pharmacokinet* **41**:691-703.
- De Ruiter C, Brinkman UAT and Frei RW (1987) Liquid Chromatographic Determination of a Substituted Benzamide in Biological Fluids Using Preconcentration and Post-Column Extraction. *Journal of Liquid Chromatography & Related Technologies* **10**:1903-1916.
- DePuy ME, Demetriades JL, Musson DG and Rogers JD (1997) Stereoselective determination of R-(+)- and S-(-)-remoxipride, a dopamine D2-receptor antagonist, in human plasma by chiral high-performance liquid chromatography. *J Chromatogr B Biomed Sci Appl* **700**:165-173.
- Graff CL and Pollack GM (2005) Nasal drug administration: potential for targeted central nervous system delivery. *J Pharm Sci* **94**:1187-1195.
- Hammarlund-Udenaes M, Paalzow LK and de Lange EC (1997) Drug equilibration across the blood-brain barrier--pharmacokinetic considerations based on the microdialysis method. *Pharm Res* **14**:128-134.
- Jansson B and Bjork E (2002) Visualization of in vivo olfactory uptake and transfer using fluorescein dextran. *J Drug Target* **10**:379-386.
- Main DC, Waterman AE and Kilpatrick IC (1996) Disposition of remoxipride in plasma and cerebrospinal fluid in sheep. *J Vet Pharmacol Ther* **19**:402-404.
- Moghaddam B and Bunney BS (1989) Ionic composition of microdialysis perfusing solution alters the pharmacological responsiveness and basal outflow of striatal dopamine. *J Neurochem* **53**:652-654.
- Nadal R (2001) Pharmacology of the atypical antipsychotic remoxipride, a dopamine D2 receptor antagonist. *CNS Drug Rev* **7**:265-282.
- Nilsson LB (1990) Determination of remoxipride in plasma and urine by reversed-phase column liquid chromatography. *J Chromatogr* **526**:139-150.
- Ogren SO, Lundstrom J and Nilsson LB (1993) Concentrations of remoxipride and its phenolic metabolites in rat brain and plasma. Relationship to extrapyramidal side effects and atypical antipsychotic profile. *J Neural Transm Gen Sect* **94**:199-216.
- Stevens J, Suidgeest E, Van der Graaf PH, Danhof M and De Lange EC (2009) A New Minimal-Stress Freely-Moving Rat Model for Preclinical Studies on Intranasal Administration of CNS Drugs. *Pharm Res* **26**:1911-1917.
- Van Zutphen LFM, Baumans V and Beynen AC (2003) *Handboek Proefdierkunde; Proefdiereen, dierproeven, alternatieven en ethiek*. Elsevier Gezondheidszorg.

- Viswanathan C, Bansal S, Booth B, DeStefano A, Rose M, Sailstad J, Shah V, Skelly J, Swann P and Weiner R (2007) Quantitative Bioanalytical Methods Validation and Implementation: Best Practices for Chromatographic and Ligand Binding Assays. *Pharmaceutical Research* **24**:1962-1973.
- Widman M, Nilsson LB, Bryske B and Lundstrom J (1993) Disposition of remoxipride in different species. Species differences in metabolism. *Arzneimittelforschung* **43**:287-297.

Systemic- and direct nose-to-brain transport in the rat; a pharmacokinetic model for remoxipride after intravenous and intranasal administration *Manuscript submitted*

J. Stevens¹, B. A. Ploeger², P. H. van der Graaf³, M. Danhof^{1,2},
E. C. M. de Lange¹.

¹ *Division of Pharmacology, LACDR, Leiden University, Leiden, The Netherlands.*

² *LAP&P Consultants B.V., Leiden, The Netherlands.*

³ *Pfizer, Pharmacometrics/Global Clinical Pharmacology, Sandwich, Kent, England.*

ABSTRACT

Intranasal (IN) administration could be an attractive mode of delivery for drugs targeting the central nervous system (CNS) potentially providing a high bio-availability due to avoidance of a hepatic first-pass effect and rapid onset of action. However, controversy remains whether a direct transport route from the nasal cavity into the brain exists. Pharmacokinetic modeling is proposed to identify the existence of direct nose-to-brain transport in a quantitative manner.

The selective dopamine D2-receptor antagonist remoxipride was administered at different dosages, in freely moving rats, by the IN and intravenous (IV) route. Plasma- and brain extracellular fluid (ECF) concentration-time profiles were obtained, and simultaneously analyzed using non-linear mixed effects modeling.

Brain ECF/plasma AUC ratios were 0.28 and 0.19 after IN and IV administration, respectively. A multi compartment pharmacokinetic model with two absorption compartments (nose-to-systemic and nose-to-brain) was found to best describe the observed pharmacokinetic data. Absorption was described in terms of bio-availability and rate. Total bioavailability following IN administration was 89%, of which 75% was attributed to direct nose-to brain transport. Direct nose-to-brain absorption rate was slow, explaining prolonged brain ECF exposure after IN compared to IV administration.

These studies explicitly provide separation and quantitation of systemic- and direct nose-to-brain transport after IN administration of remoxipride in the rat. Describing remoxipride pharmacokinetics at the target site (brain ECF) in a semi-physiology based manner would allow for better prediction of pharmacodynamic effects.

INTRODUCTION

Many diseases, including Parkinson's disease, schizophrenia and depression are related to dysfunctions of the dopaminergic system in the central nervous system (CNS). The effects of therapeutic agents following oral administration are often limited due to active first-pass clearance by the liver and restricted blood-brain barrier (BBB) transport. In theory, direct injections into the brain, by intracerebroventricular or intraparenchymal injections, are an alternative to the oral route. However, these methods are invasive and risky and therefore not suitable for application in clinical practice. Moreover, local injection does not always result in sufficient CNS target site distribution, as brain diffusion may be slow relative to elimination processes (De Lange, et al., 1995; Dhuria, et al., 2009).

Intranasal (IN) administration could be an attractive alternative mode of delivery for drugs targeting the CNS, potentially providing high bioavailability due to avoidance of a hepatic first-pass effect and rapid systemic uptake via perivascular spaces in the respiratory epithelium (Chien, et al., 1989). Apart from that, the olfactory epithelial pathway may allow therapeutic agents to diffuse into the perineural spaces, crossing the cribriform plate, ending up in the cerebrospinal fluid (CSF) (Frey, et al., 1997; Baker and Spencer, 1986). In addition, the olfactory nerve pathway may allow intracellular transport through olfactory sensory neurons, passing the cribriform plate, into the olfactory bulb (Bagger and Bechgaard, 2004). By directly targeting the brain, it has been hypothesized that IN delivery can enhance the CNS target site bioavailability and the efficacy of CNS drugs (Graff and Pollack, 2005; Illum, 2004; Jansson and Bjork, 2002).

Typically, IN administration data are compared to various other administration routes, on the basis of area under the curve (AUC) of plasma-, and CSF concentration-time profiles. However, although CSF-over-plasma AUC ratios reflect differences in exposure after IN administration (Van den Berg, et al., 2004), it does not allow the distinction between direct nose-to-brain transport and systemic uptake in terms of absorption rate and bioavailability. Consequently, the existence of a direct nose-to-brain route is still a matter of debate (Dhuria, et al., 2009). PK modeling would provide the opportunity to quantify the systemic- and direct nose-to-brain absorption separately, which is not possible on the basis of AUC comparison.

Another important factor is that CSF concentrations do not necessarily reflect target site concentrations (De Lange and Danhof, 2002). This is because of factors related to CSF turnover, intra-brain diffusion, extra-intracellular

exchange, and qualitative and quantitative differences in BBB and blood-CSF-barrier transport mechanisms. As many targets (receptors) are facing the brain extracellular fluid (ECF), brain ECF concentrations are anticipated to reflect target site concentrations best and will therefore provide a better basis to describe pharmacokinetic (PK)- and pharmacodynamic (PD) relations in a more mechanistic manner (Del Bigio, 1994; De Lange, et al., 1999; De Lange and Danhof, 2002; De Lange, et al., 2005; Watson, et al., 2009; Jeffrey and Summerfield, 2010).

Our interest is to investigate the PK-PD mechanisms that play a role in modulation of the dopaminergic system and the use of IN administration of dopaminergic drugs that often encounter very low bioavailability and/or limited BBB transport. The aim of the study was to quantitatively assess direct transport of remoxipride into the brain following IN administration. Remoxipride is a weak, but selective, dopamine D2-receptor antagonist (Farde and Von Bahr, 1990; Köhler, et al., 1990) and was prescribed as an atypical antipsychotic (Roxiam®) at the end of the eighties. Due to a few cases of aplastic anemia, the drug was withdrawn from the market (Philpott, et al., 1993). However, remoxipride is still of interest as a paradigm compound in mechanism-based PK-PD studies on the dopaminergic system.

Using our previously reported minimum stress, freely moving rat model for IN and IV drug administration (Stevens, et al., 2009), plasma- and brain ECF samples were obtained over time, following IV- and IN administration of 4, 8, or 16 mg/kg remoxipride. Compartmental PK non-linear mixed effects modeling using NONMEM (Beal and Sheiner, 1992)) was applied to quantify the direct nose-to-brain distribution in terms of absorption rate and bioavailability.

METHODS

■ Animals

All animal procedures were performed in accordance with Dutch laws on animal experimentation. The study protocol was approved by the Animal Ethics Committee of Leiden University (UDEC 6132). Male Wistar WU rats ($n = 60$, 253 ± 20 g, Charles River, The Netherlands) were housed in groups for 7-13 days (Animal Facilities, Gorlaeus Laboratoria, Leiden, The Netherlands), under standard environmental conditions (ambient temperature 21°C; humidity 60%; 12/12 hour light, background noise, daily handling), with *ad libitum* access to food (Laboratory chow, Hope Farms, Woerden, The Netherlands) and acidified water. Between surgery and experiments, the rats were kept individually in Makrolon type 3 cages for 7 days to recover from the surgical procedures.

■ Surgery

Rat surgery and experiments were performed as previously reported (Stevens, et al., 2009). In short, during anesthetized surgery, all animals received cannulas in the femoral artery and vein for serial blood sampling and drug administration respectively. Also, an IN probe (AP 12mm and L -0.5 mm relative to Bregma) for drug administration, and a microdialysis guide (caudate putamen; AP +0.4, L 3.2, V -3.5 relative to Bregma), were implanted. After 6 days, the microdialysis guide was replaced by a microdialysis probe (CMA/12, 4 mm polycarbonate membrane, cut-off 20 kD, Aurora Borealis Control, Schoonebeek, The Netherlands) for continuous brain ECF sampling (Chaurasia, et al., 2007). At 24 ± 1 hour later, the experiments were started.

■ Experiments

The rats were randomly assigned to 3 groups ($n = 20$ per group), to receive 4, 8, or 16 mg remoxipride (Tocris, Bristol, United Kingdom) per kg body-weight. Per group, at $t = 0$ min (corresponding with actual time of 10 AM ± 1 h), remoxipride in saline (B. Braun Melsungen AG, Melsungen, Germany) was administered via either a 1 minute IN infusion ($n = 10$), or a 30 minute IV infusion ($n = 10$), using an automated pump (Harvard apparatus 22, model 55-2222, Holliston, MA, USA). For the IN infusions, different remoxipride solutions were used to ensure similar flow rates (± 19 $\mu\text{l}/\text{min}$) and total IN administered volumes.

Before the experiments, perfusion fluid consisting of 145 mM NaCl, 0.6 mM KCl, 1.0 mM MgCl_2 , 1.2 mM CaCl_2 , 0.2 mM ascorbic acid, in a 2 mM potassium phosphate buffer, pH 7.4 (Moghaddam and Bunney, 1989) was prepared. From $t = -30$ to 240 min, the microdialysis probe was continuously flushed with perfusion fluid at a flow rate of 2 $\mu\text{l}/\text{min}$. Microdialysate samples were collected every 10 minutes for the first 2 hours, and every 20 minutes thereafter until the end of the experiments and collected in a cooled fraction collector (Univentor 820 Microsampler, Antec, The Netherlands). The microdialysis samples were weighed to confirm accurate sampling volumes and stored at -80°C , pending analysis. Microdialysis samples were considered accurate and further used only when their volume was within 95-105% of the expected volumes of 20 or 40 μl for 10- and 20 min samples respectively. Blood samples of 200 μl each were taken from the arterial cannula at $t = -5$ (blank), 5, 10, 20, 35, 60, 90, 120, 150, 180, and 240 min and collected in EDTA-coated vials. After centrifuging for 15 minutes at 5000 rpm, the plasma was stored at -20°C . After the experiments, the animals were decapitated following an overdose of Nembutal (1 ml, IV).

Two animals from the 4 mg/kg IN dosing group were excluded as the nasal cannula was partially blocked. At some instances during plasma sampling, the arterial cannula was blocked, thereby preventing further sampling. Ultimately, 350 plasma and 235 brain ECF samples could be obtained from 58 remoxipride treated rats and were analyzed for remoxipride. The IV study consisted of 190 plasma-, and 126 brain ECF data points, the IN study of 160 plasma-, and 109 brain ECF data points.

■ Analytical Methods

Analytical methods for the quantitation of remoxipride in small plasma- and brain microdialysate samples have been previously reported (Stevens, et al., 2010). In short, for the measurements of remoxipride concentrations in plasma, online solid phase extraction was followed by high-pressure liquid chromatography-tandem mass spectrometry (Finnigan TSQ Quantum Ultra Mass Spectrometer System, Thermo Fischer Scientific, Breda, The Netherlands).

Brain microdialysate samples were measured using high-pressure liquid chromatography-tandem mass spectrometry, without sample clean up. Remoxipride concentrations in microdialysate samples were corrected for *in vivo* recovery through the microdialysis probe and tubing (based on *in vivo* loss (20, 100 and 500 ng/ml), with mean \pm S.E.M. = 20 % \pm 0.6), to yield estimates of brain ECF concentration values (Chaurasia, et al., 2007).

Data acquisition and processing was performed using LC-Quan provided by Thermo Fisher Scientific. For constructing the calibration curve, linear regression analysis was applied using weigh factor $1/Y^2$. The lower limits of detection were 0.15 and 0.08 ng/ml remoxipride in plasma- and in microdialysate samples respectively. The lower limits of quantification were 0.5 and 0.25 ng/ml for plasma and microdialysate samples respectively. Using the obtained individual plasma- and brain ECF profiles, mean AUC \pm S.E.M values were calculated per matrix (plasma/brain ECF), dose (4, 8, 16 mg/kg) and study (IN/IV) group, using the trapezoidal rule (from $t = 0$ min until the end of experiments).

■ Pharmacokinetic model building and random variability

Nonlinear mixed effect modeling using NONMEM (version VI, level 2.0, Icon Development Solutions, Ellicott City, Maryland, USA) was used for the structural model building, performed under ADVAN 6, and the first order conditional method with interaction was used for estimation with a conver-

gence criterion of 3 significant digits in the parameter estimates. NONMEM reports an objective function value (OFV), which is the $-2 \cdot \log$ likelihood. Model hypothesis testing was done using the likelihood ratio test under the assumption that the difference in $-2 \cdot \log$ likelihood is Chi-square distributed with degrees of freedom determined by the number of additional parameters in the more complex model. Hence, with a decrease in the OFV of at least 3.84 points ($p < 0.05$) the model with one additional parameter is preferred over its parent model.

Additive, proportional, or combined residual variability models were investigated separately for the remoxipride concentrations in plasma and in brain ECF (measurement compartments). Log normal distribution of the inter-individual variability (IIV) was assumed and possible covariate correlations were taken into account. Calculation of the coefficient of variation (CV) was used to derive the uncertainty in the parameter estimates of the model and considered acceptable when lower than 50%.

By this approach, several compartmental model structures were optimized (Figure 1).

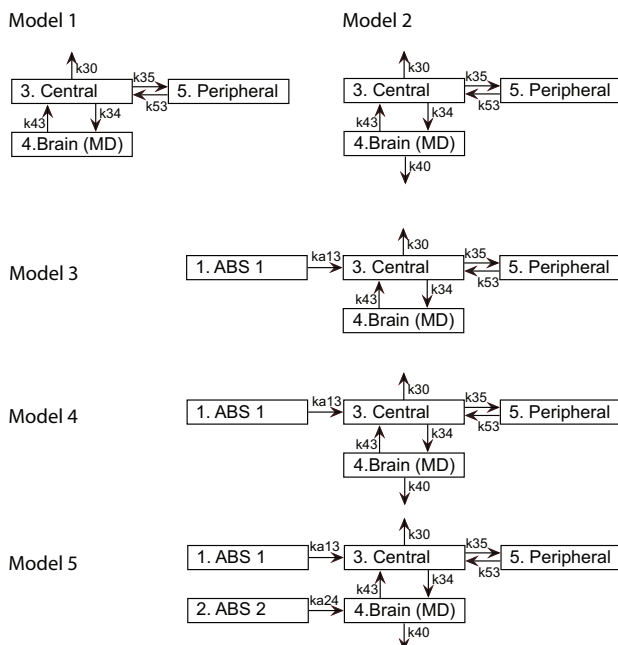
Typical values for the PK parameters clearance (CL), volume of distribution (V), and inter-compartmental clearance (Q, clearance between the compartments) were estimated, based on parameter estimates (θ). When identifiable, a term expressing IIV (η) was included (equation 1).

Equation 1; Typical value = $\theta \cdot e^\eta$

Transport of remoxipride over time between the compartments and elimination processes were defined by rate constants (equation 2) based on the typical estimated values for CL (or Q) and V.

Equation 2; $k_{x,y} = CL_{xy}/V_x$

Figure 1 Compartmental model structures. The models consists of; 1) an absorption compartment (ABS 1), 2) a second absorption compartment (ABS 2) describing direct nose-to-brain transport, 3) a central measurement compartment (Central; plasma concentrations), 4) a brain measurement compartment (Brain; brain ECF concentrations), and 5) a peripheral compartment (Peripheral) describing the distribution into other tissues and organs. k_a , absorption rate constant; k_{30}/k_{40} , first order elimination rate constants; k , rate constants with compartment-associated numbers.



In model 1, plasma and brain ECF data following IV administration of remoxipride were simultaneously modeled in a structural model consisting of a central, a brain and a peripheral compartment (Figure 1, model 1). For the elimination of remoxipride from plasma, a first order elimination rate constant was applied (k_{30}). As removal of remoxipride from the brain was underestimated, an additional first order elimination rate constant (k_{40}) was applied in a second structural model approach (Figure 1, model 2). The value for k_{40} was assumed to be smaller than k_{30} , and therefore calculated as the estimated fraction of k_{30} (equation 3).

Equation 3; $k_{40} = (\theta * e\eta) * k_{30}$

As models 1 and 2 are nested (based on identical datasets), their OFVs can be used as comparative means to identify the model that best describes the data, taking into account the number of additional parameters. These two models formed the basis for the identification of more complex model structures that include the IN dataset.

For inclusion of the IN dataset, an absorption compartment with an absorption rate constant (ka) was added to the model structure, here as ka_{13} . In the first instance, ka_{13} and bioavailability from the site of absorption to the central plasma compartment (F_1) were estimated, leaving out brain elimination (Figure 1, model 3). An improvement was made by addition of k_{40} (Figure 1, model 4) using the same approach as for model 2.

In the final model (Figure 1, model 5), a second absorption compartment was added, describing the hypothesized direct nose-to-brain transport. Absorption from the IN site of administration to the brain results from transport of compound over a longer distance when compared to systemic absorption, as the latter depends on the nasal vascular system that is closely located to the site of administration. As a result, direct nose-to-brain transport is a relatively slow process compared to systemic absorption (Dhuria, et al., 2009). Therefore, typical values for the absorption rate constants were estimated on the assumption that the absorption rate constant to the central compartment (ka_{13}) is higher than the absorption rate constant into the brain compartment (ka_{24}). The total bioavailability (F_{TOT}) was defined as the sum of the bioavailability to the central compartment (F_1) and that for the brain compartment (F_2). During model optimization, typical values for F_1 and F_{TOT} were estimated, whereas F_2 was calculated ($F_2 = F_{TOT} - F_1$). The change in amount of remoxipride (dA) in each compartment over time (dt) was described using differential equations (equations 4-8).

Equation 4; Nose-to-systemic absorption: $dA_{ABS1}/dt = -A_{ABS1} \cdot ka_{13}$

Equation 5; Nose-to-brain absorption: $dA_{ABS2}/dt = -A_{ABS2} \cdot ka_{24}$

Equation 6; Central absorption and elimination:

$$dA_{central}/dt = A_{ABS1} \cdot ka_{13} - A_{central} \cdot k_{34} + A_{brain} \cdot k_{43} - A_{central} \cdot k_{35} + A_{periph} \cdot k_{53} - A_{central} \cdot k_{30}$$

Equation 7; Brain absorption and elimination:

$$dA_{brain}/dt = A_{ABS2} \cdot ka_{24} + A_{central} \cdot k_{34} - A_{brain} \cdot k_{43} - A_{brain} \cdot k_{40}$$

Equation 8; Peripheral distribution and elimination:

$$dA_{periph}/dt = A_{central} \cdot k_{35} - A_{periph} \cdot k_{53}$$

The optimized models 3, 4 and 5 are nested and were therefore compared on the basis of OFV.

■ Model evaluation

All optimized models were internally qualified based on goodness-of-fit for individual concentration-time profiles in plasma and brain ECF. As for the intravenous administration groups, doubling of the dose leads to doubling of the plasma- and brain ECF AUC's, BBB transport of remoxipride was not considered to be subject to active influx- or efflux processes. Hence, observed remoxipride concentrations were normalized to dose (16 mg/kg) before

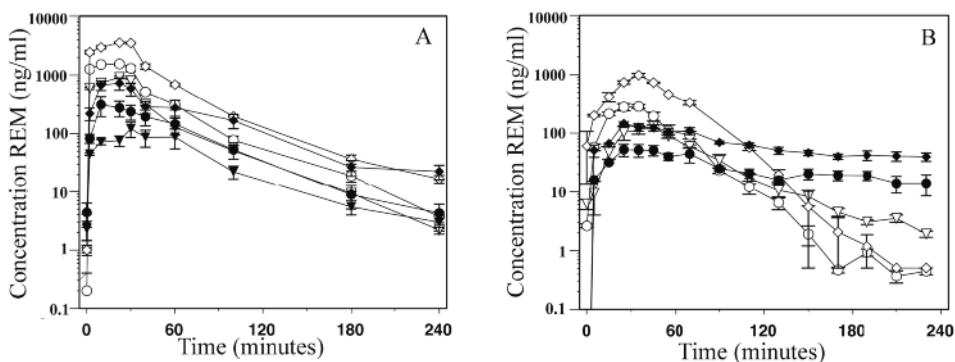
performance of a visual predictive check (VPC). The VPCs were performed using NONMEM VI, by simulating 1000 replications of the PK model and a simulation dataset that contained dosing information for one individual rat per dosing regimen and administration group. The median, 5 and 95 percentiles were calculated for each simulated time-point. The predictions at each time-point (median and 90 % prediction interval) were compared visually with the actual normalized data. Resemblance between simulated and original distributions indicates the accuracy of the model (i.e., 90 % of the observed data should fall within the predicted range for 90 % of the variability) (Post, et al., 2008).

RESULTS

■ Remoxipride plasma and brain ECF data following IV and IN administration

Plasma concentration-time profiles of remoxipride following IV- and IN administration of 4, 8 and 16 mg/kg of remoxipride are shown in figure 2A. The maximal remoxipride concentration (C_{\max}) in plasma is higher following IV administration, when compared to the C_{\max} following IN administration of a similar dose. Moreover, the slope of the concentration-time profile during the elimination phase seemed to be slower following IN compared to IV administration, and indicates slow absorption processes. The brain ECF concentration-time profiles are shown in figure 2B.

Figure 2 Mean concentration-time profiles (\pm S.E.M.) of remoxipride in plasma (2A) and brain ECF (2B), after 30-minute IV (open symbols), or 1-minute IN (closed symbols) infusion of 4, 8, or 16 mg/kg remoxipride (triangles, circles, and diamonds respectively).



The C_{\max} for brain ECF concentrations after IN administration was lower than the C_{\max} following IV administration. Furthermore, following IN administration, remoxipride brain ECF concentrations decreased slower when compared to IV administration.

As a consequence, the $AUC_{\text{brain ECF}}/AUC_{\text{plasma}}$ ratio value following IN administration was higher when compared to IV administration (Table 1). This indicates direct nose-to-brain transport (Van den Berg, et al., 2004). Doubling of the dose (4 to 8 to 16 mg/kg) resulted in doubling of the mean AUC_{plasma} and AUC_{brainECF} in both IV and IN studies (Table 1), indicating linear BBB distribution.

Table 1 Mean area's under the curve (\pm S.E.M.) from 0 to 4 hours of individual plasma- and brain ECF concentration-time profiles per study and matrix.

	Intravenous study			Intranasal study		
Dose (mg/kg)	Plasma AUC ($\mu\text{g} \cdot \text{min}/\text{ml}$)	Brain ECF AUC ($\mu\text{g} \cdot \text{min}/\text{ml}$)	Brain ECF AUC/ plasma AUC (%)	Plasma AUC ($\mu\text{g} \cdot \text{min}/\text{ml}$)	Brain ECF AUC ($\mu\text{g} \cdot \text{min}/\text{ml}$)	Brain ECF AUC/ plasma AUC (%)
4	44.9 (7.7)	7.9 (1.7)	17.5	10.8 (2.9)	-	-
8	70.1 (4.7)	14.0 (0.7)	19.9	20.0 (5.5)	4.9 (0.8)	24.7
16	173.0 (9.0)	34.6 (7.1)	20	53.9 (11.4)	16.7 (2.4)	31
Mean brain/plasma AUC per study			19 (0.8)	28 (2.6)		

- not determined.

■ **Development of the structural PK model for simultaneous analysis of IN and IV data**

The plasma- and brain ECF remoxipride concentrations following IV and IN administration were modeled in NONMEM VI. Several structural models were examined to investigate brain elimination and hypothesized direct nose-to-brain transport (see Methods for details). Table 2 summarizes the OFVs, parameter estimates with their precision (CV), IIV and residual error for all structural models. Because of linear BBB distribution, all the observed plasma- and brain ECF concentrations could be normalized to dose before performing VPCs.

Table 2 Model summary, parameter estimates with coefficients of variation, and calculated pharmacokinetic parameters.

Model summary	Model 1			Model 2			Model 3			Model 4			Model 5		
Dataset	IV			IV			IV & IN			IV & IN			IV & IN		
Brain elimination	No			Yes			No			Yes			Yes		
Absorption	No			No			1			1			2		
OFV	-1430			-1758			-2815			-3239			-3435		
Parameter estimate*	TE (CV%)	IIV		TE (CV%)	IIV		TE (CV%)	IIV		TE (CV%)	IIV		TE (CV%)	IIV	
CL3 (l/h/kg)	2.22 (12.1)	0.41		0.59 (24.1)	0.32		1.80 (15.2)	0.38		0.36 (36.2)	0.27		1.12 (10.1)	0.04	
V3 (l/kg)	0.050 (24.2)	ne		0.062 (16.6)	ne		0.073 (25.2)	ne		0.08 (14.8)	ne		0.088 (13.6)	ne	
Q4 (l/h/kg)	0.98 (9.8)	ne		1.38 (13.3)	ne		1.66 (27.3)	ne		1.59 (20.1)	ne		0.70 (19.9)	ne	
V4 (l/kg)	0.41 (39.3)	ne		1.47 (12.0)	ne		0.18 (20.7)	0.31		3.02 (40.7)	0.21		0.873 (24.1)	0.06	
Q5 (l/h/kg)	1.13 (21.6)	ne		1.18 (11.1)	ne		0.567 (12.3)	ne		1.04 (15.6)	ne		1.20 (10.2)	ne	
V5 (l/kg)	0.13 (22.4)	0.10		0.425 (7.9)	0.05		0.325 (7.14)	ne		0.36 (16.5)	ne		0.417 (8.60)	0.08	
FK40 (/h)	-	-		-	-		-	-		0.36 ***	-		0.302 (17.5)	ne	
ka ₁₃ (/h)	-	-		-	-		1.56 (19.1)	0.44		1.94 (20.7)	0.35		1.54 (11.8)	0.17	
ka ₂₄ (/h)	-	-		-	-		-	-		-	-		0.033 (43.8)	ne	
F _{TOT}	-	-		-	-		-	-		-	-		0.89 (4.60)	0.48	
F ₁	-	-		-	-		0.171 (22.6)	0.17		0.19 (19.8)	0.52		0.22 (20.1)	0.09	
RV plasma	0.0629			0.057			0.12			0.11			0.098		
RV microdialysate	0.48			0.203			0.368			0.19			0.103		
Calculated parameters															
F ₂	-			-			-			-			0.67		
k ₃₀ (/h)	44.4			9.5			24.7			4.5			12.7		
k ₄₀ (/h)	-			3.45 (8.9)**			-			1.62			3.84		

* parameter estimates are given with their compartment number, according to figure 1;

** estimated parameter;

*** fixed parameter; RV interindividual variability; FK40 k₄₀ as fraction of k₃₀; ne not estimated in model.

IV data

For data obtained following IV administration of remoxipride, model 1 consisted of a central, peripheral and brain compartment (Figure 1). Parameter estimates showed low CVs (< 25%), indicating good precision for all typical parameter estimates. A relatively large IIV was identified for CL3 and V5,

while a proportional error model best described the residual error in both measurement compartments. The median of the plasma VPC of model 1 (Figure 3), shows good prediction of the C_{\max} in plasma, but the concentrations during elimination were under-predicted. All the brain ECF concentrations were over-predicted by the model. The variability could not be adequately estimated as indicated by large confidence interval of the VPCs, when compared to the original distribution.

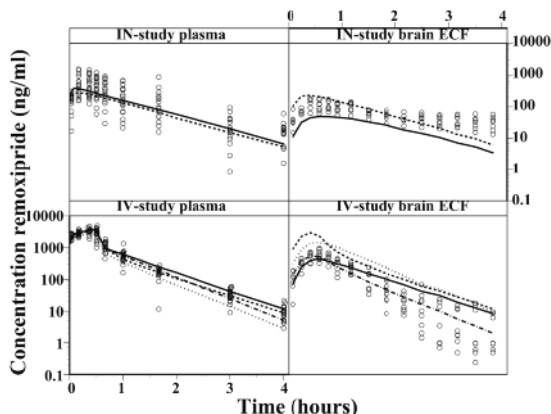
Addition of brain elimination in model 2 (Figure 1) showed improved model predictions for plasma and brain ECF observations (Figure 3). The brain ECF observations were now randomly distributed around the simulated median, indicating improved accuracy of the model. The OFV was improved compared to model 1 (328 points) and IIV was identified for the same parameters. Overall, the CVs were decreased compared to model 1, indicating better estimation of parameter estimates. Based on the overall decrease in values for IIV and residual errors (proportional), model 2 was better able to accurately estimate the variability as well.

IV and IN data

Following IN administration, a single systemic absorption compartment (Figure 1, model 3) allowed for parameter estimation with low CVs. The plasma concentrations of the IV study were well described by VPC median of model 3 (Figure 3). However, the brain ECF concentrations following IV administration were poorly predicted. Specifically, the C_{\max} was over-predicted and, although for the elimination phase the slope of the median followed the slope of the observations, there was over-prediction of the observed concentrations for the full time range. After IN administration, model 3 under-predicted the C_{\max} in plasma and the brain ECF observations were not randomly distributed around the simulated median due to over-prediction of the high concentration range (including C_{\max}) and under-predicting the lower concentration range. Significant IIV variability was identified on CL₃, V₄, ka_{13} , and F_1 , and a proportional error model best described residual error in the central- and brain compartment. Since the parameter estimates did not allow good predictions of the brain ECF observations, total bio-availability could not be accurately estimated.

Again, incorporation of brain elimination in the model (model 4) greatly improved the OFV (424 points). Also, the VPC median for the brain ECF concentration-time profiles after IV administration was better when compared to model 3 (Figure 3), albeit that still a slight under-prediction of C_{\max} and over-prediction of concentrations during the elimination phase was observed.

Figure 3 The observed remoxipride concentrations (open circles) per study and measurement compartment. The medians of the VPCs of model 1 until 4 are represented by the dotted, dash-dotted, dashed and solid lines respectively.

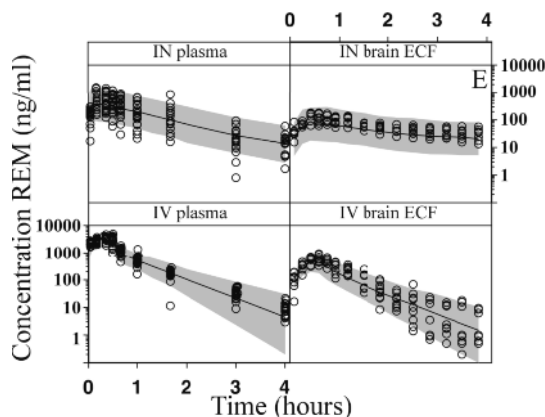


Specifically, after IN administration, the C_{\max} in brain ECF was under-predicted, as were all concentrations during the elimination phase. The uncertainties for the parameter estimates (CV) were slightly higher, IIV variability was identified on CL3, V4, ka_{13} , and F_1 , and a proportional error model best described residual error in both measurement compartments.

The final model (Figure 1, model 5) took into account a second, direct transportation route from the nasal cavity to the brain ECF compartment, as well as brain elimination. In contrast to model 4, the VPC (Figure 4) showed good prediction for both the plasma- and brain ECF concentrations after IV administration. The plasma observations after IN administration were also accurately described. The major advancement of the final model was represented in the median of the brain ECF VPC, which described the observations well, although a minor under-prediction of the C_{\max} and elimination phase was observed. This led to a highly significant improvement in goodness-of-fit compared to model 4 (OFV decrease from -3239 to -3435). The majority of the observations for IN- and IV administration were within the 90% prediction interval.

The CVs decreased for all estimated parameters, indicating improved certainty for the parameter estimations. In addition to the IIV on CL3, V4, ka_{13} , and F_1 in the previous model, IIV could also be identified for V5 and F_{TOT} . Again, proportional error models best described the residual error in both plasma and brain ECF compartments.

Figure 4 Visual predictive check of the final model, representing the observed remoxipride concentrations (open circles) per study and measurement compartment, the median concentration predictions of the model (black line), and the 90% prediction intervals (grey area).



Since the remoxipride concentrations were accurately predicted in both plasma- and brain ECF, the absorption rate constant- and bioavailability parameter estimates can be considered accurate. In the final model, the low value of the absorption rate constant to the brain (ka_{24}) represents slow transport mechanisms from the nose to the brain and showed a relatively high CV (43.8%). The bioavailability of direct nose-to-brain transport was found to be 75% (F_2/F_{TOT}) of the F_{TOT} (89%). The ka_{24} was low when compared to the ka_{13} , explaining the relative slow decrease in plasma- and brain ECF concentrations over time following IN administration. This indicates fast absorption into plasma and consecutive BBB transport, after which concentrations in brain ECF are maintained by (slower) direct nose-to-brain transport. IIV for F_{TOT} was found to be 0.48. Furthermore, the use of dense serial blood and microdialysis sampling allowed for a precise estimation of the F_{TOT} (CV of only 4.6%).

Further data analysis showed a smaller apparent total volume of distribution when comparing models 2 and 5. These factors indicate a more complex distribution from the nasal cavity to the site of measurement. Addition of absorption and/or brain compartments were considered in the early phase of the structural model building, e.g. dual (slow and fast) direct nose-to-brain transport or an extra compartment between the absorption- and brain compartment. However, additional absorption processes and/or compartments could not be identified with the present dataset from our animal model.

DISCUSSION

The aim of the study was to quantitatively assess direct transport of remoxipride into the brain following IN administration. To this end, plasma- and brain ECF concentration-time profiles were obtained following IV and IN administration of 3 different dosages, and data were analyzed using a PK modeling approach. A multi-compartment, semi-physiologically-based PK model with one absorption compartment from the nose into the systemic circulation and one from the nose into the brain compartment was found to best describe the observed data. Total bioavailability following IN administration was 0.89, of which 75% was attributed to direct nose-to brain transport. The absorption rate constant from the nose to the brain was low when compared to the absorption rate constant for systemic uptake, explaining the relatively slow decrease in plasma- and brain ECF concentrations over time following IN administration. These studies explicitly provide separation and quantitation of systemic- and direct nose-to-brain transport after IN administration.

To characterize BBB transport in rats, increasing and decreasing remoxipride concentrations in plasma- and brain ECF over time were obtained using 30 minute IV infusion. For IN administration, the duration of the intranasal administration was restricted by maximum solubility of remoxipride and the maximum administration volume in freely moving rats (Stevens, et al., 2009). Standard nonparametric analysis of our data showed that BBB transport was linear. Although no preclinical literature could be found to compare these results, in schizophrenic patients remoxipride readily passes the BBB (Farde and Von Bahr, 1990). Furthermore, as only free drug concentrations can cross the BBB, protein binding needs to be considered. Slight concentration dependent plasma binding has been reported in patients with tardive dyskinesia (Widerlov, et al., 1991), however, we did not find any indication for this in our dose range. As BBB transport appeared to be linear and measurements were taken in the plasma- and brain compartment, Q_4 represents movement of unbound remoxipride concentrations, thereby incorporating protein binding.

Despite an approximate doubling of C_{\max} in plasma and brain ECF for IV compared with IN administration, the elimination is slower for the latter (Figure 2). The slower elimination for IN indicates an absorption rate dependent elimination rate (flip-flop kinetics), being most pronounced in the brain ECF (Figure 3). The resulting increase of $AUC_{\text{brain ECF}}/AUC_{\text{plasma}}$ for IN when compared to IV administration (Table 1), suggests direct nose-to-brain transport (Van den Berg, et al., 2004). For remoxipride it seems that

a fast onset of action can be reached by the fast systemic uptake, while the slower direct nose-to-brain transport can result in a prolonged duration of effect after intranasal administration of CNS-active drugs. If this holds true, remains to be seen in our currently progressing study on remoxipride PK-PD relationship following IV and IN administration.

In model 1, the VPCs revealed misspecification of the brain ECF concentration predictions. Hepatic clearance and urinary excretion are known to result in elimination of remoxipride from plasma (Widerlov, et al., 1989; Nilsson, 1998), as was included in our model approaches by the first order elimination rate constant k_{30} . An additional parameter for brain-elimination was essential to predict both plasma- and brain ECF observations adequately (model 2), indicating that more complex processes are responsible for the clearance of remoxipride from the brain ECF. The main metabolic routes in rodents are 1) hydroxylation and 2) O-demethylation at the aromatic moiety of remoxipride. Remoxipride metabolites have been previously identified in rat brain, and have been contributed to liver metabolism and consecutive BBB transport (Ahlenius, et al., 1997). However, in another study, O-demethylase activity has been identified in rat brain (Jolival, et al., 1995), which could account for brain metabolism of remoxipride. To our knowledge, there are no studies that implicate remoxipride as a substrate for brain efflux transporters. In our model, the clearance processes in the brain were lumped in a single first order elimination rate constant (k_{40}), awaiting more mechanistic data on brain elimination processes (e.g. by *in vitro* studies) to further develop the model for specific mechanistic understanding.

Simultaneous analysis of the IV and IN datasets using models 3 and 4 yielded the consistent finding that brain elimination is essential to predict brain ECF remoxipride concentrations. However, this approach could not explain the slower decrease in remoxipride concentrations in brain ECF following IN administration. The final model took into account a second, direct transportation route from the nasal cavity to the brain ECF compartment, as well as brain elimination. This led to a highly significant improvement in goodness-of-fit for remoxipride plasma- and brain ECF concentration-time profiles as reflected in the reduction of the OFV, CVs, IIV and improved VPC. Consequently, the bioavailability parameters could be considered precise.

Regarding intra-individual variability following IN administration, one has to take into account that there are many protective barriers in the nasal cavity, such as mucociliary clearance, efflux transporter proteins and metabolizing enzymes that influence the absorption of compounds (Dhuria, et al., 2009), which may all contribute.

The low value found for the ka_{24} (0.033 /h) represents slow transport mechanisms via the olfactory epithelial- and/or olfactory nerve pathway, that are both subject to IIV. Although IIV on ka_{24} as such could not be identified, it may explain the lower precision of ka_{24} , when compared to ka_{13} , the latter which is associated with a smaller absorption distance. It would be of interest to quantify the olfactory epithelial- and nerve pathways separately, which is not possible with the current dataset. In future investigations, measuring remoxipride brain ECF concentrations simultaneously in several brain regions could allow the quantification of separate absorption rate constants for the different direct nose-to-brain transport routes.

From our studies, it is clear that brain ECF concentrations are influenced by direct nose-to-brain transport, BBB transport following systemic uptake and brain elimination processes. To understand the effect of CNS-active drugs, it is pertinent to understand the drug exposure at the target site (brain ECF) as this provides a better basis for the determination of concentration-effect relationships following IN administration. In humans, information on target site distribution is more difficult to obtain when compared to animal studies. However, based on preclinically derived semi-physiologically-based PK parameters, translational modeling would allow simulation of human brain ECF concentrations, which can form the basis of PK-PD models that will help towards increased safety and efficacy (Danhof, et al., 2008). Small scale, efficient clinical trials could subsequently provide the accuracy of these pre-clinical derived translational models.

In conclusion, by simultaneous modeling of plasma- and brain ECF concentration-time profiles obtained following IV and IN routes of administration of remoxipride, we have provided a semi-physiologically-based PK model on the target site distribution of remoxipride. The model provides quantitative evidence of direct nose-to-brain transport after IN administration. Also, pharmacokinetic modeling allowed the quantification of brain elimination, which contributed significantly to clearance of remoxipride. Further investigations on the plasma- and brain ECF PK of other compounds should lead to a more generalized model for IN administration, since direct nose-to-brain transport is compound dependent. Describing rat brain PK in a semi-physiology based manner is anticipated to allow for simulation of human brain ECF concentrations by means of translational models. This will aid in the prediction of the efficacy and safety of CNS active compounds after IN administration in man.

REFERENCES

- Ahlenius S, Ericson E, Hillegaart V, Nilsson LB, Salmi P and Wijkstrom A (1997) In Vivo Effects of Remoxipride and Aromatic Ring Metabolites in the Rat. *J Pharmacol Exp Ther* **283**:1356-1366.
- Bagger MA and Bechgaard E (2004) The potential of nasal application for delivery to the central brain-a microdialysis study of fluorescein in rats. *Eur J Pharm Sci* **21**:235-242.
- Baker H and Spencer RF (1986) Transneuronal transport of peroxidase-conjugated wheat germ agglutinin (WGA-HRP) from the olfactory epithelium to the brain of the adult rat. *Exp Brain Res* **63**:461-473.
- Beal SL and Sheiner BL (1992) NONMEM user's guide, Part 1, in *NONMEM user's guide, Part 1* University of California at San Francisco.
- Chaurasia CS, Muller M, Bashaw ED, Benfeldt E, Bolinder J, Bullock R, Bungay PM, De Lange ECM, Derendorf H, Elmquist WF, Hammarlund-Udenaes M, Joukhadar C, Kellogg DL, Jr., Lunte CE, Nordstrom CH, Rolfe H, Sawchuk RJ, Cheung BWY, Shah VP, Stahle L, Ungerstedt U, Welty DF and Yeo H (2007) AAPS-FDA Workshop White Paper: Microdialysis Principles, Application, and Regulatory Perspectives. *J Clin Pharmacol* **47**:589-603.
- Chien WY, Su KSE and Chang SF (1989) *Nasal systemic drug delivery*. Marcel Dekker, Inc..
- Danhof M, De Lange EC, Della Pasqua OE, Ploeger BA and Voskuyl RA (2008) Mechanism-based pharmacokinetic-pharmacodynamic (PK-PD) modeling in translational drug research. *Trends Pharmacol Sci* **29**:186-191.
- De Lange EC, Bouw MR, Mandema JW, Danhof M, de Boer AG and Breimer DD (1995) Application of intracerebral microdialysis to study regional distribution kinetics of drugs in rat brain. *Br J Pharmacol* **116**:2538-2544.
- De Lange EC and Danhof M (2002) Considerations in the use of cerebrospinal fluid pharmacokinetics to predict brain target concentrations in the clinical setting: implications of the barriers between blood and brain. *Clin Pharmacokinet* **41**:691-703.
- De Lange EC, De Boer BA and Breimer DD (1999) Microdialysis for pharmacokinetic analysis of drug transport to the brain. *Adv Drug Deliv Rev* **36**:211-227.
- De Lange EC, Ravenstijn PG, Groenendaal D and Van Steeg TJ (2005) Toward the prediction of CNS drug-effect profiles in physiological and pathological conditions using microdialysis and mechanism-based pharmacokinetic-pharmacodynamic modeling. *AAPS J* **7**:E532-E543.
- Del Bigio MR (1994) The ependyma: A protective barrier between brain and cerebrospinal fluid. *Glia* **14**:1-13.
- Dhuria SV, Hanson LR and Frey WH (2009) Intranasal delivery to the central nervous system: Mechanisms and experimental considerations. *Journal of pharmaceutical sciences* **99**:1654-1673.
- Farde L and Von Bahr C (1990) Distribution of remoxipride to the human brain and central D2-dopamine receptor binding examined in vivo by PET. *Acta Psychiatr Scand Suppl* **358**:67-71.
- Frey WH, Liu J, Chen X, Thorne RG, Fawcett JR, Ala TA and Rahman Y (1997) Delivery of 125-I-NGF to the brain via the olfactory route. *Drug delivery* **4**:87-92.
- Graff CL and Pollack GM (2005) Nasal drug administration: potential for targeted central nervous system delivery. *J Pharm Sci* **94**:1187-1195.
- Illum L (2004) Is nose-to-brain transport of drugs in man a reality? *J Pharm Pharmacol* **56**:3-17.
- Jansson B and Bjork E (2002) Visualization of in vivo olfactory uptake and transfer using fluorescein dextran. *J Drug Target* **10**:379-386.
- Jeffrey P and Summerfield S (2010) Assessment of the blood-brain barrier in CNS drug discovery. *Neurobiol Dis* **37**:33-37.
- Jolival C, Minn A, Vincent-Viry M, Galteau MM and Siest G (1995) Dextromethorphan Odemethylase activity in rat brain microsomes. *Neuroscience Letters* **187**:65-68.

- Köhler C, Hall H, Magnusson O, Lewander T and Gustafsson K (1990) Biochemical pharmacology of the atypical neuroleptic remoxipride. *Acta Psychiatr Scand Suppl* **358**:27-36.
- Moghaddam B and Bunney BS (1989) Ionic composition of microdialysis perfusing solution alters the pharmacological responsiveness and basal outflow of striatal dopamine. *J Neurochem* **53**:652-654.
- Nilsson LB (1998) High sensitivity determination of the remoxipride hydroquinone metabolite NCQ-344 in plasma by coupled column reversed-phase liquid chromatography and electrochemical detection. *Biomed Chromatogr* **12**:65-68.
- Ogren SO, Lundstrom J and Nilsson LB (1993a) Concentrations of remoxipride and its phenolic metabolites in rat brain and plasma. Relationship to extrapyramidal side effects and atypical antipsychotic profile. *J Neural Transm Gen Sect* **94**:199-216.
- Ogren SO, Lundstrom J, Nilsson LB and Widman M (1993b) Dopamine D2 blocking activity and plasma concentrations of remoxipride and its main metabolites in the rat. *J Neural Transm Gen Sect* **93**:187-203.
- Philpott N, Marsh JCW, Gordon-Smith EC, Bolton JS, Laidlaw ST, Snowden JA and Brown MJ (1993) Aplastic anaemia and remoxipride. *The Lancet* **342**:1244-1245.
- Post TM, Freijer JJ, Ploeger BA and Danhof M (2008) Extensions to the visual predictive check to facilitate model performance evaluation. *J Pharmacokinet Pharmacodyn* **35**:185-202.
- Stevens J, Suidgeest E, Van der Graaf PH, Danhof M and De Lange EC (2009) A new minimal-stress freely-moving rat model for preclinical studies on intranasal administration of CNS drugs. *Pharm Res* **26**:1911-1917.
- Stevens J, Van den Berg D-J, De Ridder S, Niederlander HAG, Van der Graaf PH, Danhof M and De Lange ECM (2010) Online solid phase extraction with liquid chromatography-tandem mass spectrometry to analyze remoxipride in small plasma-, brain homogenate-, and brain microdialysate samples. *Journal of Chromatography B* **878**:969-975.
- Van den Berg MP, Verhoef JC, Romeijn SG and Merkus FW (2004) Uptake of estradiol or progesterone into the CSF following intranasal and intravenous delivery in rats. *Eur J Pharm Biopharm* **58**:131-135.
- Watson J, Wright S, Lucas A, Clarke KL, Viggers J, Cheetham S, Jeffrey P, Porter R and Read KD (2009) Receptor occupancy and brain free fraction. *Drug Metab Dispos* **37**:753-760.
- Widerlov E, Andersson U, Von Bahr C and Nilsson MI (1991) Pharmacokinetics and effects on prolactin of remoxipride in patients with tardive dyskinesia. *Psychopharmacology (Berl)* **103**:46-49.
- Widerlov E, Termander B and Nilsson I (1989) Effect of urinary pH on the plasma and urinary kinetics of remoxipride in man. *European Journal of Clinical Pharmacology* **V37**:359-363.
- Widman M, Nilsson LB, Bryske B and Lundstrom J (1993) Disposition of remoxipride in different species. Species differences in metabolism. *Arzneimittelforschung* **43**:287-297.

Mechanism-based PK-PD model for the prolactin biological system response following a dopamine inhibition challenge - quantitative extrapolation to humans

J. Stevens¹, B. A. Ploeger², M. Hammarlund-Udenaes³, G. Osswald⁴,
P. H. van der Graaf⁵, M. Danhof^{1,2}, E. C. M. de Lange¹.

¹ *Division of Pharmacology, LACDR, Leiden University, Leiden, The Netherlands.*

² *LAP&P Consultants B.V., Leiden, The Netherlands.*

³ *Uppsala University, Uppsala, Sweden.*

⁴ *AstraZeneca R&D, Södertälje, Sweden.*

⁵ *Pfizer, Pharmacometrics/Global Clinical Pharmacology, Sandwich, Kent, England.*

ABSTRACT

The aim of this investigation was to develop a mechanism-based pharmacokinetic-pharmacodynamic (PK-PD) model for the biological system prolactin response following a dopamine inhibition challenge using remoxipride as a paradigm compound.

After assessment of baseline variation in prolactin concentrations, the prolactin response of remoxipride was measured following 1) single intravenous doses of 4, 8 and 16 mg/kg and 2) following double dosing of 3.8 mg/kg with different time intervals. The mechanistic PK-PD model consisted of; i) a PK model for remoxipride concentrations in brain extracellular fluid; ii) a pool model incorporating prolactin synthesis, storage in lactotrophs, release into- and elimination from plasma; iii) a positive feedback component interconnecting prolactin plasma concentrations and prolactin synthesis; and iv) a dopamine antagonism component interconnecting remoxipride brain extracellular fluid concentrations and stimulation of prolactin release. The most important finding was the positive feedback on prolactin synthesis in the lactotrophs, in contrast to the negative feedback in the previous models on the PK-PD correlation of remoxipride.

An external validation was performed using a dataset obtained in rats following intranasal administration of 4, 8, or 16 mg/kg remoxipride. Following simulation of human remoxipride brain extracellular fluid concentrations, pharmacodynamic extrapolation from rat to humans was performed, using allometric scaling in combination with independent information on the values of biological system

specific parameters as prior knowledge. The PK-PD model successfully predicted the system prolactin response in humans, indicating that positive feedback on prolactin synthesis and allometric scaling thereof could be a new feature in describing complex homeostatic mechanisms.

INTRODUCTION

Prolactin release is a common side-effect of antipsychotic drugs (Petty, 1999) and several clinical pharmacokinetic-pharmacodynamic (PK-PD) models have been published on the relationships between dopaminergic drug- and prolactin concentrations. In 1995, a PK-PD model was proposed to describe the effects of double intravenous dosing of the dopamine D2/D3-receptor antagonist remoxipride on the prolactin release (Movin-Osswald and Hammarlund-Udenaes, 1995). The basis was a pool model describing prolactin synthesis, storage in lactotrophs, release into- and elimination from plasma. This model was found to be less suitable to describe the data of subsequent clinical studies following chlorprothixene treatment (D1/D2/D3-receptor antagonist). Next, as regulation of prolactin synthesis and secretion involves both negative (e.g. dopamine) and positive (e.g. oxytocin, estrogen) regulators (Freeman, et al., 2000), putative dopamine concentrations were used to describe mechanistic (biological system) feedback in an agonist-antagonist interaction model (Bagli, et al., 1999). However, actual dopamine concentrations could not be obtained, hence limiting quantitation of system-specific parameters. A next improvement included a circadian prolactin release model, following risperidone and paliperidone (D2-receptor antagonists) treatment (Friberg, et al., 2008). Most recently, the pool- and agonist-antagonist interaction models were compared after remoxipride administration. The agonist-antagonist interaction model proofed superior, based on better descriptive properties for the baseline prolactin release, although the data following remoxipride treatment were slightly better described by the pool model (Ma, et al., 2010).

An important restriction of these models may lie in the fact that its constituents –e.g. drug effect, (negative) system feedback and circadian rhythmicity– drive a single parameter for prolactin release into plasma, which complicates the separation of these constituents of the model. Taken together, these studies indicate that a general model for prolactin release following administration of dopaminergic drugs has yet to be developed. In order to do so, drug- and biological-system specific parameters should be separated in a quantitative, mechanistic manner (De Lange, et al., 2005; Danhof, et al., 2007; Ploeger, et al., 2009; Gabrielsson and Green, 2009), including expressions for target site distribution.

For dopaminergic compounds, the target site is the brain extracellular fluid (ECF) surrounding the dopamine receptors. As obtainment of this data in humans is highly restricted and expensive, information should be derived from *in vivo* animal studies using translational pharmacology approaches (Danhof, et al., 2008). Quantitative measurement of unbound drug concentrations in brain ECF over time is available *in vivo* in animals by intracerebral microdialysis (De Lange, et al., 2000). By using animal experimentation techniques, models can be challenged by administering larger dose ranges than allowed in human studies, resulting in a broader concentration range and thus more precise description of concentration–effect relationships. In animals, mechanism-based PK-PD models describing prolactin release have not yet been explored, but could provide a more mechanistic basis. Earlier translational investigations to predict drug effects in humans have already shown that preclinical derived drug- and biological-system specific parameters in mechanism-based PK-PD models can be used with reasonable degree of success (Yassen, et al., 2007; Zuideveld, et al., 2007). Such investigations were based on allometric scaling of PK parameters (Boxenbaum, 1982) and independent information on the values of system specific parameters (e.g. target binding). Subsequent simulation studies can provide insight on the clinical applicability of a drug, at an early stage in drug development. Also, clinical studies suffice with fewer individuals and less samples per individual, for proof of concept in man.

In this study we aim to develop a mechanism-based PK-PD model for prolactin response following dopamine inhibition challenge in rats, using remoxipride as a paradigm compound. To that end, remoxipride concentration-time profiles were obtained in plasma and brain ECF, following a single dose of 4, 8, or 16 mg/kg and double dosing of 3.8 mg/kg remoxipride by 30 min intravenous infusions. After assessing the baseline variation in prolactin plasma concentrations, the effects of remoxipride on prolactin plasma concentrations were determined. Using nonlinear mixed effects modeling, we developed a population-based mechanism-based PK-PD model consisting of; i) a previously proposed pharmacokinetic model (chapter 5), ii) a pool model, iii) a positive feedback component interconnecting prolactin plasma concentrations and the synthesis of prolactin and iv) a dopamine antagonism component interconnecting remoxipride brain ECF concentrations and prolactin release.

As external validation, prolactin plasma concentrations from an intranasal remoxipride administration study were compared to model predictions. By translational modeling approaches, the PK and PD were then simulated in humans and compared to a clinical dataset (Movin-Osswald and Hammarlund-Udenaes, 1995).

METHODS

■ Animals

All animal procedures were performed in accordance with Dutch laws on animal experimentation. The study protocol was approved by the Animal Ethics Committee of Leiden University (UDEC nr. 6023 and 6132). Male Wistar WU rats ($n = 92$, mean weight \pm standard deviation = 245 ± 18 gram, Charles River, The Netherlands), were housed in groups for 7-13 days (Animal Facilities, Gorlaeus Laboratoria, Leiden, The Netherlands), under standard environmental conditions (Ambient temperature 21°C; humidity 60%; 12/12 hour light, 8AM lights on (circadian time 0), background noise, daily handled), with *ad libitum* access to food (Laboratory chow, Hope Farms, Woerden, The Netherlands) and acidified water. Between surgery and experiments, the animals were kept individually in Makrolon type 3 cages for 7 days to recover from surgical procedures.

■ Surgery

Rat surgery and experiments were performed as previously reported (Stevens, et al., 2009). In short, during anaesthetized surgery, all animals received cannulas in the femoral artery and vein, for serial blood sampling and drug administration respectively. Also, an intranasal probe (AP 12 mm, L -0.5 mm) for drug administration, and a microdialysis guide (CMA/12, Schoonebeek, The Netherlands, AP +0.4, L 3.2, V -3.5) for continuous brain ECF sampling were implanted. After 6 days, 24 ± 1 hour before the experiments, the microdialysis guide was replaced by a probe (CMA/12, 4 mm polycarbonate membrane, cut-off 20 kDa, Aurora Borealis Control, Schoonebeek, The Netherlands). For the natural 24 hour circadian rhythmicity study, the animals only received a chronically implanted cannula in the femoral artery for blood sampling.

■ Experiments

The control study investigated the natural 24 hour rhythmicity of prolactin in 8 rats by obtaining 20 μ l blood samples from the arterial cannula every 30 minutes for a period of 25 hour.

In the placebo study, the effects of handling and experimental techniques on prolactin release were investigated by 30 minute intravenous infusion of 500 μ l saline ($n = 7$) and 30 second intranasal infusion of 10, 20, or 40 μ l saline ($n = 8, 10$, and 9 respectively) by an automated pump (B. Braun Mel-

sungen AG, Melsungen, Germany). Blood samples of 200 μ l were taken from the arterial cannula at $t = 0, 5, 10, 20, 35, 60, 90, 120, 150,$ and 180 min.

In the separate remoxipride administration study, prolactin data were acquired following two intravenous remoxipride administration protocols; a single dose and a double dosing study. The experimental procedures for single dose remoxipride administration have been previously reported (Stevens, et al., 2009). In short, 3 experimental groups ($n = 10$ per group) received a single dose of 4, 8 or 16 mg/kg remoxipride in during a 30 minute intravenous infusion. Blood samples of 200 μ l were taken from the arterial cannula at $t = -5$ (blank), 2, 10, 22, 30, 40, 60, 100, 180, and 240 min. Consecutive remoxipride dosing experiments were performed under similar conditions, but with twice dosing of 3.8 mg/kg of remoxipride during 30 minute intravenous infusions, at different time intervals; 0–1, 0–2, 0–4, 0–6, 2–6, and 4–6 hours ($n = 3, 4, 3, 2, 2,$ and 3 respectively). A number of 20 blood samples of 100 μ l were taken at different time points per group.

For the external validation data set, remoxipride experiments were performed under identical experimental techniques as the single dose studies, but with 1 minute intranasal infusion of 4, 8 or 16 mg/kg remoxipride ($n = 10$ per group).

For all animal experiments, blood samples were collected in EDTA-coated vials and, after centrifuging for 15 minutes at 5000 rpm, plasma was stored at -20°C pending analysis. After the experiments the animals were sacrificed with an overdose of Nembutal (1 ml, intravenously).

For comparison of rat-to-human prediction, a clinical dataset was obtained from a previously published study (Movin-Osswald and Hammarlund-Udenaes, 1995). In short, eight healthy volunteers (mean weight \pm standard deviation = 76 ± 10 kg) received two 30 minute intravenous infusions of 50 mg remoxipride in different time intervals in a randomized, six period cross-over design. The time intervals between the first dose at $t = 0$ and the second dose were 2, 8, 12, 24, and 48 hours. Remoxipride- and total prolactin plasma concentrations were obtained in 13 or more plasma samples per individual.

■ Analytical Methods

For all single dose animal experiments, remoxipride concentrations were measured in plasma and brain ECF using online solid phase extraction with liquid chromatography–tandem mass spectrometry (Stevens, et al., 2010).

For all plasma samples taken in all remoxipride administration studies, prolactin concentrations were measured with a commercially available enzyme-linked immunosorbent assay (Rat prolactin ELISA (AER011), Biocode-Hycl, Belgium), according to the instructions of the manufacturer. Data acquisition was performed on a uQuant Universal Microplate Spectrophotometer (BioTek, Germany). Concentrations were calculated using R 2.5.0 (The R Foundation for Statistical Computing, Vienna, Austria). Individual prolactin concentration-time plots were generated and apparent outliers were excluded from the dataset if exceeding 1.5 times the interquartile range of the median concentration at that time point. Also, prolactin data below the limit of quantification (0.36 ng/ml) were excluded from the dataset.

■ PK-PD model building and random variability

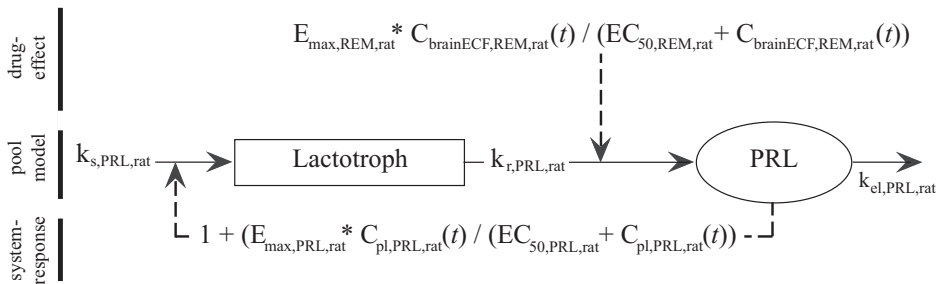
Nonlinear mixed effect modeling using NONMEM (version VI, level 2.0 Icon Development Solutions, Ellicott City, Maryland, USA) was used for modeling of the single- and double intravenous remoxipride administration studies. A sequential PK-PD modeling approach was applied, in which the individual PK parameters were fixed to the posthoc parameter estimates from the previously published population PK model for remoxipride in rat plasma and brain ECF (chapter 5). The structural model building was performed under ADVAN 9, and the first order conditional method with interaction was used for estimation with a convergence criterion of 3 significant digits in the parameter estimates. NONMEM reports an objective function value (OFV) which is the $-2 \times \log$ likelihood. Model hypothesis testing was done using the likelihood ratio test under the assumption that the difference in $-2 \times \log$ likelihood is Chi-square distributed with degrees of freedom determined by the number of additional parameters in the more complex model. Hence, with decrease in the OFV of at least 3.84 points ($p < 0.05$) the model with one additional parameter is preferred over its parent model. Additive, proportional, or combined residual variability models were investigated for the prolactin concentrations in plasma. Log normal distribution of the inter-individual variability was assumed and possible covariate correlations were taken into account.

The structural model is depicted in figure 1. The general structure of the PD model consists of a pool model which was based on the original pool model (Movin-Osswald and Hammarlund-Udenaes, 1995). Briefly, this model consists of a lactotroph- and a plasma prolactin compartment.

The change in prolactin concentration in the lactotrophs ($dC_{1a,PRL, rat}$) over time (dt) is determined by a zero-order rate constant for the synthesis of prolactin ($k_{s,PRL, rat}$) and a first-order rate constant for the release of prolactin from the lactotrophs ($k_{r,PRL, rat}$).

Figure1 Compartmental structure of the final model, including the E_{\max} concentration-effect relations of the drug-effect- and biological system effect models on the turnover model.

$k_{s,PRL,rat}$ synthesis rate constant of prolactin in lactotrophs; $k_{r,PRL,rat}$ release rate constant of prolactin into plasma; $k_{el,PRL,rat}$ elimination rate constant of prolactin from plasma; $C_{brainECF,REM,rat}(t)$, rat brain extracellular fluid concentrations of remoxipride over time; $C_{pl,PRL,rat}(t)$, rat plasma prolactin concentrations over time; E_{\max} , maximal effect of prolactin (PRL) or remoxipride (REM); EC_{50} , concentration PRL/REM inducing 50% of the E_{\max} .



The change in prolactin concentration over time in the plasma compartment ($dC_{pl,PRL,rat}$) is described by a turnover model, which consists of the $k_{r,PRL,rat}$ and a first-order rate constant for the elimination of prolactin from plasma ($k_{el,PRL,rat}$). At $t = 0$, in absence of remoxipride, prolactin concentration in the plasma compartment ($C_{pl,PRL,rat}$) equals the baseline plasma prolactin concentration (BSL_{rat}), and total prolactin synthesis, release, and elimination are in equilibrium, according to principles of mass-balance ($k_{s,PRL,rat} = BSL_{rat} * k_{el,PRL,rat}$) (Ma, et al., 2010). In this pool model, the relatively low value for $k_{s,PRL,rat}$ causes lactotroph depletion after remoxipride administration, and drives therefore the tachyphylaxis component of the model. Positive homeostatic feedback on the $k_{s,PRL,rat}$ is anticipated to correct for this.

The physiological basis for the positive feedback (PF) model lies in the fact that synthesis and release of neurotransmitters are two separate processes that can be independently regulated in a biological system. Prolactin receptor activation in the cell membrane of lactotrophs (Morel, et al., 1994) activates a wide range of transcription factors and immediate early genes in the nucleus via JAK/STAT (Watson and Burdon, 1996) and MAPK pathways (Piccoletti, et al., 1994). Endogenous compounds that increase prolactin

synthesis (like e.g. estrogen) also use MAPK activation (Singh, et al., 1999, Ben-Jonathan, et al., 2008), suggesting that prolactin receptor activation can increase prolactin synthesis. In short, the PF model describes the physiological process by which release of prolactin by lactotrophs (depletion) increases the prolactin synthesis to “refill” the lactotrophs. The PF component was described by applying linear-, log-linear-, E_{\max} - and sigmoidal E_{\max} concentration-response relationships (equations 1-4) between plasma prolactin concentrations ($C_{pl,PRL,rat}$), normalized to BSL_{rat} , and the value of $k_{s,PRL,rat}$. The terms $E_{\max,PRL,rat}$ and $EC_{50,PRL,rat}$ correspond to the values of maximal prolactinergic feedback and the plasma prolactin concentration that induces 50% of the $E_{\max,PRL,rat}$, respectively, and c is the slope of the plasma prolactin concentration feedback relationship.

Equation 1; $PF_{linear} = c * (C_{pl,PRL,rat} - BSL_{rat})$

Equation 2; $PF_{log-linear} = c * \log(C_{pl,PRL,rat} - BSL_{rat})$

Equation 3; $PF_{E_{\max}} = E_{\max,PRL,rat} * (C_{pl,PRL,rat} - BSL_{rat}) / (EC_{50,PRL,rat} + (C_{pl,PRL,rat} - BSL_{rat}))$

Equation 4; $PF_{Sigmoidal E_{\max}} = E_{\max,PRL,rat} * (C_{pl,PRL,rat} - BSL_{rat})^y / (EC_{50,PRL,rat}^y + (C_{pl,PRL,rat} - BSL_{rat})^y)$

Consequently, for equations 1, 3 and 4, $PF = 0$ when $C_{pl,PRL,rat}$ returns to BSL_{rat} . While investigating on the log-linear concentration response relationships, $PF_{log-linear}$ was reset to 0 when $C_{pl,PRL,rat}$ returned to BSL_{rat} . During the modeling process, the parameter estimates for BSL_{rat} were estimated separately for the single- and double remoxipride dosing studies.

A dopamine antagonist component of the drug effect (DE) describes the drug–effect relationship between unbound remoxipride concentrations in brain ECF ($C_{brainECF,REM,rat}$) and the $k_{r,PRL,rat}$. In the early phase of structural model building, an E_{\max} -model (equation 5) described the DE relation, in terms of maximal remoxipride induced prolactin response ($E_{\max,REM,rat}$), and the remoxipride concentration that induces half the $E_{\max,REM,rat}$ ($EC_{50,REM,rat}$).

Equation 5; $DE = E_{\max,REM,rat} * C_{brainECF,REM,rat} / (EC_{50,REM,rat} + C_{brainECF,REM,rat})$

Incorporating the components for PF and DE results in differential equations 6 and 7 for $dC_{la,PRL,rat}/dt$ and for $dC_{pl,PRL,rat}/dt$, respectively.

The terms $C_{la,PRL,rat}$ and $C_{pl,PRL,rat}$ represent the prolactin concentration in the lactotroph- and plasma compartment at time = t , respectively.

Equation 6;
$$dC_{la,PRL,rat}/dt = k_{s,PRL,rat} * (1+PF) - C_{la,PRL,rat} * k_{r,PRL,rat} * (1+DE)$$

Equation 7;
$$dC_{pl,PRL,rat}/dt = C_{la,PRL,rat} * k_{r,PRL,rat} * (1+DE) - C_{pl,PRL,rat} * k_{el,PRL,rat}$$

Based on decrease in OFV and individual goodness-of-fit, the best model for the PF component was selected. Then, the DE component was re-evaluated by applying log-linear and sigmoidal- E_{max} concentration–effect relationships.

Prior information for parameter estimation was used for the values of $EC_{50,REM,rat}$ of the dopamine D2-receptor and for the $k_{el,PRL,rat}$. The equilibrium binding dissociation constant of remoxipride for the D2-receptor is reported to be 41.9 ng/ml, with a standard deviation of 50 ng/ml (Mohell, et al., 1993). Our microdialysis experiments allowed measurement of brain ECF remoxipride concentrations being close to, or equal to the target site (D2-receptor) concentrations. As remoxipride is an antagonist, the EC_{50} can be assumed to be similar to the equilibrium binding dissociation constant of remoxipride binding to the D2-receptor.

Secondly, based on the first-order elimination rate of endogenous prolactin from plasma, the $t_{1/2}$ of prolactin in rats is 6.9 minutes, with a confidence of 6.3 – 7.7 minutes (Chi and Shin, 1978). This allows calculation of the $k_{el,PRL,rat}$ by $\ln 2/t_{1/2}$. The NWPRI subroutine in NONMEM was used, which allowed a penalty function based on a frequency prior to be specified and added to the -2log likelihood function (Gisleskog, et al., 2002), to estimate the $EC_{50,REM,rat}$ and $k_{el,PRL,rat}$.

■ PK–PD model evaluation

A bootstrap procedure, in which the final model was optimized on at least 1000 datasets obtained by random sampling with replacement from the original dataset, was used to derive the uncertainty in the parameter estimates of the final model. From the bootstrap estimation the median and 2.5th and 97.5th percentiles were obtained to represent the non-parametric 95% confidence limits.

The bootstrapped parameter estimates were then used in an internal qualification of the model by means of a visual predictive check (VPC). The VPCs were performed using NONMEM, by simulating 1000 replications of the model and a simulation dataset that contained intravenous dosing information for one individual per dosing regimen. The median, 5th and 95th percentiles were calculated for each simulated time-point. The predictions at each time-point (median and 90 % prediction interval) were compared visually with the actual data. Resemblance between simulated and original distributions indicates the accuracy of the model i.e., 90 % of the observed data should fall within the predicted range for 90 % of the variability (Post, et al., 2008).

The model was also externally validated. To this end, a VPC was performed using an external dataset obtained following intranasal administration of remoxipride. 1000 replications of the model and a simulation dataset containing intranasal dosing information for one individual per dosing regimen were generated. Again, the median, 5th and 95th percentiles were calculated for each simulated time-point and visually compared at each time point with the actual data. Resemblance between simulated and original distributions indicates the predictive value of the model for the intranasal administration route.

■ Translation from rat to human

Our ultimate goal was to predict the prolactin response in humans on the basis of our preclinical PK-PD model. Berkeley-Madonna software (Berkeley Madonna 8.3.9, Berkeley Madonna Inc., University of California (REGENTS), Berkeley, California, USA) was used for the simulation of the time course of the prolactin plasma concentrations in humans, which was then compared to the plasma data from the clinical dataset.

To translate the preclinical pool model to that for the human situation, allometric scaling (Boxenbaum, 1982) was applied for estimation of the human prolactin release- and elimination rate constants (equation 8).

Equation 8; $k_{\text{hum}} = k_{\text{rat}} * (\text{bodyweight}_{\text{hum}}/\text{bodyweight}_{\text{rat}})^{-0.25}$

As $k_{\text{S,PRL, rat}}$ is initially defined by $k_{\text{el,PRL, rat}} * \text{BSL}_{\text{rat}}$ and the same structural model is applied for the human situation, the human prolactin synthesis rate constant is automatically scaled as well. The clinical value for BSL_{hum} (9.4 ng/ml) was obtained from literature (Movin-Osswald and Hammarlund-Udenaes, 1995).

Concerning the extrapolation of the PF, to our knowledge, no clinical data are available on the $E_{\max, \text{PRL, hum}}$ and $EC_{50, \text{PRL, hum}}$. However, from a physiological perspective, interspecies differences in these parameters are expected (Ben Jonathan, et al., 2008) and an empiric approach on translation of these parameters was necessary. As prolactin is synthesized in lactotrophs, the interspecies difference in number of lactotrophs forms a basis for extrapolation of the $E_{\max, \text{PRL, hum}}$. The average lactotroph density in the young adult male rat pituitary (LD_{rat}) is reported to be 37.9 % (Dada, et al., 1984; Phelps, 1986) and in the human pituitary (LD_{hum}) 16.9 % (Asa, et al., 1982). Consequently, the $E_{\max, \text{PRL, hum}}$ was extrapolated according to equation 9.

Equation 9; $E_{\max, \text{PRL, hum}} = E_{\max, \text{PRL, rat}} * (LD_{\text{hum}}/LD_{\text{rat}})$

Little information is available on the physiological activity of prolactin on lactotrophs in man. In cell proliferation studies, the EC_{50} of human prolactin on the human prolactin receptor was determined (8.74 mg/l: Utama, et al., 2009). Although this does not represent the prolactin elevation of the $K_{s, \text{PRL, hum}}$ at a nucleus level, this pharmacological activity of prolactin forms a basis for extrapolating the interspecies difference in our simulation approach and this value was used for the $EC_{50, \text{PRL, hum}}$.

In the present investigations, to translate the DE model, the PK of remoxipride of the clinical dataset were reanalyzed using a 2-compartmental approach in NONMEM VI, to obtain PK parameter estimates for volume of distribution (V), clearance (CL) and intercompartmental clearance (Q) of remoxipride in humans. Based on the mean parameter estimates and their standard deviation, calculation of the coefficient of variation (CV) was used to derive the uncertainty in the parameter estimates of the model, which is considered acceptable when lower than 50%. For visual comparison of the model and the actual data, remoxipride concentration-time profiles were plotted for all dosing regimens.

In the preclinical PK-PD model, the DE model is related to the unbound brain ECF concentrations of remoxipride, which are described in a third (brain) compartment. Such information is not available for humans. Our approach was therefore to simulate the human brain ECF concentrations, by assuming that the ratio of concentrations in the brain- and peripheral compartment is equal in rats and man (equation 10 and 11). The human PK parameters for the brain- ($PK_{\text{brain, hum}}$) and peripheral compartment ($PK_{\text{periph, hum}}$) are calculated based on the human parameter estimate from

the clinical model (peripheral compartment, $\theta_{\text{periph,hum}}$) and the preclinical parameter estimates (θ_{rat}) for the brain- and peripheral compartment.

Equation 10;
$$PK_{\text{brain,hum}} = \theta_{\text{periph,hum}} * (\theta_{\text{brain, rat}} / (\theta_{\text{brain, rat}} + \theta_{\text{periph, rat}}))$$

Equation 11;
$$PK_{\text{periph,hum}} = \theta_{\text{periph,hum}} * (\theta_{\text{periph, rat}} / (\theta_{\text{brain, rat}} + \theta_{\text{periph, rat}}))$$

For extrapolation of the DE component, the values for $E_{\text{max,REM}}$ and $EC_{50,REM}$ in humans had to be acquired. In the clinical dataset, the observed maximum prolactin concentrations after remoxipride administration are the combined result of the pool-, DE- and PF model components. The observed maximal prolactin concentration 70 ng/ml (Movin-Osswald and Hammarlund-Udenaes, 1995) minus BSL_{hum} therefore overestimates the required value of $E_{\text{max,REM,hum}}$, as the PF is not taken into account. However, for our simulation purposes this approximation on the value of $E_{\text{max,REM,hum}}$ was considered acceptable. As remoxipride is a dopamine antagonist and the DE is based on simulated brain ECF concentrations that are close to, or at the target site, the $EC_{50,REM,hum}$ was considered similar to the remoxipride equilibrium binding dissociation constant. In literature, the equilibrium binding dissociation constant of remoxipride for the human D2-receptor is reported to be 5.936 mg/l (Burstein, et al., 2005), and thus incorporated in the model.

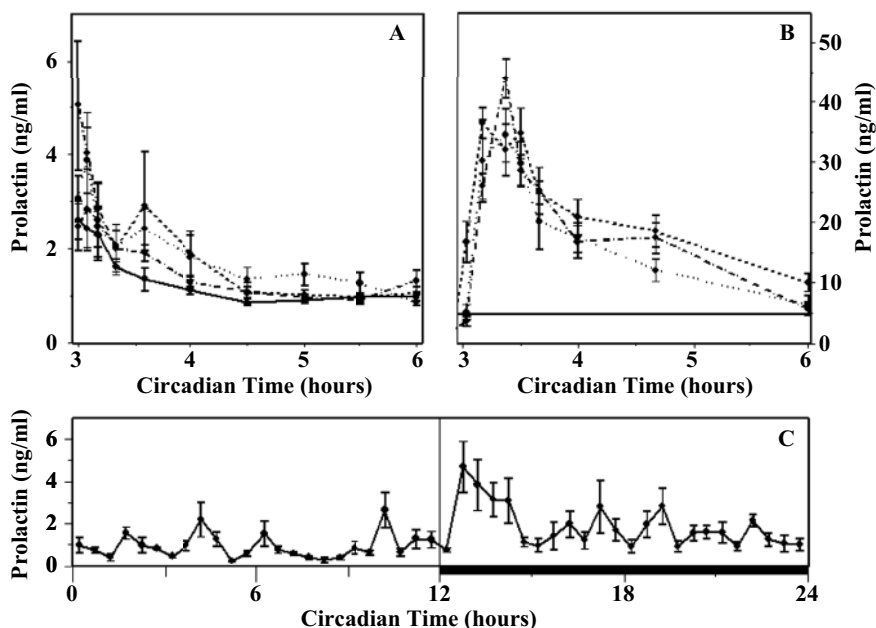
RESULTS

The control and placebo studies show low mean prolactin concentration when compared to the prolactin response after intravenous remoxipride administration (Figure 2). Also, the variations in baseline prolactin concentrations were low, and no handling- or experimental influences on prolactin release were found.

The baseline concentrations of prolactin proved similar to previous findings in individually housed animals (Perello, et al., 2006). As a result, $k_{\text{r,PRL, rat}}$ can be considered a rate constant at the baseline, in absence of remoxipride. Following remoxipride administration, a maximal prolactin peak was observed, which is equal for all dosing regimens. Upon visual assessment, the area under the curve of the prolactin concentration time curve seemed to increase with increase of remoxipride dose. After performing the second, double dosing study of remoxipride, no full second response could be generated at short dosing intervals, as expected based on the previously reported tachyphylactic properties of prolactin release. The intravenous single- and

double remoxipride dosing studies provided 190- and 295 prolactin concentrations, respectively.

Figure 2 Average prolactin concentrations (\pm SEM) under different conditions over circadian time; A) 500 μ l intravenous-, and 20, 30, and 40 μ l intranasal saline administration (solid-, dash-dotted-, dotted-, and dashed lines respectively), B) 30 min intravenous infusion of 4, 8 and 16 mg/kg remoxipride (dash- dotted-, dotted- and dashed lines respectively), the solid line represents the highest average prolactin concentration after saline administration. C) 24 hour sampling (solid line), the dark phase (12-24 hours) is represented by the dark bar.



■ PK-PD modeling

Applying the E_{\max} -model for the remoxipride brain ECF concentration–effect relationship allowed reasonable description of the prolactin concentrations in plasma for the groups that received a single remoxipride dose and for groups that received double dosing of remoxipride at longer intervals. However, without a PF component, the model underestimated a second plasma prolactin peak in plasma following double remoxipride dosing at short intervals. Next, PF of plasma prolactin concentrations on the $k_{s,PRL, rat}$ was described by linear- and log-linear concentration–effect relationships,

with OFV of 2148 and 2074 respectively. The lowest OFV (2057) was achieved by an E_{\max} relationship, while a sigmoidal- E_{\max} model caused over-parameterization. As a result of the E_{\max} -model for PF, all individual plasma prolactin concentration-time profiles were now adequately described for all dosing intervals.

Next, the drug–effect relationships between unbound remoxipride brain ECF concentrations and plasma prolactin concentrations were re-evaluated. Log-linear relationships and sigmoidal- E_{\max} relationships increased the OFV approximately 60 points, so optimization of the model was continued with an E_{\max} -model for both the PF- and DE components. Based on a decrease in OFV, a combined proportional- and additive error model best described the residual variability in the prolactin response compartment for all model structures. Inter-individual variability was identified for BSL_{rat} .

Single inclusion of prior information on the value $k_{el,PRL, rat}$ resulted in more realistic estimations for $E_{\max, REM, rat}$ and, as expected, the estimation for $EC_{50, REM, rat}$ was closer to the equilibration binding association constant (OFV 1975). Adding prior information only to the parameter for $EC_{50, REM, rat}$ in the drug–effect relationship, decreased the OFV to 1966. However, the resulting estimation of $E_{\max, REM, rat}$ now increased three-fold from earlier model expectations, which is probably caused by the large predefined standard deviation in the penalty function.

When adding prior information for both parameter estimates, the OFV dropped to 1953 points and the parameter estimation for $E_{\max, REM, rat}$ was now in similar range of previous model expectations, although the covariance step was now aborted by NONMEM. Table 1 summarizes the parameter estimates, IIV and residual error. Describing the PF- and DE components by E_{\max} -relationships resulted in the best predictions for all doses and dosing regimens in all individual rats, as depicted for a typical individual in every double dosing regimen (Figure 3).

■ PK-PD model evaluation

The parameter estimates after 1096 bootstrap replications of the dataset were very close to the NONMEM estimates of the final model (Table 1). Also, the estimates for IIV and residual error were similar, confirming the stability of the model.

Figure 3 Individual predicted (solid line) and observed (open circles) plasma prolactin concentration over time in hours (h) for the repeated (3.8 mg/kg) remoxipride dosing study. Per dosing regimen (dose, with time interval in hours after the start of the experiments), a typical single individual is plotted.

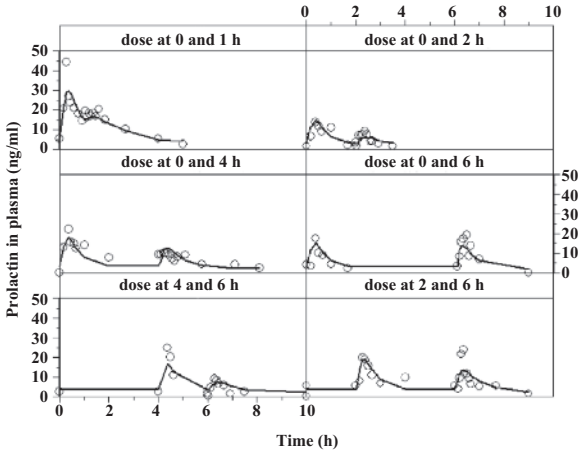


Table 1 NONMEM parameter estimates and bootstrap results.

parameter	Final model estimates	Bootstrap (n = 1096)		
		median	95% CL	CV (%)
Pool model				
BSL _{sd, rat} (ng/ml)	6.2	6.1	4.4-7.2	12.1
BSL _{dd, rat} (ng/ml)	3.9	3.9	2.4-5.6	17.8
k _{r, PRL, rat} (h ⁻¹)	0.6	0.6	0.4-0.7	12.6
k _{el, PRL, rat} (h ⁻¹)	5.7	5.8	5.1-6.3	5.4
Positive feedback model				
E _{max, PRL, rat} (ng/ml)	3.5	3.7	3.0-6.8	25.1
EC _{50, PRL, rat} (mg/L)	12.4	12.0	8.5-16.8	17.2
Drug-effect model				
E _{max, REM, rat} (ng/ml)	25.0	24.6	18.8-44.6	24.0
EC _{50, REM, rat} (ng/ml)	0.08	0.08	0.04-0.12	22.30
Error				
σ additive	0.06	0.06	0.04-0.10	23.81
σ proportional	6.73	6.54	2.91-11.70	35.47
η BSL	0.07	0.07	0.04-0.10	21.39

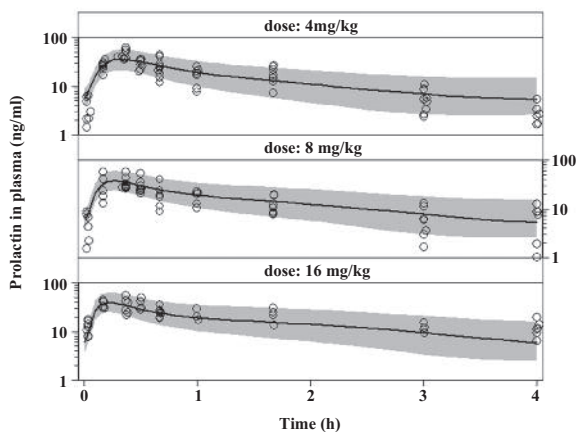
95% CL, confidence limits calculated as 2.5th and 97.5th percentiles;
CV, coefficient of variation calculated from mean bootstrap parameter estimates;
BSL, baseline prolactin concentration in the single- (sd) and double (dd) remoxipride dosing study; parameters as defined in figure 1;
σ, residual error;
η, interindividual error calculated as single estimate for both BSL_{sd, rat} and BSL_{dd, rat}.

95% CL, confidence limits calculated as 2.5th and 97.5th percentiles;
CV, coefficient of variation calculated from mean bootstrap parameter estimates;
BSL, baseline prolactin concentration in the single- (sd) and double (dd) remoxipride dosing study; parameters as defined in figure 1;
σ, residual error;
η, interindividual error calculated as single estimate for both BSL_{sd, rat} and BSL_{dd, rat}.

In an internal evaluation of the model, the VPC visualized accurate prediction of observed prolactin concentrations following single dose intravenous administration of remoxipride (Figure 4).

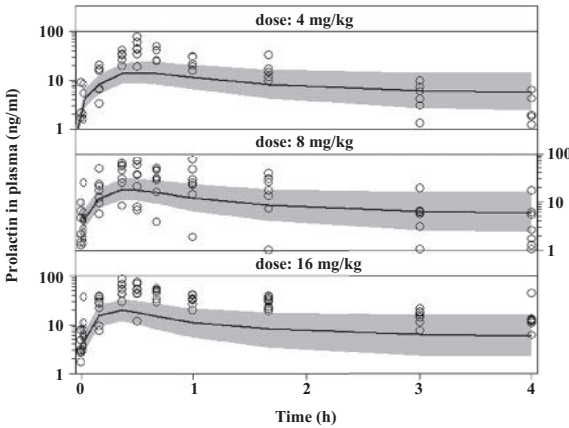
In general, for all single dose groups, the maximal observed prolactin concentrations were well described by the median of the VPC. Although negligible, the observed concentrations at $t = 2$ min were slightly overestimated by the median of the model for the 4- and 8 mg/kg dose groups and in the 16 mg/kg dose group a slight underestimation of the lower concentration range was observed. Most observations lie within the 90% confidence interval, indicating that the variability was well estimated.

Figure 4 Visual predictive checks of preclinical PK-PD model. The plots represent the simulated median of the plasma prolactin concentration predictions (solid line), and the 90% prediction interval (grey area) over time per dose, following intravenous remoxipride administration. The open circles represent plasma prolactin concentrations measured in the intravenous single dose remoxipride experiments.



The placebo study proved that intranasal administration as such does not influence baseline prolactin concentrations (Figure 2A). As a result, the biological-system parameters were considered equal for intravenous- and intranasal administration of remoxipride. Consequently, the data from the intranasal remoxipride administration study could be used for external validation of the final model. When a VPC was performed (Figure 5), the maximum prolactin plasma concentrations were underestimated ($\sim 10\%$), as was the time to maximal prolactin concentration. Also, a higher percentage of the observations were outside the 90% confidence interval. As the PD variability of the PK-PD model is based on the intravenous administration datasets, this indicates different variability after intranasal administration.

Figure 5 Visual predictive checks of the external validation dataset. The plots represent the simulated median of the plasma prolactin concentration predictions (solid line), and the 90% prediction interval (grey area) over time per dose, following intranasal remoxipride administration. The open circles represent plasma prolactin concentrations measured in the intranasal single dose remoxipride experiments.



■ Translation from rat to human

The pharmacokinetics of remoxipride in human plasma could be well described by a two-compartmental approach. The parameter estimates for in the human PK model were close to the values estimated earlier (Movin-Osswald and Hammarlund-Udenaes, 1995) and the low CVs indicates accurate parameter estimation (Table 2).

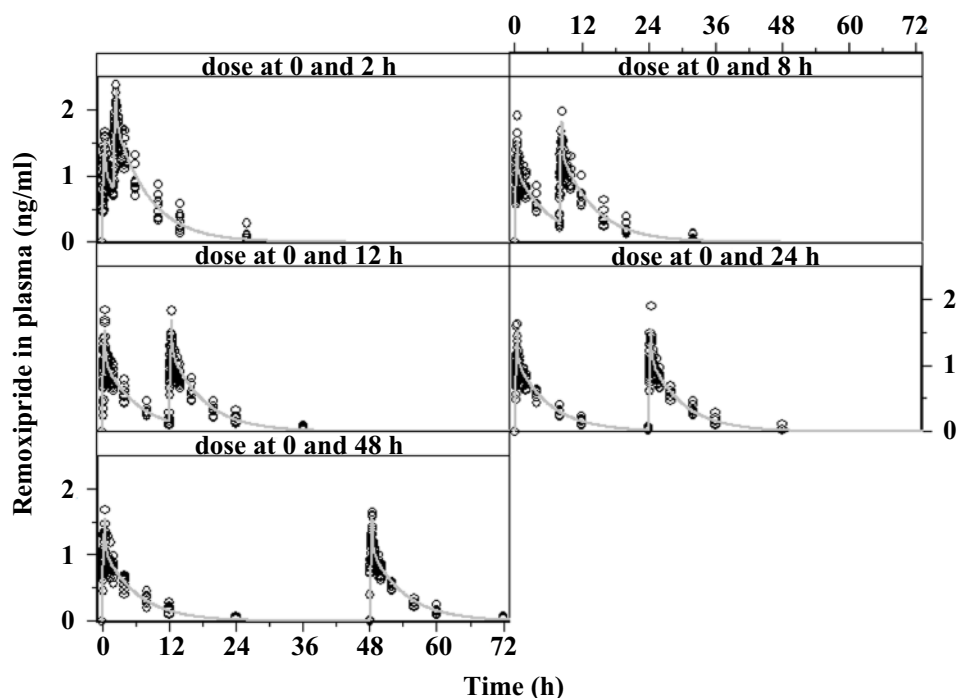
Table 2 NONMEM pharmacokinetic parameter estimates for remoxipride in humans.

parameter	human PK model estimate (CV in %)	η	Movin-Osswald and Hammarlund-Udenaes, 1995 estimate	η
plasma compartment				
CL (l/h)	7.4 (5.2)	0.03	6.84	0.14
V (l)	12.2 (3.1)	-		
peripheral compartment				
Q (l/h)	137 (11.3)	0.1		
V (l)	34.7 (6)	0.03		
Error				
σ additive	0.03			
σ proportional	0.14			
Vtotal			40	0.09

η , inter-individual variability; σ , residual variability; CL, clearance; V, volume of distribution; Q, intercompartmental clearance; Vtotal, total volume of distribution in steady state.

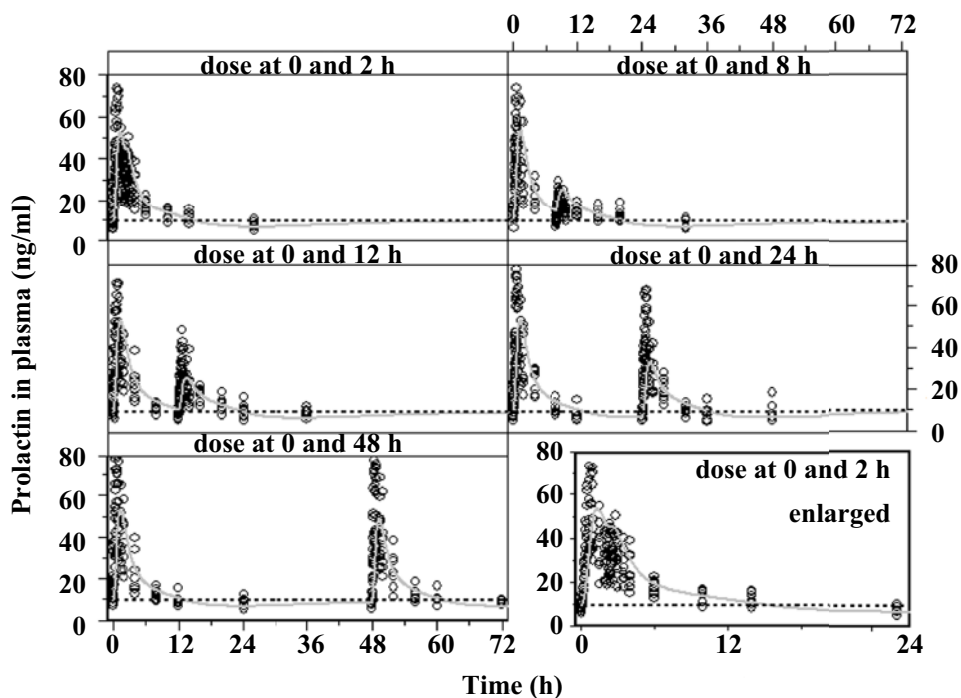
In the preclinical model, the drug-effects are related to brain ECF concentrations in a brain-PK compartment. To allow extrapolation of drug-effect in rats to humans, human brain ECF concentrations were estimated by converting the human two-compartmental- into a three-compartmental PK model. The hence acquired PK model showed accurate description of the remoxipride concentration time profiles in human plasma (Figure 6), for all dosing regimens. Compared to remoxipride plasma concentrations after intravenous administration of remoxipride, brain ECF concentration-time profiles generally showed lower maximal concentrations and a longer time to reach the maximal concentration, due to nose-to-brain distribution characteristics (chapter 5). As no human data are available on remoxipride brain ECF concentrations, no comparison can be made. The predicted human remoxipride brain ECF profiles showed lower maximal concentrations and a short delay in time to maximal concentration when compared to the plasma concentration-time profiles, as expected.

Figure 6 Translation of preclinical to clinical PK (three-compartment PK model). The solid, grey lines represent the prediction of remoxipride concentrations in plasma over time for different dosing regimens. The open circles represent measured remoxipride concentrations, obtained in the clinical dataset (Movin-Osswald and Hammarlund-Udenaes, 1995).



In general, the translational mechanism-based PK-PD simulation described the human prolactin plasma concentrations following the repeated intravenous administration of remoxipride adequately (Figure 7). The time to full equilibrium of the pool model (return to baseline prolactin concentration), is concurrent with the time at which a full second response can be generated in humans (dosing interval 0–48).

Figure 7 Translation of preclinical to clinical PK-PD. The solid, grey lines represent the prediction of plasma prolactin concentrations over time for different dosing regimens. The open circles represent measured prolactin concentrations, obtained in the clinical dataset (Movin-Osswald and Hammarlund-Udenaes, 1995).



DISCUSSION

Our aim was to develop a mechanistic PK-PD model for the prolactin response following administration of dopamine receptor antagonists. To this end, the interrelationships between the time course of remoxipride concentrations in brain ECF and the time course of the plasma prolactin concentrations were assessed under different conditions. A previously proposed pool

model, which accounted for tachyphylaxis upon repeated administration of remoxipride in humans, constituted the backbone of the novel mechanism-based PK-PD model (Movin-Osswald and Hammarlund-Udenaes, 1995).

Prolactin is released into plasma by lactotrophs in the anterior pituitary and is tonically suppressed by three types of hypothalamic dopaminergic neurons. Tuberoinfundibular neurons release dopamine into long portal veins that empty in pituitary sinusoids. Periventricular hypothalamic- and tubero-hypophysial dopaminergic neurons project directly to the pituitary (Freeman, et al., 2000). Thus, dopamine antagonists increase prolactin release into plasma, limited by depletion of the prolactin content. Less is known about regulation of the synthesis of prolactin after such depletion. Interestingly, we found a positive feedback of prolactin plasma concentrations on its synthesis. In physiological terms this can be regarded as a homeostatic mechanism, restoring basal conditions of the biological system.

In the original pool model (Movin-Osswald and Hammarlund-Udenaes, 1995), lactotroph depletion and the value of $k_{s,PRL, rat}$ have been identified as rate limiting steps in prolactin release following remoxipride administration, but could not adequately describe the plasma prolactin concentrations at short dosing intervals in subsequent studies. Likewise, in our animal studies, sole use of a pool model underestimated the prolactin response following remoxipride administration at a short interval. To correct for this, previously proposed (clinical) PK-PD model approaches included baseline circadian rhythmicity, linear DE and (negative) linear system feedback, that all drive the single parameter estimate for $k_{r,PRL}$ and thereby complicate separation of these model constituents. By strict separation of model constituents in an animal experimental setup, we provided a basis to quantitate the biological system parameters of prolactin release and the drug-effects thereon.

First, circadian rhythmicity in baseline prolactin plasma concentrations was low, if not neglectible, compared to the magnitude of the prolactin response following administration of remoxipride (Figure 2). Therefore, $k_{r,PRL, rat}$ could be considered constant.

Secondly, to identify drug-specific parameters in a quantitative, semi-mechanistic manner, we obtained remoxipride plasma- and target site (brain ECF) concentration-time profiles. A broader remoxipride dosing regimen was applied than would be allowed in humans, to increase the remoxipride concentration range and thereby the descriptive properties of the DE model. In

our model approach, we included previous literature data on the pharmacology of remoxipride ($EC_{50,REM,rat}$) and prolactin ($k_{el,PRL,rat}$) in a penalty function. The resulting DE model allowed accurate description of a maximal drug–effect relationship between remoxipride brain ECF concentrations and $k_{r,PRL,rat}$ and can be considered more mechanistic compared to previously proposed clinical models that identified (linear) drug–effect relationships between remoxipride plasma drug concentrations and $k_{r,PRL}$.

Thirdly, the use of a positive feedback mechanism between plasma prolactin concentrations and $k_{s,PRL,rat}$ allowed strict distinction between the drug–effect (on $k_{r,PRL,rat}$) and system-effect. Addition of a positive feedback model allowed accurate description of the time course of prolactin concentrations in plasma following a second remoxipride dose, for all dosing regimens (Figure 3). The increase in prolactin synthesis includes a physiological limit, represented by the $E_{max,PRL,rat}$ -parameter estimate. Consequently, both lactotroph depletion and the $E_{max,PRL,rat}$ are the rate limiting steps for prolactin release in plasma.

Bootstrapping proved high stability and VPCs showed good predictive properties of the preclinical PK-PD model in the mechanistic description of the drug–effect and biological system response when using prolactin as a PD endpoint following remoxipride administration.

In the external validation, the simulations showed underestimation of the C_{max} and time-to- C_{max} following intranasal administration of remoxipride to rats. In the previously PK-model (chapter 5), maximum observed remoxipride brain ECF concentrations (~ 0.1 mg/l) are close to the estimated $EC_{50,REM,rat}$ (0.08 mg/l). We also reported slight underestimation of the maximum remoxipride concentration in brain ECF and higher variability on pharmacokinetic parameters following intranasal administration. Both factors contribute to the underestimation of prolactin release and consequently delayed lactotroph depletion as displayed in the VPC (Figure 4). This leads to believe that the value of $EC_{50,REM}$ is slightly overestimated in the final PK-PD model and/or that the prediction bias may come from the PK model. The lowest value for the $EC_{50,REM,rat}$ within the confidence limits of the bootstrap, is 0.04 mg/l. The expectation is that such a low value will cause the observed maximal brain ECF concentrations to induce lactotroph depletion and therefore correct the C_{max} and time-to- C_{max} . Optimization of study design (e.g. dose regimen and sampling times) in subsequent studies would allow for identification of a sigmoidal E_{max} drug-effect relationship (Hill-coefficient) to verify this assumption. However, taking these factors into account, the evaluation shows that the model predicts the prolactin-

ergic effects relatively well after intranasal administration of remoxipride, implying that the mechanism-based PK-PD model has predictive power towards this other routes of administration, rather than only describing the intravenous dataset.

In the extrapolation from rat to human PK-PD, the simulation of human brain ECF concentrations is a critical factor. As remoxipride brain ECF concentrations depend on unbound plasma drug concentrations, interspecies differences in plasma binding (Widman, et al., 1993) should be considered when scaling between species. As data from the clinical study were available, an easier approach was to construct a clinical two-compartment PK model in NONMEM that describes total remoxipride concentrations in plasma and unbound remoxipride concentrations in the peripheral compartment. In this model, the PK parameter estimates proved to match previously published data (Table 2). As remoxipride is reported to rapidly cross the blood-brain barrier in both rat and man (Farde and Von Bahr, 1990; Kohler, et al., 1992), we assumed that the ratio of unbound remoxipride in brain and periphery would be comparable in rat and human (equations 10 and 11). By this approach, we were able to simulate remoxipride brain-ECF concentrations in humans in the translational PK model.

Prolactin synthesis, release pathways, homeostatic feedback, and plasma elimination half-life are well understood and have been found to be structurally similar in rats and man (Ben Jonathan, et al., 2008). For that reason, as well as because prolactin concentrations can be measured relatively easily in plasma samples in both rat and man, prolactin comprises all prerequisites for a translational biomarker (Danhof, et al., 2005) for dopaminergic activity in the brain. We used the simulated brain ECF concentrations in the clinical PK model as the basis for the rat-to-human simulation of the PD effect. The rate constants in the pool model were allometrically scaled, leading to a $k_{el,PRL,hum}$ of 1.4 h^{-1} , which is in agreement with previous studies, that report $k_{el,PRL,hum}$ to range between 1 and 2.09 h^{-1} (Movin-Osswald and Hammarlund-Udenaes, 1995; Bagli, et al., 1999; Ma, et al., 2010). The human BSL values were obtained from literature. As limited information is available on the remaining E_{max} and EC_{50} parameter values, further research (e.g. by *in vitro* bioassays) should validate actual values and thus improve the translational properties of the model, as may the previously proposed inclusion of circadian rhythmicity in prolactin release. The PK-PD model was successful in describing both the PK and PD in humans.

An important question is how to further validate the proposed translational PK-PD model for prediction of the prolactin biological system response, as reflected by prolactin plasma concentrations. An interesting approach is to challenge the model with a training set of different compounds as has previously been successfully applied in the development of mechanistic PK-PD models for adenosine A1-receptor agonists (Van der Graaf, et al., 1997), GABA-ergic compounds (Visser, et al., 2002) and 5-HT1a-receptor agonists (Zuideveld, et al., 2004). Administration of other dopaminergic antagonists in rats will be subject to different drug–effect relationships, but the values describing the biological system response should essentially remain identical. Also, unique physicochemical properties of new chemical entities that are not (yet) approved for use in man can be studied, alternative routes of administration can be explored more easily, as can *in vitro-in vivo* correlations. This provides additional data for the validation of the pool- and positive feedback models. Finally, small scale clinical studies on (intranasal) administration of dopaminergic compounds allows validation on this new structural approach on prolactinergic turnover and homeostatic feedback in humans.

Summarizing, we accomplished the development of a mechanism-based PK-PD model describing prolactin release in plasma in rats following remoxipride administration in different dosages and dosing regimens. The most important finding, relative to previous investigations on the PK-PD correlation of remoxipride, was the identification of a positive feedback of prolactin plasma concentrations on the zero-order rate constant for synthesis of prolactin in the lactotrophs. The use of allometric scaling, literature values of clinical drug-specific- and biological system specific parameters, and simulation of brain ECF concentration-time-profiles allowed extrapolation to humans with reasonable degree of success. This indicates that the structure of the model adequately describes prolactin release in both rats and humans, and that positive feedback of prolactin plasma concentrations on its own synthesis in the lactotrophs and allometric scaling thereof could be a new feature in describing complex homeostatic mechanisms.

REFERENCES

- Asa SL, Penz G, Kovacs K and Ezrin C (1982) Prolactin cells in the human pituitary. A quantitative immunocytochemical analysis. *Arch Pathol Lab Med* **106**:360-363.
- Bagli M, Suverkrup R, Quadflieg R, Hoflich G, Kasper S, Moller HJ, Langer M, Barlage U and Rao ML (1999) Pharmacokinetic-pharmacodynamic modeling of tolerance to the prolactin-secreting effect of chlorprothixene after different modes of drug administration. *J Pharmacol Exp Ther* **291**:547-554.
- Ben Jonathan N, LaPensee CR and LaPensee EW (2008) What Can We Learn from Rodents about Prolactin in Humans? *Endocr Rev* **29**:1-41.
- Boxenbaum H (1982) Interspecies scaling, allometry, physiological time, and the ground plan of pharmacokinetics. *J Pharmacokinet Biopharm* **10**:201-227.
- Burstein ES, Ma J, Wong S, Gao Y, Pham E, Knapp AE, Nash NR, Olsson R, Davis RE, Hacksell U, Weiner DM and Brann MR (2005) Intrinsic Efficacy of Antipsychotics at Human D₂, D₃, and D₄ Dopamine Receptors: Identification of the Clozapine Metabolite N-Desmethylclozapine as a D₂/D₃ Partial Agonist. *J Pharmacol Exp Ther* **315**:1278-1287.
- Chi HJ and Shin SH (1978) The effect of exposure to ether on prolactin secretion and the half-life of endogenous prolactin in normal and castrated male rats. *Neuroendocrinology* **26**:193-201.
- Dada MO, Campbell GT and Blake CA (1984) Pars distalis cell quantification in normal adult male and female rats. *J Endocrinol* **101**:87-94.
- Danhof M, De Jongh J, De Lange EC, Della Pasqua O, Ploeger BA and Voskuyl RA (2007) Mechanism-based pharmacokinetic-pharmacodynamic modeling: biophase distribution, receptor theory, and dynamical systems analysis. *Annu Rev Pharmacol Toxicol* **47**:357-400.
- Danhof M, De Lange EC, Della Pasqua OE, Ploeger BA and Voskuyl RA (2008) Mechanism-based pharmacokinetic-pharmacodynamic (PK-PD) modeling in translational drug research. *Trends Pharmacol Sci* **29**:186-191.
- De Lange EC, De Boer AG and Breimer DD (2000) Methodological issues in microdialysis sampling for pharmacokinetic studies. *Adv Drug Deliv Rev* **45**:125-148.
- De Lange EC, Ravenstijn PG, Groenendaal D and Van Steeg TJ (2005) Toward the prediction of CNS drug-effect profiles in physiological and pathological conditions using microdialysis and mechanism-based pharmacokinetic-pharmacodynamic modeling. *AAPS J* **7**:E532-E543.
- Farde L and Von Bahr C (1990) Distribution of remoxipride to the human brain and central D₂-dopamine receptor binding examined in vivo by PET. *Acta Psychiatr Scand Suppl* **358**:67-71.
- Freeman ME, Kanyicska B, Lerant A and Nagy G (2000) Prolactin: structure, function, and regulation of secretion. *Physiol Rev* **80**:1523-1631.
- Friberg LE, Vermeulen AM, Petersson KJF and Karlsson MO (2008) An Agonist-Antagonist Interaction Model for Prolactin Release Following Risperidone and Paliperidone Treatment. *Clin Pharmacol Ther* **85**:409-417.
- Gabrielsson J and Green AR (2009) Quantitative Pharmacology or Pharmacokinetic Pharmacodynamic Integration Should Be a Vital Component in Integrative Pharmacology. *J Pharmacol Exp Ther* **331**:767-774.
- Gisleskog PO, Karlsson MO and Beal SL (2002) Use of prior information to stabilize a population data analysis. *J Pharmacokinet Pharmacodyn* **29**:473-505.
- Kohler C, Radesater AC, Karlsson-Boethius G, Bryske B and Widman M (1992) Regional distribution and in vivo binding of the atypical antipsychotic drug remoxipride. A biochemical and autoradiographic analysis in the rat brain. *J Neural Transm Gen Sect* **87**:49-62.
- Ma G, Friberg LE, Movin-Osswald G and Karlsson MO (2010) Comparison of the agonist-antagonist interaction model and the pool model for the effect of remoxipride on prolactin. *British Journal of Clinical Pharmacology* **70**:815-824.

- Mohell N, Sallemark M, Rosqvist S, Malmberg A, Hogberg T and Jackson DM (1993) Binding characteristics of remoxipride and its metabolites to dopamine D2 and D3 receptors. *European Journal of Pharmacology* **238**:121-125.
- Morel G, Ouhtit A, Kelly PA (1994) Prolactin Receptor Immunoreactivity in Rat Anterior Pituitary. *Neuroendocrinology* **59**:78-84.
- Movin-Osswald G and Hammarlund-Udenaes M (1995) Prolactin release after remoxipride by an integrated pharmacokinetic-pharmacodynamic model with intra- and interindividual aspects. *J Pharmacol Exp Ther* **274**:921-927.
- Perello M, Chacon F, Cardinali DP, Esquifino AI and Spinedi E (2006) Effect of social isolation on 24-h pattern of stress hormones and leptin in rats. *Life Sciences* **78**:1857-1862.
- Petty RG (1999) Prolactin and antipsychotic medications: mechanism of action. *Schizophr Res* **35 Suppl**:S67-S73.
- Phelps CJ (1986) Immunocytochemical analysis of prolactin cells in the adult rat adenohypophysis: distribution and quantitation relative to sex and strain. *Am J Anat* **176**:233-242.
- Piccoletti R, Maroni P, Bendinelli P, and Bernelli-Zazzera (1994) Rapid stimulation of mitogen-activated protein kinase of rat liver by prolactin. *Biochem J* **303**: 429-433
- Ploeger BA, Van der Graaf PH and Danhof M (2009) Incorporating receptor theory in mechanism-based pharmacokinetic-pharmacodynamic (PK-PD) modeling. *Drug Metab Pharmacokinet* **24**:3-15.
- Post TM, Freijer JJ, Ploeger BA and Danhof M (2008) Extensions to the visual predictive check to facilitate model performance evaluation. *J Pharmacokinet Pharmacodyn* **35**:185-202.
- Prado MAM, Reis RAM, Prado VF, De Mello MC, Gomez MV, de Mello FG (2002) Regulation of acetylcholine synthesis and storage. *Neurochemistry International* **41**: 291-299
- Singh M, Se'ta'lo' Jr G, Guan X, Warren M, Toran-Allerand CD (1999) Estrogen-induced activation of mitogen-activated protein kinase in cerebral cortical explants: convergence of estrogen and neurotrophin signaling pathways. *J Neurosci* **19**:1179-1188
- Stevens J, Suidgeest E, Van der Graaf PH, Danhof M and De Lange EC (2009) A new minimal-stress freely-moving rat model for preclinical studies on intranasal administration of CNS drugs. *Pharm Res* **26**:1911-1917.
- Stevens J, Van den Berg D-J, De Ridder S, Niederlander HAG, Van der Graaf PH, Danhof M and De Lange ECM (2010) Online solid phase extraction with liquid chromatography-tandem mass spectrometry to analyze remoxipride in small plasma-, brain homogenate-, and brain microdialysate samples. *Journal of Chromatography B* **878**:969-975.
- Utama FE, Tran TH, Ryder A, LeBaron MJ, Parlow AF and Rui H (2009) Insensitivity of Human Prolactin Receptors to Nonhuman Prolactins: Relevance for Experimental Modeling of Prolactin Receptor-Expressing Human Cells. *Endocrinology* **150**:1782-1790.
- Van der Graaf PH, Schaick EA, Mathot RAA, Ijzerman AP and Danhof M (1997) Mechanism-Based Pharmacokinetic-Pharmacodynamic Modeling of the Effects of N6-Cyclopentyladenosine Analogs on Heart Rate in Rat: Estimation of in Vivo Operational Affinity and Efficacy at Adenosine A1 Receptors. *J Pharmacol Exp Ther* **283**:809-816.
- Visser SAG, Gladdines WWFT, Van der Graaf PH, Peletier LA and Danhof M (2002) Neuroactive Steroids Differ in Potency but Not in Intrinsic Efficacy at the GABAA Receptor in Vivo. *J Pharmacol Exp Ther* **303**:616-626.
- Watson CJ and Burdon TG (1996) Prolactin signal transduction mechanisms in the mammary gland: the role of the Jak/Stat pathway. *Reviews of Reproduction* **1**: 1-5.
- Widman M, Nilsson LB, Bryske B and Lundstrom J (1993) Disposition of remoxipride in different species. Species differences in metabolism. *Arzneimittelforschung* **43**:287-297.
- Yassen A, Olofsen E, Kan J, Dahan A and Danhof M (2007) Animal-to-human extrapolation of the pharmacokinetic and pharmacodynamic properties of buprenorphine. *Clin Pharmacokinet* **46**:433-447.

- Zuideveld KP, Van der Graaf PH, Peletier LA and Danhof M (2007) Allometric scaling of pharmacodynamic responses: application to 5-HT_{1A} receptor mediated responses from rat to man. *Pharm Res* **24**:2031-2039.
- Zuideveld KP, Van der Graaf PH, Newgreen D, Thurlow R, Petty N, Jordan P, Peletier LA and Danhof M (2004) Mechanism-Based Pharmacokinetic-Pharmacodynamic Modeling of 5-HT_{1A} Receptor Agonists: Estimation of in Vivo Affinity and Intrinsic Efficacy on Body Temperature in Rats. *J Pharmacol Exp Ther* **308**:1012-1020.

Conclusions and general discussion

For dopaminergic agents, oral dosing is the most common route of administration. Absorption via this route is largely influenced by gastrointestinal- and first-pass metabolic processes. Medicinal Chemistry programs in this field have typically faced significant challenges to overcome high first-pass clearance and deliver clinical candidates which could provide sufficient systemic exposure following oral administration (Attkins, et al., 2009). Moreover, for compounds active in the central nervous system (CNS), transport across the blood-brain barrier (BBB) may restrict the distribution to the target site in the brain (El Ela, et al., 2004). As a consequence, relatively high doses are required to obtain efficacious concentrations in the brain (Deleu, et al., 2002), which increases the risk of adverse events driven by peripheral mechanisms, such as cardiac valve fibrosis in the treatment of Parkinson's disease. Another complicating factor may be the relatively slow onset of the effect in e.g. the treatment of sexual dysfunction (Attkins, et al., 2009). Therefore investigations have focused on alternative routes of administration.

The existence of a direct nose-to-brain transport route has been reported in numerous studies, although very few studies allow quantification of drug transport by this route. Consequently, although intranasal administration is generally accepted as an alternative route for drug administration, controversy remains on direct absorption from the nasal cavity into the brain. This controversy is fueled by limitations of currently used animal models in terms of attainable data and sampling techniques. In general, there is a strong demand for less invasive animal models, that allow measurement of drug and biomarker concentrations at the target site, which is the brain extracellular fluid (ECF) for most drugs acting in the CNS (Jansson and Bjork, 2002; De Lange and Danhof, 2002; Illum, 2004; Graff and Pollack, 2005a; Dhuria, et al., 2009; Watson, et al., 2009).

The objective of the investigations described in this thesis was to develop a scientific basis for the translational pharmacology of dopaminergic drugs following systemic and intranasal administration, focusing on the brain distribution kinetics and biomarker responses. After recognizing the main scientific challenges and opportunities to achieve this goal (chapter 2), we first developed a new, minimal stress rat model, in which the pharmacokinetics and pharmacodynamics (PK-PD) following intranasal administration of compounds can be compared to intravenous control administration

in freely moving rats (chapter 3, (Stevens, et al., 2009)). These experimental techniques allowed serial blood- and brain ECF sampling, by using intracerebral microdialysis (De Lange, et al., 1999; Chaurasia, et al., 2007). To measure the concentrations of the dopamine D2-receptor antagonist remoxipride as a paradigm compound in mechanism-based PK–PD studies, new analytical methods were developed for remoxipride measurements in small plasma, brain ECF and brain homogenate samples (chapter 4, (Stevens, et al., 2010)). Subsequently, nonlinear mixed effect modeling (Beal and Sheiner, 1992) was applied to develop the PK model of remoxipride in plasma and brain ECF (target site for remoxipride (Nadal, 2001)) following intranasal and intravenous administration. This advanced mathematical modeling approach proved, for the first time in a strictly quantitative manner, the existence of a direct nose-to-brain transport route for remoxipride (chapter 5). Next, the effects of remoxipride on prolactin as translational biomarker for dopaminergic system activity were assessed. Based on intravenous remoxipride administration studies in the rat, a novel mechanism-based PK–PD model was developed. With use of translational modeling approaches, the model allowed good prediction of human remoxipride PK–PD (chapter 6).

In addition, we provide evidence that, following intranasal administration of remoxipride, the time to maximal drug concentrations in plasma and brain ECF is almost equal to that following intravenous administration (chapters 3 and 5). This shows that for remoxipride the absorption from the nasal cavity into the brain is fast. Therefore, intranasal administration can be of added value in diseases for which a fast time to onset of action is required and intravenous administration is highly impractical (e.g. off-phase symptoms of Parkinson's disease, menopausal hot flashes, migraine, epilepsy). Also, for remoxipride, the direct nose-to-brain transport route appears to be responsible for prolonged brain ECF exposure. As a consequence, enhanced brain distribution following intranasal administration may indeed result in smaller efficacious doses (compared to e.g. oral dosage), and has therefore the potential to reduce (peripheral) side effects.

In this thesis, in further studies, the effects of remoxipride were assessed using prolactin as a translational biomarker for dopaminergic system activity. Based on intravenous remoxipride administration studies in the rat, a novel mechanism-based PK–PD model was developed. This model is based on the concept of a physiological indirect response model with a pool depletion component (Movin-Osswald and Hammarlund-Udenaes, 1995). Detailed analysis of the prolactin profiles following single and repeated intravenous administrations of remoxipride revealed that a more elaborate

model was needed to describe the data. The new aspects in this model consisted of; i) a biological system response model, describing homeostatic feedback on the synthesis of prolactin and; ii) a dopamine antagonism component based on target site- (brain ECF) rather than plasma concentrations. This model could predict the prolactin response of remoxipride following intranasal administration, thereby confirming the validity of the model. Moreover, the model allowed good prediction of the prolactin response in humans on basis of scaling of the model in rats, indicating good translational properties (chapter 6).

Below, the main findings of the investigations are summarized. In addition, the implications and future prospects are discussed.

MAIN FINDINGS

- a novel chronically instrumented animal model allows quantification of the PK, brain distribution and PD of dopaminergic drugs following intranasal administration under minimal stress conditions
- a novel semi-physiological compartmental PK model has been developed which allows quantification of the direct nose-to-brain transport of dopaminergic drugs following intranasal administration
- a novel mechanism-based PK-PD model has been developed to describe the prolactin response following remoxipride administration. Special features of the model are; i) remoxipride target site concentrations (brain ECF) that drive the effect on prolactin release and ii) prolactin plasma concentrations that drive prolactin synthesis to allow description of the tachyphylaxis component of prolactin release in rats
- the novel mechanism-based PK-PD model was successfully applied in animal to human extrapolation. Special features of the translational approach are; i) use of simulated human target site (brain ECF) concentrations; ii) literature values of drug-specific- and biological system specific parameters, and iii) allometric scaling of prolactin turnover. This resulted in a reasonable prediction of human plasma prolactin response profiles.

IMPLICATIONS AND FUTURE RESEARCH

■ Rate and extent of brain distribution following intranasal administration

This thesis provides, for the first time, quantitative insight in the rate and extent of transport of a drug after intranasal administration. This was achieved by using a novel chronically instrumented rat model for stress free intranasal administration, using intracerebral microdialysis to measure brain

target site drug concentrations combined with advanced mathematical modeling. This approach opens the possibility of systematic investigations on the CNS distribution of drugs following intranasal administration. In terms of nasal morphology and physiology, potential routes of transport into the brain include the respiratory- and olfactory epithelium pathway, as described in chapter 2. Following absorption across the respiratory epithelium, compounds diffuse into trigeminal nerves which may allow compounds to further enter the brain. Compounds that enter the brain by the olfactory epithelial pathway may diffuse into the perineural spaces that cross the cribriform plate. This ends up in the cerebrospinal fluid of the subarachnoid space, and compounds may further diffuse throughout the brain. The olfactory epithelial pathway also allows intracellular transport through the sensory neurons, into the olfactory bulb. On the cell surface of sensory neurons, transporter proteins (glycoproteins) are present allowing compounds to bind and to be absorbed via endocytosis. After intracellular transport, the compound is exocytosed in the olfactory bulb. Which specific pathway is responsible for direct nose-to-brain transport is therefore likely to depend on the physico-chemical properties of drugs (e.g. lipophylicity, ionization, osmotic properties). Furthermore, it has been suggested that certain intranasal administration devices may favor specific pathways (Dhuria, et al., 2009).

The nose has its barriers to prevent entrance of compounds or particles into the body. The secreted nasal mucus helps to identify and destroy viruses, prevents bacteria from entering the nasal epithelium, and plays an eminent role in immunology (Jones, 2001). For drugs, the presence of nasal mucus may counteract nose-to-brain transport. Then, also nose-to-brain barriers exist, as nasal tissues express specific metabolic enzymes, as well as specific influx- and efflux transporters and mechanisms that may differ between the respiratory- and olfactory epithelium. As an example, both the olfactory epithelium and the endothelial cells surrounding the olfactory bulb express the efflux transporter P-glycoprotein (P-gp) (Graff and Pollack, 2003; Graff and Pollack, 2005b). This will obviously have an impact on nose-to-brain transport of P-gp substrates.

Specific knowledge on all these factors is important to predict target site exposure for CNS drugs following intranasal versus systemic administration. Then, to specifically predict nose-to-brain transport following intranasal administration in humans, several additional challenges must be overcome, like e.g. correcting for difference in olfactory surface area (absorption) and characterizing the impact of disease on the physiological state of the nasal epithelium and mucocilliary clearance, as has been reported for Alzheimer's

disease (Talamo, et al., 1989). For that, simultaneous modeling of data obtained in preclinical- and small scale human studies is useful to validate nose-to-brain distribution in man (chapter 6).

■ Mechanism-based PK–PD model

Information on target site exposure is important as it drives the PD. However, measurement of CNS concentrations in humans is highly restricted. In animals, intracerebral microdialysis can be applied, providing data on the free drug in the brain ECF that is close to or even indistinguishable from target site concentrations, which may be distinctively different from plasma concentrations because of the influence of e.g. BBB transport, intra-brain distribution and brain elimination of the drug (De Lange, et al., 2005).

This thesis describes the development of a mechanism-based PK–PD model for the prolactin response in plasma following remoxipride administration. This population-based model consists of; i) semi-physiological PK model for remoxipride (chapter 5); ii) a pool model incorporating the synthesis-, lactotroph storage-, plasma release-, and central elimination of prolactin; iii) an innovative biological system response model, describing homeostatic feedback by interconnecting prolactin plasma concentrations and the synthesis of prolactin, and; iv) a dopamine antagonism component interconnecting free remoxipride brain ECF concentrations and prolactin release. The structure of the model is adequate in describing prolactin response profiles in rats and humans alike. Consequently, mechanism-based PK–PD modeling of dopaminergic agents in preclinical studies *in vivo* can help to predict efficacious doses and the time-course of dopaminergic drug effects in man.

Dopaminergic modulation is a combination of complex processes, and theoretically there is no limit to the number of biological system responses (feedback) that can/should be included. However, without some way of quantifying functional biomarkers, they remain hypothetical. To this end, animal experimental methods are critical as these allow serial measurement of functional PK–PD biomarkers in both plasma and brain ECF. This is important as the BBB and blood-cerebrospinal-fluid-barrier may prevent free distribution of CNS biomarkers into plasma. E.g. it would be of much interest to obtain dopamine concentrations in brain ECF, to directly monitor dopaminergic modulation over time.

The pool- and biological system response structures of the preclinical (rat) PK–PD model are based on physiological processes and can therefore be considered mechanistic (Ben Jonathan, et al., 2008). In the mechanism-based PK–PD model this is parameterized in terms of positive feedback of prolactin on its own synthesis. Using *in vitro* bioassays and lactotroph cell cultures,

it would be of considerable interest to obtain detailed information on the kinetics of the prolactinergic feedback in both rat and man. In such an approach, following prolactin exposure, target occupancy and signal transduction should be monitored in a quantitative manner, in terms of prolactin transcription and –storage. This improves the mechanistic properties of the model, while simultaneously providing a comparative tool for the positive feedback parameter estimates found in these studies.

The preclinical PK–PD model for dopaminergic inhibition by remoxipride administration as developed in this thesis can be seen as an essential first step. An important feature is the validation of this proposed model. A crucial step in this respect is to demonstrate that the system specific parameters are independent from the drug parameters. In this respect it is important to administer different dopaminergic partial agonists and antagonists. While for dopaminergic antagonist only affinity (receptor occupancy) plays a role, for agonists also intrinsic efficacy should be taken into account. Such can be done in a similar preclinical setting. Subsequent modeling using the proposed mechanism-based PK–PD model should result in changes in the estimation of drug–effect parameters (absorption rate constant, maximal effect, concentration of drug that induces 50% of the maximal effect and the Hill-factor), but not in the pool- and biological system parameters. Hence, the pool- and system feedback models can be validated. Such an approach has been successfully applied in the development of mechanistic PK–PD models for adenosine A1-receptor agonists (Van der Graaf, et al., 1997), GABA-ergic compounds (Visser, et al., 2002), and 5-HT1a-receptor agonists (Zuideveld, et al., 2004).

While prolactin concentrations in plasma are considered an adequate biomarker in plasma that reflects inhibition of the dopaminergic system, it is not useful as biomarker for full dopaminergic stimulation. This is because baseline prolactin concentrations in rats are low and dopamine stimulation would cause prolactin concentrations to quickly drop below the limit of quantification. As a result, it will be extremely difficult to describe a drug–effect relationship. Therefore, inclusion of other dopaminergic system activity biomarkers should be considered, to expand the mechanism-based PK–PD model and allow description of stimulatory dopaminergic system functionality. Specifically the measurement of oxytocin in plasma should be considered, as its release into plasma is increased by dopamine receptor activation. Moreover, it would be of much interest to include this mechanism in the currently proposed PK–PD model, as interaction between oxytocin and prolactin is well documented (Freeman, et al., 2000). In the early stage of the experimental studies for this thesis, we considered measuring oxytocin con-

centrations. However, at the time of the experiments, no analytical methods were yet available to quantitatively measure oxytocin in small plasma samples. Next to these biomarkers that refer to physiological measurement in the integral biological system (type 4), measurement of functional biomarkers that refer to the degree of dopaminergic target occupancy (type 2, e.g. Positron Emission Tomography) and target site activation (type 3, electroencephalograms and functional Magnetic Resonance Imaging) should be pursued (chapter 2). These non-invasive techniques provide additional information on the causal chain between drug PK and effect and can be performed easily in both rats and humans.

In general, inclusion of multiple biomarkers for mechanisms on the causal chain between dose administration and effect will increase the mechanistic properties of the PK–PD model. In such approaches, information on target occupancy and transduction should be included, both in rat and human, as previously proposed (Danhof, et al., 2007; Ploeger, et al., 2009). Consequently, obtainment of multiple functional biomarkers (biomarker “fingerprint”), to reflect dopaminergic modulation in the brain, will increase the power of the model to predict the PK–PD relationships for other dopaminergic compounds, but also for the translation to the human situation. Ultimately, mechanistic understanding of dopaminergic modulation can be applied in models for disease progression in diseases related to dopaminergic dysfunction like e.g. Parkinson’s disease, schizophrenia and depression.

SUMMARIZING

For mechanism-based investigations on PK–PD relationships following intranasal administration, the use of advanced animal models and analytical techniques are crucial. As described in this thesis, quantitative information on distinction between extent as well as rate of absorption between nose-to-systemic and nose-to-brain distribution can now be obtained. Using plasma prolactin concentrations as a biomarker for dopamine D2 inhibition, a mechanism-based PK–PD model was developed. Most important aspects in this approach were incorporation of target site exposure (brain ECF) of remoxipride and a biological system response (positive feedback) mechanism on the synthesis of prolactin, thereby increasing the mechanistic insight in modulation of the dopaminergic system in rats. Simulating remoxipride brain ECF concentrations in humans, allometric scaling and use of independent information on interspecies differences proved that the structural model is applicable in both rats and man.

REFERENCES

- Atkins NJ, Heatherington AC, Phipps J, Verrier H and Huyghe I (2009) Predictability of in tranasal pharmacokinetics in man using pre-clinical pharmacokinetic data with a dopamine 3 receptor agonist, PF-219061. *Xenobiotica* **39**:523-533.
- Beal SL and Sheiner BL (1992) NONMEM user's guide, Part 1, in *NONMEM user's guide, Part 1* University of California at San Francisco.
- Ben Jonathan N, LaPensee CR and LaPensee EW (2008) What Can We Learn from Rodents about Prolactin in Humans? *Endocr Rev* **29**:1-41.
- Chaurasia CS, Muller M, Bashaw ED, Benfeldt E, Bolinder J, Bullock R, Bungay PM, De Lange ECM, Derendorf H, Elmquist WF, Hammarlund-Udenaes M, Joukhadar C, Kellogg DL, Jr., Lunte CE, Nordstrom CH, Rollemma H, Sawchuk RJ, Cheung BWY, Shah VP, Stahle L, Ungerstedt U, Welty DF and Yeo H (2007) AAPS-FDA Workshop White Paper: Microdialysis Principles, Application, and Regulatory Perspectives. *J Clin Pharmacol* **47**:589-603.
- Danhof M, De Jongh J, De Lange EC, Della Pasqua O, Ploeger BA and Voskuyl RA (2007) Mechanism-based pharmacokinetic-pharmacodynamic modeling: biophase distribution, receptor theory, and dynamical systems analysis. *Annu Rev Pharmacol Toxicol* **47**:357-400.
- De Lange EC and Danhof M (2002) Considerations in the use of cerebrospinal fluid pharmacokinetics to predict brain target concentrations in the clinical setting: implications of the barriers between blood and brain. *Clin Pharmacokinet* **41**:691-703.
- De Lange EC, De Boer BA and Breimer DD (1999) Microdialysis for pharmacokinetic analysis of drug transport to the brain. *Adv Drug Deliv Rev* **36**:211-227.
- De Lange EC, Ravenstijn PG, Groenendaal D and Van Steeg TJ (2005) Toward the prediction of CNS drug-effect profiles in physiological and pathological conditions using microdialysis and mechanism-based pharmacokinetic-pharmacodynamic modeling. *AAPS J* **7**:E532-E543.
- Deleu D, Northway MG and Hanssens Y (2002) Clinical pharmacokinetic and pharmacodynamic properties of drugs used in the treatment of Parkinson's disease. *Clin Pharmacokinet* **41**:261-309.
- Dhuria SV, Hanson LR and Frey WH (2009) Intranasal delivery to the central nervous system: Mechanisms and experimental considerations. *Journal of pharmaceutical sciences* **99**:1654-1673.
- El Ela AA, Härtter S, Schmitt U, Hiemke C, Spahn-Langguth H, Langguth P (2004) Identification of P-glycoprotein substrates and inhibitors among psychoactive compounds—implications for pharmacokinetics of selected substrates. *J Pharm Pharmacol* **56**:967-75.
- Freeman ME, Kanyicska B, Lerant A and Nagy G (2000) Prolactin: structure, function, and regulation of secretion. *Physiol Rev* **80**:1523-1631.
- Graff CL and Pollack GM (2003) P-Glycoprotein attenuates brain uptake of substrates after nasal instillation. *Pharm Res* **20**:1225-1230.
- Graff CL and Pollack GM (2005a) Nasal drug administration: potential for targeted central nervous system delivery. *J Pharm Sci* **94**:1187-1195.
- Graff CL and Pollack GM (2005b) Functional Evidence for P-glycoprotein at the Nose-Brain Barrier. *Pharmaceutical Research* **22**:86-93.
- Illum L (2004) Is nose-to-brain transport of drugs in man a reality? *J Pharm Pharmacol* **56**:3-17.
- Jansson B and Bjork E (2002) Visualization of in vivo olfactory uptake and transfer using fluorescein dextran. *J Drug Target* **10**:379-386.
- Jones N (2001) The nose and paranasal sinuses physiology and anatomy. *Adv Drug Deliv Rev* **51**:5-19.
- Movin-Osswald G and Hammarlund-Udenaes M (1995) Prolactin release after remoxipride by an integrated pharmacokinetic-pharmacodynamic model with intra- and interindividual aspects. *J Pharmacol Exp Ther* **274**:921-927.
- Nadal R (2001) Pharmacology of the atypical antipsychotic remoxipride, a dopamine D2 receptor antagonist. *CNS Drug Rev* **7**:265-282.36

- Ploeger BA, Van der Graaf PH and Danhof M (2009) Incorporating receptor theory in mechanism-based pharmacokinetic-pharmacodynamic (PK-PD) modeling. *Drug Metab Pharmacokinet* **24**:3-15.
- Stevens J, Suidgeest E, Van der Graaf PH, Danhof M and De Lange EC (2009) A new minimal-stress freely-moving rat model for preclinical studies on intranasal administration of CNS drugs. *Pharm Res* **26**:1911-1917.
- Stevens J, Van den Berg D-J, De Ridder S, Niederlander HAG, Van der Graaf PH, Danhof M and De Lange ECM (2010) Online solid phase extraction with liquid chromatography-tandem mass spectrometry to analyze remoxipride in small plasma-, brain homogenate-, and brain microdialysate samples. *Journal of Chromatography B* **878**:969-975.
- Talamo BR, Rudel R, Kosik KS, Lee VM, Neff S, Adelman L and Kauer JS (1989) Pathological changes in olfactory neurons in patients with Alzheimer's disease. *Nature* **337**:736-739.
- Van der Graaf PH, Schaick EA, Mathot RAA, Ijzerman AP and Danhof M (1997) Mechanism-Based Pharmacokinetic-Pharmacodynamic Modeling of the Effects of N6-Cyclopentyladenosine Analogs on Heart Rate in Rat: Estimation of in Vivo Operational Affinity and Efficacy at Adenosine A1 Receptors. *J Pharmacol Exp Ther* **283**:809-816.
- Visser SAG, Gladdines WWFT, van der Graaf PH, Peletier LA and Danhof M (2002) Neuroactive Steroids Differ in Potency but Not in Intrinsic Efficacy at the GABAA Receptor in Vivo. *J Pharmacol Exp Ther* **303**:616-626.
- Watson J, Wright S, Lucas A, Clarke KL, Viggers J, Cheetham S, Jeffrey P, Porter R and Read KD (2009) Receptor occupancy and brain free fraction. *Drug Metab Dispos* **37**:753-760.
- Zuideveld KP, Van der Graaf PH, Newgreen D, Thurlow R, Petty N, Jordan P, Peletier LA and Danhof M (2004) Mechanism-Based Pharmacokinetic-Pharmacodynamic Modeling of 5-HT1A Receptor Agonists: Estimation of in Vivo Affinity and Intrinsic Efficacy on Body Temperature in Rats. *J Pharmacol Exp Ther* **308**:1012-1020.

APPENDICES

NEDERLANDSE SAMENVATTING

Het dopaminerge systeem is betrokken bij vele neurologische functies in het centrale zenuwstelsel, waaronder regulatie van gedrag, (vrijwillige) beweging, motivatie- en beloningssystemen, inhibitie van prolactine afgifte, slaap, stemmingswisselingen, aandacht en leerprocessen. Veel ziekten van het centrale zenuwstelsel vinden dan ook hun oorsprong in het disfunctioneren van dit belangrijke systeem. Voorbeelden hiervan zijn de ziekte van Parkinson, schizofrenie, en seksuele aandoeningen.

De therapieën die beschikbaar zijn voor de behandeling van neurologische aandoeningen waarin het dopaminerge systeem een rol speelt laten echter nog veel te wensen over. Verbeteringen zijn te verwachten door:

- onderzoek naar betere toedieningsroutes
- het ontwikkelen van mathematische modellen met een beter voorspellende waarde.

Veel dopaminerge stoffen hebben een lage en/of zeer variabele orale biologische beschikbaarheid. Dit tengevolge van beperkte absorptie vanuit de darm en/of een groot First-pass effect. Daarnaast is het bloedhersen-barrière transport van een aantal dopaminerge stoffen beperkt. Het is daarom belangrijk te zoeken naar alternatieve toedieningsroutes.

Intranasale toediening omzeilt de problemen met betrekking tot darmpassage en First-pass effect. Daarnaast zou er via deze route mogelijk een selectieve verhoging van de hersendistributie plaats kunnen vinden wanneer er direct neus-naar-hersenen transport zou plaatsvinden. Om deze redenen zou intranasale toediening van belang kunnen zijn voor centraal werkende dopaminerge stoffen.

Verder is voor het ontwikkelen van betere therapieën meer kennis nodig van de biologische mechanismen die bepalend zijn voor het concentratie-tijd profiel (farmacokinetiek, PK) van de toegediende stof op de plaats van werking en het daarmee samenhangend verloop van het farmacologisch effect (farmacodynamiek, PD).

Voor centraal werkende dopamine agonisten en antagonisten is de plaats van werking de extracellulaire vloeistof in de hersenen (hersen ECF) waaraan de membraangebonden dopamine receptoren zijn blootgesteld. Het is belangrijk om informatie over de PK van de stof op de plaats van werking te hebben omdat daarmee een beter onderscheid gemaakt kan worden tussen de stof- en de biologisch systeem-specifieke eigenschappen, die samen de PK-PD relatie van de stof bepalen. Dit onderscheid is nodig voor de ontwikkeling van meer mechanistische PK-PD modellen met een hogere voorspellende waarde.

De technieken die in onderzoek naar PK-PD relaties van centraal werkende stoffen in de mens toegepast kunnen worden beperken zich tot seriële bloedafname, in zeer beperkte mate het afnemen van lumbale cerebrospinaal vloeistof, en beeldvormende technieken waarmee op niet-invasieve wijze de bezetting van receptoren in het centrale zenuwstelsel zichtbaar gemaakt kan worden. Dit is op zich onvoldoende voor het verkrijgen van meer mechanistische informatie en er zal daarom gebruik gemaakt moeten worden van geavanceerde en goed gecontroleerde dierexperimenten. Vervolgens moet er dan speciale aandacht worden besteed aan de translatie van de PK-PD relatie in het proefdier naar dat in de mens.

Voor het bestuderen van de PK-PD relatie van een centraal werkende dopaminerge stof is het essentieel om te beschikken over een goed gekarakteriseerde biomarker die de dopaminerge activiteit in de hersenen weerspiegelt. Daarnaast zou deze biomarker bij voorkeur in het bloed gemeten moeten worden zodat het mogelijk is om dit zowel in het proefdier als in de mens te bepalen en vervolgens met elkaar in verband te brengen.

Het hormoon prolactine is mogelijk een geschikte functionele en translationele biomarker voor dopaminerge hersenactiviteit. Prolactine wordt geproduceerd in lactotrofen die zich in de hypofyse bevinden en uitgescheiden in het bloed, waarin het vervolgens gemeten kan worden. De afgifte van prolactine vanuit de lactotrofen wordt mede gereguleerd door dopaminerge hersenactiviteit. Daarnaast is er veel kennis beschikbaar over prolactine afgifte in meerdere biologische systemen, waaronder de rat en de mens. De vraag of prolactine geschikt is als translationele biomarker moet echter nog worden beantwoord. Dit kan worden onderzocht door prolactine spiegels in dier en mens te bestuderen na beïnvloeding van dopaminerge hersenactiviteit door toediening van dopamine (ant)agonisten.

In een aantal klinische studies is de PK-PD relatie tussen de PK van dopamine antagonist in plasma en de resulterende prolactine plasma spiegels als PD reeds onderzocht. Op basis hiervan zijn er een aantal humane PK-PD modellen ontwikkeld, waarin echter belangrijke informatie ontbreekt met betrekking tot de distributie van de antagonist naar de plaats van werking. Zoals reeds genoemd is deze informatie van bijzonder belang voor het maken van een onderscheid tussen de stof- en de biologisch systeem-specifieke eigenschappen, en daarmee voor het *voorspellen* van PK-PD relaties onder condities die anders zijn dan die waarvoor het model ontwikkeld is. Hierbij valt te denken aan een andere vorm van toediening, een andere (nieuw ontwikkelde) stof, een ziekte, en/of een ander biologisch systeem (dier vs. mens). In dat laatste geval is het noodzakelijk om voldoende informatie te hebben over de verschillen tussen de biologische systemen (*hoofdstuk 2*).

Dit proefschrift betreft het onderzoek naar de PK-PD relatie van de modelstof remoxipride, als centraal werkende dopamine antagonist. Hierin zijn prolactine plasma spiegels gebruikt als PD biomarker voor dopaminerge functionaliteit. Eerst is de PK-PD relatie onderzocht in de rat, na intranasale toediening in vergelijking tot intraveneuze toediening. Hierbij is de PK van remoxipride op de plaats van werking expliciet gemeten. Op basis van de intraveneuze data is een PK-PD model ontwikkeld. Vervolgens is getoetst of dit de PK-PD relatie na intranasale toediening zou kunnen *voorspellen*. Het uiteindelijke onderzoek betrof het toetsen van de voorspellende waarde van het PK-PD model voor de PK-PD relatie in de humane situatie na intraveneuze toediening van remoxipride.

Een nieuw, vrij-bewegend diermodel onder minimale stress omstandigheden voor preklinische studies na intranasale toediening van stoffen die actief zijn in het centraal zenuwstelsel

Voor de ontwikkeling van mechanistische PK-PD modellen is het cruciaal om te beschikken over diermodellen waarin de PK op de plaats van werking kan worden bepaald in samenhang met het verloop van het effect in vrij bewegende dieren onder minimale stress condities. Voor de intranasale toediening van stoffen voldeden de beschikbare methoden niet doordat gebruik werd gemaakt van anesthesie/fixatie tijdens het experiment, waardoor de fysiologie van het neus-epitheel beïnvloed wordt. Aangezien intranasale toediening in de mens niet plaatsvindt onder dergelijke omstandigheden, werd een nieuw model voor stressvrije intranasale toediening in de vrijbewegende rat ontwikkeld.

In de rat werden vier chronische implantaties uitgevoerd; i) een nieuw-ontwikkelde toedienings-canule in de neusholte voor de intranasale toediening, ii) een canule in de vena femoralis voor de intraveneuze toediening van remoxipride, iii) een intracerebrale microdialyse canule voor seriële opvang van microdialysaat monsterfracties (hersens ECF) en iv) een canule in de arteria femoralis voor seriële afname van bloedmonsters. De ratten kregen vervolgens een week rust voor herstel van de operatie en anesthesie alvorens de experimenten werden gestart. In dit nieuwe diermodel bleek de intranasale toediening van de kleurstof Evans Blue via de intranasale canule vooral het nasale olfactorisch epitheel aan te kleuren. Als biomarker voor de mate van stress werden corticosteron concentraties in plasma gemeten tijdens- en na een 1 minuut durende intranasale infusie van 10, 20 en 40 µl fysiologisch zout oplossing. Ter vergelijking werd dit tevens gemeten na intraveneuze toediening van deze oplossing. Hieruit bleek dat de ratten geen verhoogde stressrespons vertoonden als gevolg van intranasale toediening of experimentele handelingen in vergelijking tot die na intraveneuze toediening. Van paracetamol, als modelstof voor lineaire distributie, werd de PK in plasma- en in de hersens ECF bepaald, na intraveneuze en intranasale toediening van

equimolaire doses. Deze studie toonde aan dat de opname van paracetamol in de neus erg snel is en, zoals verwacht, werden er identieke waarden voor plasma en hersen ECF PK parameters gevonden (*hoofdstuk 3*).

Nieuwe analytische methoden voor de bepalingen van remoxipride concentraties in kleine plasma-, hersen homogenaat en hersen microdialysaat monsters

Voor het ontwikkelen van een mechanistisch PK-PD model voor dopaminerge stoffen werd de dopamine D2-antagonist remoxipride gekozen als modelstof. In de literatuur zijn diverse analytische methoden beschikbaar voor het bepalen van remoxipride concentraties in plasma en in cerebrospinaal vloeistof. Deze methoden zijn gebaseerd op monstervolumes van respectievelijk 0.5 tot 2 ml, met bijbehorende bepalinglimieten van 0.7-20 ng/ml.

De volumina van monsters verkregen uit proefdieren zijn echter veel kleiner; (maximaal) 200 µl bloed, wat overeenkomt met ~100 µl plasma, terwijl de microdialysaatmonsters rond de 20-40 µl liggen. Bepalingen in deze kleine volumina vereisen zeer gevoelige analytische technieken die voor de studies in dit proefschrift ontwikkeld moesten worden. Voor het bepalen van remoxipride in hersenhomogenaatmonsters was geen analyse beschikbaar.

Om remoxipride te meten in kleine plasma-, hersenhomogenaat en microdialyse monsters werd gebruik gemaakt van *vaste stof extractie en gecombineerde vloeistofchromatografie - massaspectrometrie*. **Hoofdstuk 4** beschrijft de ontwikkeling van deze methode, met optimalisatie en validatie in termen van calibratie curven, mate van extractie, de bepalinglimiet, de nauwkeurigheid, en de intra-dag en inter-dag variatie.

De remoxipride analyses werden met succes ontwikkeld en in grote aantallen plasma-, hersen ECF- en hersenhomogenaatmonsters werden de concentraties van remoxipride met hoge gevoeligheid en goede reproduceerbaarheid gemeten.

Distributie naar de hersenen: een nieuw mechanistisch farmacokinetisch model voor remoxipride na intranasale en intraveneuze toediening

Bovenstaande dierexperimentele- en analytische technieken werden gebruikt om de PK van remoxipride in plasma en hersen ECF te bepalen na intranasale- en intraveneuze toediening van 3 doseringen (4, 8 en 16 mg/kg). De PK van remoxipride werd beschreven met behulp van compartimentele PK *non-linear mixed effects modeling* (NONMEM).

Diverse geoptimaliseerde mathematische PK modelstructuren werden op kwantitatieve wijze met elkaar vergeleken en het beste model werd geselecteerd voor verdere PK modelontwikkeling. Op basis van de data verkregen uit de intrave-

neuze studies was een PK modelstructuur nodig bestaande uit een plasma-, een hersen ECF- en een perifeer compartiment. Elk compartiment werd beschreven door parameters voor volume van distributie en (intercompartimentele) klaring. Eliminatie van remoxipride uit de hersenen bleek essentieel om de PK in hersen ECF te kunnen omschrijven.

Vervolgens werden de intranasale data toegevoegd om de absorptieroutes te karakteriseren in termen van de mate van absorptie (biologische beschikbaarheid) en de absorptiesnelheid. Er werden drie absorptieroutes getoetst; neus-naar-systemische circulatie, neus-naar-hersenen en de combinatie van deze twee routes. De laatste omschreef de data het beste en resulteerde in een mathematisch PK model met *als primeur* het *kwantitatieve onderscheid* tussen de absorptie vanuit de neus naar de systemische circulatie en de directe absorptie vanuit neus naar de hersenen.

De totale biologische beschikbaarheid van remoxipride naar de hersenen was hoog (89%) en een groot deel daarvan (75%) kon worden toegeschreven aan voor deze stof trage directe absorptie van neus naar hersenen. De absorptiesnelheidsconstante voor het directe transport van de neus naar de hersenen was laag vergeleken met de absorptiesnelheidsconstante voor systemische opname vanuit de bloedbaan. Dit verklaarde de relatief langzame eliminatie van remoxipride uit plasma- en met name hersen ECF na intranasale toediening. Het PK model was hiermee in staat om zowel de intraveneuze als de intranasale kinetiek van remoxipride in plasma en op de plaats van werking te beschrijven (*hoofdstuk 5*).

Preklinisch mechanistisch PK-PD model en de translatie van rat-naar-mens

Er is redelijk veel bekend over het verband tussen dopaminerge activiteit in de hersenen en het verloop van de concentratie van het hormoon prolactine in plasma. Het hormoon prolactine wordt aangemaakt in de lactotrofen die zich in de hypofyse bevinden. De prolactine afgifte aan het bloed wordt onder meer gereguleerd door dopamine in de hersenen. Dopamine remt de afgifte van prolactine terwijl dopamine antagonisten de afgifte stimuleren. De homeostase wordt vervolgens weer hersteld doordat de lactotrofen prolactine aanmaken en zich daarmee weer vullen.

Op basis van de PK en PD data werd een PK-PD model ontwikkeld. Hierin bleek dat de afgiftesnelheid van prolactine vanuit de lactotrofen aan het bloed bepaald wordt door de PK van remoxipride in hersen ECF. Voor de aanmaaksnelheid van prolactine in de lactotrofen waren data nodig, verkregen na herhaalde toediening van remoxipride. Hierbij werd het tijdsinterval tussen de eerste en tweede toediening gevarieerd, analoog aan de klinische studie waarvan de PK-PD waarden beschikbaar werden gesteld voor toetsing van de voorspellende waarde van het ontwikkelde PK-PD model. Ook werd een postieve homeostatische terug-

koppeling van prolactine concentraties in plasma op de aanmaak van prolactine in de lactotrofen in het model ingebouwd. Circadiane ritmiek, zoals in klinische PK-PD modellen als onderdeel werd gepubliceerd, bleek voor het preklinische model niet identificeerbaar. Zo werd er een nieuw mechanistisch PK-PD model ontwikkeld bestaande uit de volgende componenten:

1. Het PK model voor remoxipride concentraties op de plaats van werking.
2. Een pool-model dat de prolactine aanmaak en opslag in lactotrofen, en de prolactine afgifte naar en de prolactine eliminatie uit plasma beschrijft.
3. De positieve terugkoppeling (homeostase) voor de fysiologische relatie tussen prolactine concentraties in plasma en de aanmaaksnelheid van prolactine in de lactotrofen, en
4. De relatie tussen remoxipride hersen ECF concentraties en prolactine afgifte (dopamine antagonist model).

Dit mechanistische PK-PD model bleek de lagere afgifte van prolactine aan plasma na herhaalde dosering van remoxipride op verschillende tijdstippen goed te beschrijven.

Het model maakt vervolgens een onderscheid tussen stof (remoxipride) afhankelijke effecten en de homeostatische terugkoppeling van het biologische systeem middels prolactine plasma concentraties. Deze *positieve terugkoppeling* is een *nieuwe bevinding* die het inzicht in dit biologische systeem verdiept. Daarnaast bleek het mechanistische PK-PD model de PK-PD relatie van remoxipride na intranasale toediening in de rat goed te kunnen voorspellen.

Voor de volgende stap, de translatie naar de mens, moest eerst een aantal parameters van het biologische systeem "rat" naar "mens" aangepast worden. Zo werd in het pool-model gebruik gemaakt van allometrische schaling op basis van lichaamsgewicht voor de parameters voor prolactine aanmaak-, afgifte- en eliminatiesnelheidsconstanten. Voor de aanpassing van de positieve homeostatische terugkoppeling werden gegevens uit de literatuur gebruikt om te corrigeren voor het verschil in dichtheid van de lactotrofen in de hypofyse tussen rat en mens. Voor de bindingsaffiniteit van remoxipride voor de dopaminerge receptor werd in het dopamine antagonist model de literatuurwaarde gebruikt zoals bepaald in *in vitro* experimenten met menselijke lactotrofen. Omdat in de mens geen hersenconcentraties gemeten waren (/konden worden) en het verband tussen plasma- en hersenconcentraties van remoxipride in de rat lineair is, werd de aanname gemaakt dat de verhouding tussen concentraties in de compartimenten die de vrije fractie beschrijven in de rat dezelfde is als die voor de mens. Met deze aanpassingen naar het menselijke biologische systeem bleek het model in staat de PK-PD van remoxipride in de mens te voorspellen, ook na herhaalde intraveneuze toediening (*hoofdstuk 6*).

Samenvattend zijn de belangrijkste resultaten en bevindingen:

- De ontwikkeling van een nieuw verfijnd proefdiermodel voor intranasale toediening onder nagenoeg stressvrije omstandigheden.
- De ontwikkeling van gevoelige analyse methoden voor het meten van remoxipride in diverse matrices in kleine monstervolumina.
- De ontwikkeling van een nieuw semi-fysiologisch compartimenteel PK model waarin voor de eerste keer is aangetoond dat het mogelijk is het transport vanuit de neus naar het bloed zowel als het directe transport vanuit neus naar hersenen in kwantitatieve termen van zowel mate als snelheid te beschrijven.
- De ontwikkeling van een nieuw mechanistisch PK-PD model waarmee de prolactine respons na intraveneuze en intranasale toediening van remoxipride beschreven kan worden, waarbij de postieve terugkoppeling van prolactine concentraties in plasma op de aanmaak van prolactine in de lactotrofen voor het eerst gekarakteriseerd is.
- De aanpassing van het nieuwe mechanistische PK-PD model voor het humane biologische systeem, waarmee de prolactine respons na toediening van remoxipride in de mens voorspeld kan worden.

Het in kwantitatieve termen kunnen beschrijven van de diverse absorptieroutes van stoffen na intranasale toediening is een *absolute primeur* en geeft de mogelijkheid om een strict onderscheid te kunnen maken tussen de invloed van de specifieke stof- en formuleringseigenschappen en de systeem-specifieke eigenschappen. Hierdoor kan er een grote vooruitgang geboekt worden in de kennis van de intranasale toediening en de toepassing daarvan.

De ontwikkeling van het preklinische PK-PD model voor dopaminerge inhibitie door remoxipride toediening kan worden gezien als een eerste stap naar een alomvattend translationeel mechanistisch PK-PD model voor dopaminerge modulatie. Het model is ontwikkeld voor de dopamine antagonist remoxipride. Voor verdere ontwikkeling van het model zijn er een aantal belangrijke stappen te nemen.

Zo zou het translationele mechanistische PK-PD model verder gevalideerd en uitgebreid moeten worden voor andere dopamine antagonisten en vervolgens voor dopamine agonisten. Voor de dopamine agonisten speelt naast dopamine receptor affiniteit ook de intrinsieke effectiviteit een rol. Door samenvoegen van data verkregen in preklinische studies voor dopamine agonisten met verschillende intrinsieke effectiviteit zal uiteindelijk informatie beschikbaar komen over het maximale effect dat in een bepaald biologisch systeem te behalen valt. Daarnaast zouden de systeem specifieke parameters constant moeten blijven waardoor deze gevalideerd kunnen worden.

Voor dopamine agonisten is het gebruik van de prolactine plasma concentraties als biomarker voor dopaminerge modulatie in de rat minder geschikt. De concentraties van prolactine in plasma in de rat zijn onder basale condities erg laag en een verdere verlaging door dopaminerge stimulatie zou mogelijk niet goed te bepalen zijn. Dit betekent dat er in het mechanistische PK-PD model een biomarker voor dopamine stimulatie opgenomen zou moeten worden. Hiervoor zou de plasma concentratie van het hormoon oxytocine mogelijk geschikt zijn. Tevens zijn ook de verandering in het electro-encephalogram (EEG) en veranderingen in functionele magnetische resonantie beelden geschikt als translationele biomarkers. Uitbreiding van het model zou verder mogelijk zijn door het incorporeren van informatie over dopaminerge receptor bezetting, zoals zowel in de rat als in de mens te bepalen is, met behulp van positron emissie tomografie (PET). Met de combinatie van deze translationele biomarkers (biomarker “finger-print”) zal het mechanistische gehalte van het translationele PK-PD model, en daarmee de voorspellende waarde, sterk verbeterd worden.

Uiteindelijk zal het mechanistische begrip voor functionaliteit van het dopaminerge systeem geïncorporeerd kunnen worden in modellen voor ziekteprogressie in ziekten van het dopaminerge systeem, zoals de ziekte van Parkinson, schizofrenie en depressie.

NAWOORD

Een promotietraject is een tijdrovende en drukke periode. De rode lijnen die ten grondslag lagen aan dit proefschrift namen een hoge plaats in op mijn prioriteitenlijst. Nu dit traject is afgerond kan ik terugblikken en dringt het pas echt door hoeveel mensen direct danwel indirect aan een geweldige periode hebben bijgedragen.

Ik wil de gehele afdeling *Farmacologie* bedanken voor de prettige werksfeer en een paar personen in het bijzonder.

Joost, we hebben vanuit de J&J kamer talloze uren gespendeerd op werkgebied. Omdat onze projecten directe raakvlakken hebben, kon jij mijn ideeën inhoudelijk bekritisieren en ik die van jou, wat de kwaliteit ten goede kwam. Naast werk hebben we ook vele persoonlijke gesprekken gehad en plezier gemaakt.

Elke, bedankt voor de hulp die je mij gegeven hebt in het begin van mijn modelleer-perikelen, en voor het ontbijt na de 24-uurs studie van Ernst en mij.

Max, I want to thank you for the help you provided in my early stages of modeling. Also thanks for providing a place where we could play D&D, and many thanks for your hospitality when I visited Lodi.

Ernst, ik wil je bedanken voor het samen voorbereiden en uitvoeren van dier- experimenten en de ontwikkeling van het nieuwe diermodel. Daarnaast was je vrijgezellenfeest ook een van de hoogtepunten.

Robin, ook jij bedankt voor je bijdrage aan de dierexperimentele interpretaties.

Verder wil ik, in de volgorde van samenwerking, *Margret en Dirk-Jan* bedanken voor de onmisbare hulp die ze zijn geweest bij het uitvoeren van de analytische aspecten in dit proefschrift. Ik heb ontzettend veel van jullie geleerd.

Dank ben ik ook verschuldigd aan twee studenten die delen van de experimenten hebben uitgevoerd; *Sanne en Joëlle*. Jullie hebben echt goed en secuur werk afgeleverd, waardoor de vervolgstappen voor mij vergemakkelijkt werden.

Binnen de *LACDR borrelcommissie* wil ik specifiek *Miranda en Kjeld* bedanken voor de “vergaderingen”, lunchafspraken, een dubieus feest in Rotterdam en uiteraard de borrels zelf.

Ook ben ik *Joost en Bart*, werkzaam bij *LAP&P Consultants*, zeer dankbaar. Zonder jullie kennis, hulpvaardigheid en geduld had ik niet een dergelijk mechanistisch PK-PD model kunnen ontwikkelen.

Lieve ouders en vrienden, heel erg bedankt voor jullie belangstelling in mijn werk. Ik kan moeilijk uitleggen hoe nuttig het voor mij is geweest dit werk uit te leggen aan mensen die niet in dit specialistische vakgebied werkzaam zijn. Dat moeten jullie dus maar aannemen.

Lieve Nienke, aan jou ben ik enorm veel dank verschuldigd. Naast het feit dat je mijn privé-leven bijzonder veel glans geeft, ben je ook een goede steun in de rug geweest tijdens het werk dat ik heb verricht voor dit proefschrift. Je weet op welke momenten je mij kunt stimuleren met je optimisme, mij moet laten doorworstelen met een probleem of mij afstand moet laten nemen.

LIST OF PUBLICATIONS

- Stevens J, Suidgeest E, Van der Graaf PH, Danhof M and De Lange EC (2009) A new minimal-stress freely-moving rat model for preclinical studies on intranasal administration of CNS drugs. *Pharm Res* **26**:1911-1917.
- Stevens J, Van den Berg D-J, De Ridder S, Niederländer HAG, Van der Graaf PH, Danhof M and De Lange ECM (2010) Online solid phase extraction with liquid chromatography-tandem mass spectrometry to analyze remoxipride in small plasma-, brain homogenate-, and brain microdialysate samples. *Journal of Chromatography B* **878**:969-975.
- Stevens J, Ploeger BA, Van der Graaf PH, Danhof M, De Lange ECM Systemic- and direct nose-to-brain transport in the rat; a pharmacokinetic model for remoxipride after intravenous and intranasal administration.
Manuscript submitted
- Stevens J, Ploeger BA, Hammarlund-Udenaes M, Osswald G, Van der Graaf PH, Danhof M, De Lange ECM Mechanism-based PK-PD model for the prolactin biological system response following a dopamine inhibition challenge - quantitative extrapolation to humans.
Manuscript ready to be submitted

ABBREVIATIONS

AUC	area under the curve
BBB	blood-brain barrier
BSL	baseline
CL	clearance
C_{max}	maximum concentration
CN	hysphere silica based cyano propyl phase
CNS	central nervous system
CSF	cerebrospinal fluid
CORT	corticosterone
CV	coefficient of variation
DE	drug effect
EC₅₀	concentration inducing 50% of the E _{max}
ECD	electrochemical detection
ECF	extracellular fluid
EDTA	ethylenediaminetetraacetic acid
E_{max}	maximal effect
F	bioavailability
GP	resin general phase
HPLC	high pressure liquid chromatography
ID	internal diameter
IIV	interindividual variability
IN	intranasal
IS	internal standard
IV	intravenous
k	rate constant
k_a	absorption rate constant
LC	liquid chromatography
LLOD	lower limit of detection
LLOQ	lower limit of quantitation
MCX	mixed mode cationic exchange
MS-MS	tandem mass spectrometry
MQ	purified Millipore water
OFV	objective function value
PD	pharmacodynamic

PF	positive feedback
PK	pharmacokinetic
QC	quality control
RP	reverse phase
SD	standard deviation
SEM	standard error of the mean
SH	resin strong hydrophobic phase
SPE	solid phase extraction
VPC	visual predictive check
V	volume of distribution
WCX	weak cationic exchange
Q	intercompartmental clearance

COLOFON

Uitgave: september 2011

ISBN 978-90-9026283-3

Dit proefschrift zal ook in een digitale versie beschikbaar komen via het Leiden Repository (www.openaccess.leidenuniv.nl).

Grafische verzorging

ETCETERA (Jan Stevens, Assen)

Foto achterzijde

Nienke Heijes, Den Haag

© **Jasper Stevens**

stevens.jasper@gmail.com